THE CARDIOVASCULAR PROTECTIVE ROLE OF SALVIANIC ACID A IN DIABETES WITH ELEVATED HOMOCYSTEINE LEVEL

GAO LEI

Ph.D

The Hong Kong Polytechnic University

2018

The Hong Kong Polytechnic University

Department of Health Technology and Informatics

The Cardiovascular Protective Role of Salvianic Acid A in Diabetes with Elevated Homocysteine Level

GAO LEI

A thesis submitted in partial fulfillment of the requirements for the degree of Doctor of Philosophy

September 2017

CERTIFICATE OF ORIGINALITY

I hereby declare that this thesis is my own work and that, to the best of my knowledge and belief, it reproduces no material previously published or written, nor material that has been accepted for the award of any other degree or diploma, except where due acknowledgement has been made in the text.

_____ (Signed)

GAO LEI
_____(Name of student)

Abstract

Cardiovascular disease (CVD) is the most common cause of death in people with diabetes mellitus (DM). Compared to the non-diabetic population, individuals with DM have a higher risk for left ventricular hypertrophy (LVH) and endothelial dysfunction (ED), especially for those comorbid with elevated homocysteine (Hcy) level. Few studies have addressed the effectiveness of traditional Chinese medicine (TCM) in relieving CVD burdens for diabetic patients with elevated Hcy level.

Salvianic acid A (SAA) is an important ingredient extracted from *Salvia Miltiorrhiza* (*Danshen*) and has been widely applied in the treatment of CVD. A previous animal study indicated that SAA could ameliorate ED and lower the blood Hcy level in hyperhomocysteinemic rats without DM, but whether these observed beneficial effects might also be found in diabetic rodents remains unclear, particularly the effects on LVH and ED. Therefore, the primary aims of my thesis were to (1) investigate the protective effects of SAA against LVH and ED in *db/db* mice with elevated blood Hcy level, and (2) decipher whether the observed cardiovascular protective effects of SAA are associated with Hcy metabolism by modulating the methylation potential and redox status in the liver of the *db/db* mice with elevated blood Hcy level. A secondary objective of my thesis was to determine the antidiabetic activity of SAA, together with other structurally similar compounds.

My findings suggest that an 8-week oral treatment of SAA can significantly slow the progression of left ventricular mass in the DM group compared to other DM groups without SAA. Moreover, the chronic SAA administration ameliorated ED in the

diabetic mice with elevated Hcy level. In another *ex vivo* experiment, we found that SAA was able to induce vasorelaxation via a calcium channel-dependent pathway. Furthermore, the serum Hcy level in the methionine-diet DM group that received SAA treatment for 8 weeks was significantly reduced compared to the methionine-diet DM group without taking SAA treatment, along with an increased level of glutathione production in their liver. Lastly, I found that SAA was not a good antidiabetic agent. However, some compounds that could be extracted from *S. Miltiorrhiza,* such as Salvianolic Acid A and Salvianolic Acid B, were structurally similar to that of SAA but possessing better antidiabetic potential than SAA.

In conclusion, my thesis underlines the protective effects of SAA treatment against LVH and ED in diabetic mice with elevated Hcy. These observed beneficial effects are likely due to an improved redox status induced by the antioxidant effect of SAA itself, and to a certain extent associated with increased production of glutathione via activated trans-sulphuration pathway.

Publications

Publication based on the work presented in this thesis

(Published)

- **Lei Gao,** Parco M. Siu, Shun Wan Chan, Christopher W.K. Lai (2017). Cardiovascular protective effects of Salvianic Acid A in *db/db* mice with elevated homocysteine level. *Oxidative Medicine and Cellular Longevity, 2017, 1-10.*

Other publications during the period of my PhD study

(Published)

- **Lei Gao,** Yiu-Wa Kwan, Andrew Bulmer, and Christopher W.K. Lai (2018). Noninvasive real-time characterization of kidney function in diabetic Mice after receiving Danshensu treatment. *Oxidative Medicine and Cellular Longevity, 2018.*
- Arijit Ghosh, **Lei Gao,** Abhimanyu Thakur, Parco M. Siu and Christopher W. K. Lai (2017). Role of free fatty acids in endothelial dysfunction. *Journal of Biomedical Science, 24(1), 50.*
- Wilson KC Leung, **Lei Gao,** Parco M Siu, Christopher W.K. Lai (2016). Diabetic nephropathy and endothelial dysfunction: Current and future therapies, and emerging of vascular imaging for preclinical renal-kinetic study. *Life sciences, 166, 121-130.*

Awards

Scholarship Award

- Eurasia-Pacific-Ernst Mach Scholarships Award 2016–2017

Oral Presentation Award (2nd Prize)

- **Lei GAO,** Parco SIU, and Christopher W.K. LAI.

  The Relationship Between Hyperhomocysteinemia and Endothelial Dysfunction in Diabetes and the Potential Beneficial Effect of Salvianic Acid A. HTI Postgraduate symposium 2016. Hong Kong. (Oral presentation)

Conference Presentations

- **Lei GAO,** Christopher W.K. LAI, Yiu-Wa KWAN, Adelheid BRANTNER. Cardioprotective Effect of Salvianic Acid A in db/db Mice with Elevated Homocysteine Level. 3rd Global Summit on Herbals & Traditional Medicine, Osaka, Japan, 2017. (Oral Presentation)

- **Lei GAO,** Christopher W.K. LAI, Adelheid BRANTNER, Gerald WOELKART. Cardioprotective Effect of Salvianic Acid A in *db/db* Mice with Elevated Homocysteine Level. PHYTOPHARM 2017 and 10th Anniversary of the TCM Research Center Graz, Graz, Austria, 2017. (Poster Presentation)

- **Lei GAO,** Christopher W.K. LAI.

  Cardiac function and endothelial function assessment in diabetic mice with hyperhomocysteinemia. 17th Diabetes and Cardiovascular Risk Factors – East Meets West Symposium, Hong Kong, 2015. (Poster Presentation)

Acknowledgement

I would like to take this precious and unique opportunity to express my sincere gratitude to my chief supervisor Dr. Christopher W.K. LAI for his truly professional guidance, as well as the enormous amount of time and energy he dedicated in his supervision during the past 4 years. He is the mentor who directed me to step into the real scientific research domain and provided unlimited support, immense knowledge, encouragement, inspiration, and invaluable suggestions, with which I made every step of progression of experiments and publications. There could be never enough words for me to express my deep appreciation to him.

I would like to express my gratefulness to Dr. Parco Siu and Dr. Patrick Lai for their guidance, and Dr. Helen Law, Prof. Iris Benzie and Dr. Chung for their technical support and constructive comments.

I sincerely thank Prof. Y.W. Kwan from the Chinese University of Hong Kong and Dr. S.W. Chan from the Technological and Higher Education Institute of Hong Kong for their great support of my study, and Dr. Rachel Li from the Chinese University of Hong Kong for the technical support in the myograph experiment.

I would also like to sincerely thank Prof. Adelheid Brantner from the University of Graz, Austria for being my host for the Eurasia-Pacific Ernst Mach Scholarships Award, from whom I learned quite a lot of pharmacological knowledge, and Prof. Tamás from the University of Pécs, Hungary for his kind guidance in my experiments.

I am grateful to the support from all the technical staff in the Centralized Animal

Facility, the HTI lab, and all my friends in the office of research students, Y607.

I would also like to appreciate the financial support from the Hong Kong Polytechnic University and the Eurasia-Pacific Scholarships Uninet.

Finally, I would like to give my appreciation to my beloved family, my parents who gave me my life and the way to be a real man, my sister, Dr. Lingling GAO from the Jacobs University, Germany, her husband, Dr. Dong Li from the University Medical Center Hamburg-Eppendorf, Germany, and my little honey angels, Amboer and Beryl, who support me with warmest family love always wherever I am.

Table of Contents

List of Figures

List of Tables

List of Abbreviations

AA	arachidonic acid
ACE	angiotensin-converting enzyme
Ach	acetylcholine
ADMA	asymmetric dimethylarginine
AGEs	advanced glycated end products
AHA	American Heart Association
ALT	alanine transaminase
ARB	angiotensin receptor blocker
ARE	antioxidant-response element
AS	atherosclerosis
AST	aspartate transaminase
ATP	adenosine triphosphate
AW	anterior wall
BH4	tetrahydrobiopterin
BHMT	betaine homocysteine methyltransferase
CAD	coronary artery disease
CAT	cationic amino acid transporter
CBS	cystathionine b-synthase
cGMP	cyclic GMP
CGS	cystathionine g-synthase
CHD	coronary heart disease
CHOP/GADD153	growth arrest- and DNA-damage inducible gene153
COX	cyclooxygenase
CVD	cardiovascular disease

cyclic GMP	guanosine 3':5'-cyclic monophosphate
DAG	diacylglycerol
DDAH	dimethylarginine dimethylaminohydrolase
DM	diabetes mellitus
EC	endothelial cell
ED	endothelial dysfunction
EDHF	endothelium-derived hyperpolarizing factor
EF	ejection fraction
eNOS	endothelial nitric oxide synthase
ER	endoplasmic reticulum
FFA	free fatty acids
FS	fractional shortening
GPx1	glutathione peroxidase-1
GSH	glutathione
GSSG	glutathione disulfide
HbA1c	glycated hemoglobin
Hcy	homocysteine
HF	hepatic fibrosis
HHcy	hyper-homocysteinemia
HO-1	heme oxygenase-1
HPLC	high-performance liquid chromatography
HR	heart rate
HRWE	heat reflux water extraction
HUVEC	human umbilical vein endothelial cells
ICAM-1	intercellular adhesion molecule
INDO	indomethacin
IRE1	inositol-requiring enzyme 1

IRS-1	insulin receptor substrate-1
IVS	interventricular septal thicknesses
IVSd	interventricular septal thicknesses (diastole)
IVSs	interventricular septal thicknesses (systole)
LNNA	Nω-nitro-L-arginine
LV	left ventricular
LVH	left ventricular hypertrophy
LVID	left ventricular internal dimensions
LVIDd	left ventricular internal dimensions (diastole)
LVIDs	left ventricular internal dimensions (systole)
MAO	monoamine oxidase
MAPK	mitogen-activated protein kinases
MS	methionine synthase
MTHFR	5,10-methylenetetrahydrofolate reductase
NADPH	nicotinamide adenine dinucleotide phosphate
NE	norepinephrine
NO	nitric oxide
NOS	nitric oxide synthase
Nrf2	NF-E2 p45-related factor 2
$O^{\cdot 2-}$	superoxide
O^2	oxygen
ODQ	quinoxalin-1-one
OH	hydroxyl
OS	oxidative stress
PARP	poly (ADP-ribose) polymerase
PBS	phosphate buffered saline
PD	Parkinson’s disease

PERK	protein kinase ER kinase
PG	prostaglandin
PGI_2	prostacyclin
PI-3	phosphoinositide-3
PKC	protein kinase C
pNP	p-nitrophenol
pNPG	p-nitrophenol-D-glucopyranoside
PPARγ	peroxisome proliferator-activated receptor gamma
PRMT	protein-arginine methyltransferase
PTPs	protein tyrosine phosphatases
PW	posterior wall
PWd	posterior wall thicknesses (diastole)
PWs	posterior wall thicknesses (systole)
RAGE	receptor of advanced glycated end products
RIPA	radio immunoprecipitation assay buffer
RNS	reactive nitrogen species
ROS	reactive oxygen species
SAA	Salvianic Acid A
SAH	s-adenosyl homocysteine
SalA	Salvianolic Acid A
SalB	Salvianolic Acid B
SAM	s-adenosyl methionine
SDS	sodium dodecyl sulfate
sGC	soluble guanylyl cyclase
-SH	sulfhydryl
SHMT	serine hydroxymethyltransferase
SNP	sodium nitroprusside

STZ	streptozotocin
TCM	traditional Chinese medicine
TDAG51	T-cell death-associated gene 51
TNF	tumor necrosis factor
UPR	unfolded protein response
VCAM-1	vascular cell adhesion molecule
VEGF	vascular endothelial growth factor
VEGFR-1	VEGF receptor 1
VSM	vascular smooth muscle
VSMC	vascular smooth muscle cells
WAE-W	microwave-assisted extraction with water

Chapter 1 Introduction

1.1 Cardiovascular Disease

Cardiovascular disease (CVD) remains the world's top mortality factor (Binno 2016; Townsend, Wilson et al. 2016). According to the report provided by the Global Burden of Disease, in 2013, a total number of 17.3 million deaths globally were due to CVD, which accounts for 31.5% of all deaths and twice that of cancer (Abubakar, Tillmann et al. 2015). As estimated by World Health Organization, more than 23 million people will die from CVD by 2030 (Mendis, Puska et al. 2011). In addition, in 2015, CVD contributed up to 1,197 billion USD in the treatment costs of diabetic patients (American-Diabetes-Association 2016). Patients with type 2 diabetes have a 2-4 times higher risk of developing CVD than the subjects without diabetes, which is due to the presence of hyperglycemia, insulin resistance, oxidative stress, obesity, and high cholesterol.

CVD is defined as a series of disorders occurring in the heart and blood vessels, including coronary artery diseases, cardiomyopathy, hypertensive heart disease, rheumatic heart disease, congenital heart disease, deep vein thrombosis, and peripheral arterial disease (Mendis, Puska et al. 2011; Abubakar, Tillmann et al. 2015). Specifically, this thesis will focus on two important cardiovascular disorders that are commonly found in diabetic patients: endothelial dysfunction (ED) and left ventricular hypertrophy (LVH).

1.1.1 Cardiomyopathy

The American Heart Association Scientific Statement defines cardiomyopathy as "*Cardiomyopathies are a heterogeneous group of diseases of the myocardium associated with mechanical and/or electrical dysfunction that usually (but not invariably) exhibit inappropriate ventricular hypertrophy or dilatation and are due to a variety of causes that frequently are genetic. Cardiomyopathies either are confined to the heart or are part of generalized systemic disorders, often leading to cardiovascular death or progressive heart failure-related disability*." (Maron, Towbin et al. 2006). Cardiomyopathies can be divided into four common types (Thiene, Corrado et al. 2004): 1) Dilated cardiomyopathy, which can be induced by coronary artery disease and is characterized by stretched muscles and expanded chambers of the heart due to heart muscle weakness; 2） Hypertrophic cardiomyopathy, which can be induced by persistent high blood pressure and diabetes, and is characterized by left ventricular hypertrophy; 3) Restrictive cardiomyopathy, which can be induced when stiffened ventricles hinder diastolic ventricular filling; and 4) Arrhythmogenic right ventricular dysplasia, which occurs when the cardiac muscle, especially the muscle tissue in the right ventricle, is replaced by extra fibrous tissue and fat, leading to subsequent abnormal heart rhythms (Maron, Towbin et al. 2006; AmericanHeartAssociation 2016; Story 2017).

Hypertrophic cardiomyopathy is the most common type of cardiomyopathies and is morphologically characterized by left ventricular hypertrophy (LVH) in the absence of other heart diseases, which could increase the wall thickness. The common causes of LVH include left ventricular outflow tract obstruction, myocardial ischemia, autonomic dysfunction, diastolic dysfunction, and mitral regurgitation (Gersh, Maron

et al. 2011). Hypertrophic cardiomyopathy is usually diagnosed by detection of left ventricular wall thickness using 2-dimensional echocardiography and can be found in the presence of ECG alteration (Maron, Towbin et al. 2006). It is also suggested that patients with hypertrophic cardiomyopathy are at a higher risk of atrial fibrillation, which is a high morbidity risk factor and an important indicator of hypertrophic cardiomyopathy-related heart failure, death, and stroke (Kitaoka 2001; Olivotto, Cecchi et al. 2001).

The occurrence of cardiomyopathy is commonly subsequent to heart failure, which is either due to mechanical (e.g., induced by systolic dysfunction) or arrhythmic problems of the heart. A previously published study indicated that the hypertrophic cardiomyopathy was the top inducer of sudden cardiac death in young subjects, and was significantly correlated with heart failure disability (Maron, Towbin et al. 2006). Today, the recommended therapies for the treatment of LVH rely on invasive operations, such septal reduction therapy, surgical septal myectomy, alcohol septal ablation, and mitral valve replacement. However, effective medical therapy that aims to slow down or regress LVH progression remains unclear and requires further verification (Gersh, Maron et al. 2011).

1.1.2 Vascular Endothelial Dysfunction

The endothelium plays a significant role in the maintenance of normal vascular physiological activity (Park and Park 2015; Gimbrone and García-Cardeña 2016).

The endothelium is comprised of a single layer of endothelial cells (EC) that line the inner surface of the vascular lumen, acting as a physical barrier in the blood vessel that separates the flowing blood and vascular smooth muscle cells (VSMC). More than a barrier, ECs also make significant contributions to maintaining overall homeostasis by participating in a series of physiological alternations, such as pro-inflammatory, anti-inflammatory, and VSMC growth stimulation and inhibition. Moreover, ECs play a dominant role in regulating vasculature homeostasis by modulating the VSMC via a series of chemical mediators under various physiological conditions (Calles-Escandon and Cipolla 2001) (**Table 1-1**). ED can be described as an imbalance between vasodilation and vasoconstriction regulated by the endothelium, and such an imbalance condition has been suggested as a risk marker in the process of CVD (Deanfield, Donald et al. 2005).

Table 1-1. Chemicals and mediators related to endothelial function (Calles-Escandon and Cipolla 2001).

Vasoconstriction	Endothelin Angiotensin II Endothelin-1 Thromboxane A2 Prostaglandin H2
Vasodilation	Nitric Oxide (NO) Bradykinin Hyperpolarizing factor
Growth Stimulation	Platelet growth-derived factor Fibroblast growth factor Insulin-like growth factor-1 Endothelin Angiotensin II
Growth Inhibition	NO Prostacyclin (PGI2)
Proinflammatory	Vascular cell adhesion molecule-1 Intercellular cell adhesion molecule-1
Antithrombotic	Prostacyclin Tissue plasminogen activator
Prothrombotic	Type 1 plasminogen activator inhibitor

The principal substance that controls vasodilation, the endothelium-derived relaxing factors, has generally been recognized as nitric oxide (NO) (Félétou and Vanhoutte 1999). As an endogenous vasodilator, NO also works as an inhibitor of platelet and leukocyte adhesion, aggregation, proliferation, and permeability. As a dominant factor maintaining the normal vessel function and endothelium response, a decrease of NO quantity or bioavailability could be a significant pathological factor leading to various CVDs (Moncada, Palmer et al. 1991). NO, an endothelial-derived vasodilator, dominantly mediates the normal vasorelaxation and contributes to the homeostasis of vessel tone. Whereas, in DM status, hyperglycemia, activated oxidative stress, and pre-inflammation significantly diminish the bioactivity and availability of NO, which leads to a disordered endothelial response and a declined endothelial self-repair capacity (Van den Oever, Raterman et al. 2010). Moreover, insulin residence, obesity, and hypertension in DM also damage the normal endothelial function in multiple pathways, and lead to the ED in DM characterized by pathological changes in proliferation, barrier function, and altered susceptibility to apoptosis, which induce CVD, as well as diabetic retinopathy and nephropathy (Favaro, Miceli et al. 2008). Several detailed major mechanisms involved in the progress of ED in DM are introduced as the following content.

In ECs, endogenous NO is produced from the conversion of the L-arginine to L-citrulline, catalyzed by the NO-synthase (NOS). Multiple isoforms of this enzyme have been isolated in various organs and tissues. The type III NOS that has been isolated from endothelial cells is endothelial-NOS (eNOS), which catalyzes the derivation of NO from endothelium. NO then infiltrates into the VSMC and subsequently induce the rise of guanosine 3': 5'-cyclic monophosphate (cyclic GMP), which leads to the final vasodilation.

Over many decades, multiple clinical studies and animal experiments have revealed an impairment of endothelium-dependent vasodilation in diabetes (Bijlstra, Smits et al. 1995). Therefore, the detection of such defective vasodilation function has been playing a significant role in detecting and symbolizing the existence of ED in diabetes (Hink, Li et al. 2001).

1.2 Heart and Vascular Complications in Diabetes

1.2.1 Diabetic Cardiomyopathy

Around 50% of individuals with DM will develop heart failure, which significantly contributes to the CVD mortality, especially in those receiving insulin and rosiglitazone treatment (Singh, Loke et al. 2007; American-Diabetes-Association 2016). Diabetic cardiomyopathy (heart disease in diabetics, ultimately leading to heart failure) was firstly described by Rubler et al. in a study of the post-mortem histology of four patients who had heart failure without ischemic, hypertensive or vascular heart disease (Rubler, Dlugash et al. 1972). The current definition highlights the structural and functional changes in the myocardium of the patients in the absence of coronary artery disease or hypertension, which is induced by metabolic disorder caused in diabetes and leading to heart failure (Nunes, Rolo et al. 2017).

Interstitial and perivascular fibrosis are typical histological changes associated with diabetic cardiomyopathy, the progression of which is correlated the hypertrophy of the heart, particularly in the left ventricle (Van Hoeven and Factor 1990). Increased collagen deposition and cross-linking of collagen fibers have been suggested to contribute to the cardiomyocyte hypertrophy and ventricular hypertrophy in diabetic cardiomyopathy (Fischer, Barner et al. 1984). Also, increased sensitivity to the ischemia/reperfusion injury in diabetes is another significant character of diabetic cardiomyopathy (Alegria, Miller et al. 2007). As a result, the clinical phenotype of diabetic cardiomyopathy included the left ventricular (LV) hypertrophy and LV diastolic and systolic dysfunction (Bonito, Moio et al. 2005; Velagaleti, Gona et al. 2010).

The exact mechanism of diabetic cardiomyopathy pathogenesis has not been thoroughly investigated. Generally, in the diabetic cardiomyopathy progression, excess generation of advanced glycation end-products (AGEs) in DM significantly deactivate NO (nitric oxide) and impair coronary vasodilation capacity (Creager, Goldin et al. 2006). On the other hand, sustained hyperglycemia causes the excess formation of mitochondrial ROS leading to contractile dysfunction of the myocardium. Moreover, increased ROS production also reduces NO bioactivity, causing myocardial inflammation and ED mediated by activated PARP [poly (ADP-ribose) polymerase] (Serpillon, Floyd et al. 2009). In addition, the severity of diastolic dysfunction also correlates with HbA1c (glycated hemoglobin) and AGEs levels, which induce the formation of ROS and result in myocardial collagen deposition and fibrosis.

Other Possible mechanisms include the following factors:

(1) Impaired calcium homeostasis leads to the alternation of Ca^{2+} transient and sensitivity to contractile elements in cardiomyocytes, which can be detected prior to the onset of systolic ventricular dysfunction (Gallego, Alday et al. 2009)
(2) Diminished glucose oxidation in diabetic hearts, which is induced by the inhibited expression of GLUT4/GLUT1, leads to an impaired response to insulin and a disordered glucose supply and utilization (Deng, Huang et al. 2007).
(3) Activated receptor of advanced glycated end products (RAGE) can be responsible for blunted nitric oxide production, which contributes to the stiffening of coronary media, diminished angiogenesis, and leads to impaired coronary blood flow reserve in the heart of diabetics (Zieman, Melenovsky et al. 2007).

(4) In the presence of defective glucose metabolism, free fatty acids (FFA) act as a competitive energy substrate with glucose. Glucose utilization is reduced, and oxidation is induced, which ultimately lead to increased glucose level and insulin resistance (Khullar, Al-Shudiefat et al. 2010).

Until now, consistently verified prevention or treatment strategies for diabetic cardiomyopathy have not been described. The therapy of diabetic cardiomyopathy is basically focused on glucose control, including 1) physical training; 2) blood pressure management, such as angiotensin-converting enzyme (ACE) inhibitors; 3) blood glucose management, such as insulin-sensitizing agents; and 4) lipid management, such as statins (Nunes, Rolo et al. 2017).

In summary, diabetic cardiomyopathy is a remarkable mortality factor for patients with diabetes. The mechanism involved in the progression of pathogenesis is multifactorial. However, consistently accepted pharmacological options are still lacking in the clinical practice. Therefore, new drugs with positive therapeutic potential will greatly help to fill the research gap in this aspect and contribute to the pharmacological development of diabetic patients with risk of cardiomyopathy.

1.2.2 Diabetes-induced Vascular Burdens

Diabetics are more vulnerable to the formation of atherosclerotic plaques, thrombosis, and develop coronary artery disease (CAD) and atherosclerosis (AS) than non-diabetics (Atlas 2015). Many studies suggested that ED is the primary factor that initiates the progression of an early CVD event (Avogaro, Fadini et al. 2006). There are many proposed mechanisms to explain the pathogenesis of ED in DM, including 1) oxidative stress, 2) a defective Akt/eNOS signaling pathway; and 3) impaired vascular endothelial growth factor response.

1.2.2.1 Oxidative Stress

Oxidative stress (OS) could be triggered by hyperglycemia via increased production of reactive oxygen species (ROS), including free radicals such as superoxide ($O\cdot_2$-) and hydroxyl ($OH\cdot$), as well as reactive nitrogen species (RNS). Others OS markers, such as lipid peroxidation, protein oxidation, and a decreased antioxidant capacity have also been found in the diabetic model (Comin, Gazarini et al. 2010). Additionally, a significant intracellular antioxidant, glutathione (GSH), has also been proven to be decreased in diabetic rats, together with superoxide dismutase, another important antioxidant enzyme. Together, these pathological changes ultimately lead to an impaired antioxidant defense (Kuhad and Chopra 2008).

Moreover, hyperglycemia increases the generation of another substance, advanced glycated end products (AGEs). The cell surface RAGE can subsequently lead to the production of intracellular ROS (Wright, ScismBacon et al. 2006). Additionally,

hyperglycemia can lead to a reduction of nicotinamide adenine dinucleotide phosphate (NADPH) oxidases by activating the diacylglycerol (DAG) protein kinase C (PKC) pathway, which will lead to the subsequent flux of ROS production (Gupte, Labinskyy et al. 2010).

Another significant source of OS is uncoupled eNOS. Normally, eNOS is responsible for the generation of NO with the presence of an essential cofactor, tetrahydrobiopterin (BH4). Meanwhile, eNOS also participates in the reduction of oxygen (O_2) to superoxide anion ($O_2^{-\cdot}$) (Vásquez-Vivar, Kalyanaraman et al. 1998). However, BH4 could be easily oxidized due to excessive superoxide anion that generated in triggered OS. Subsequently, the diminished BH4 bioavailability could lead to eNOS uncoupling, which further aggravate OS. Therefore, some studies with animal model and human diabetic subjects have demonstrated this mechanism and suggested that additive supply of BH4 could upregulate NO production and thus improve endothelial function (Pieper 1997; Alp, Mussa et al. 2003).

As mentioned in Section 1.1.2, NO is an endothelium-derived relaxing factor. In normal physiological condition, there is a balance between NO and $O_2^{-\cdot}$, within which NO could be reacted with $O_2^{-\cdot}$ at an extremely rapid rate within cells in the extracellular space. Homeostasis of the endogenous antioxidant defense system has been proposed to diminish this intercommunication and preserve the redox stability. However, under certain disease conditions, such as DM, increased generation of ROS could lead to the degradation of NO and thus damage the endothelial-dependent vasorelaxation(Cai and Harrison 2000).

1.2.2.2 AKT/eNOS Signaling Pathway

Insulin has been suggested to promote eNOS production. Previous studies have suggested that the combination of insulin and receptor in EC can result in an insulin receptor substrate-1 (IRS-1) phosphorylation, which is followed by enhancement of eNOS *via* the PI3 kinase/Akt expression level (Zeng, Nystrom et al. 2000). Also, NO production induced by insulin can be blocked by the inhibitor of PI3 kinase/Akt (Muniyappa, Montagnani et al. 2007; Tousoulis, Kampoli et al. 2012). On the other hand, in mice with a mutation in the insulin receptor gene, eNOS expression and endothelial function were reduced (Duncan, Crossey et al. 2008). Also, diabetic rats with insulin resistance have been shown to have a less active PI3 kinase/Akt pathway and attenuated NO bioavailability (Jiang, Lin et al. 1999). In this regard, with the presence of insulin resistance in DM, inhibited insulin-mediated activation of eNOS *via* PI3kinase/Akt might play a significant role in the development of CVD in DM.

On the other hand, insulin resistance damages the normal pathway, where insulin activates the PI-3 kinase and Akt signaling. The mitogen-activated protein kinase (MAPK) pathways are over-triggered by a high insulin level, which leads to an imbalance between PI-3 kinase and Akt signaling and causes a disordered insulin function (Van den Oever, Raterman et al. 2010). This has been proposed as a possible mechanism for the reduced NO generation and over-produced endothlin-1. As a vasoconstrictor, endothlin-1 activates the serine phosphorylation of insulin receptor substrate-1 and leads to impaired activity of the PI-3 kinase in vascular smooth muscle cells. Moreover, phosphoinositide-3 (PI-3) kinase is a significant signaling protein involved in the NO stimulation by insulin and phosphorylation of eNOS.

Akt signaling pathway-mediated apoptosis is another possible mechanism for DM-

induced CV burden. A previous study indicated that the PI3K/Akt/NO pathway mediates the protection of EC from apoptosis induced by high glucose (Ho, Lin et al. 2006). After long-time high glucose exposure, Akt signaling was reduced, and apoptosis was observed. However, in the early stage, under high glucose status, the PI3K/Akt/eNOS/NO pathway was upregulated, and the endothelial cells were protected from apoptosis. This protective activity, as well as eNOS expression, was able to be inhibited by PI3K inhibitors (Ho, Lin et al. 2006). All these observations suggest the importance of the Akt/eNOS pathway in insulin signaling-mediated ED in DM (**Figure 1-1**).

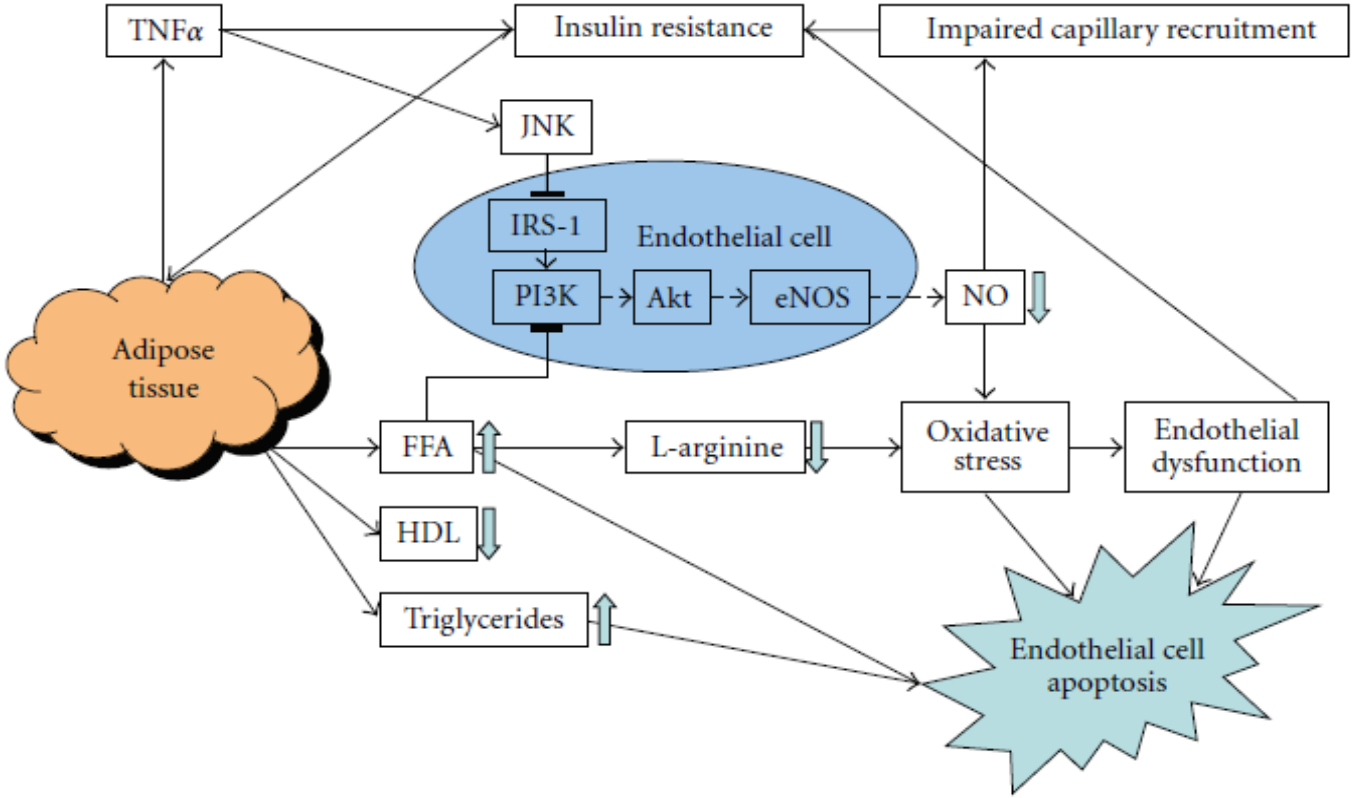

Figure 1-1. The mechanism of insulin resistance and Akt involved in endothelial dysfunction and endothelial cell apoptosis.

NO, nitric oxide; eNOS, endothelial nitric oxide synthesis; HDL, High-density lipoproteins; FFA, free fatty acids; TNF-α, Tumor Necrosis Factor-α (Van den Oever, Raterman et al. 2010).

1.2.2.3 Vascular Endothelial Growth Factor

The vascular endothelial growth factor (VEGF) is responsible for regulating virtually all fields of endothelial and vascular function, including migration, permeability, proliferation, anti-apoptotic, and the production of NO. Therefore, inhibition of VEGF will be associated with ED. In diabetics, monocyte function was shown to be impaired (Ferrara, Gerber et al. 2003). As the monocytes expression can functionally active VEGFR-1 (VEGF receptor 1) on their surface, there is diminished VEGF-related signal transduction in monocytes isolated from diabetic individuals. Such an impaired VEGR response will be regarded as a reduced chemotactic response and VEGF resistance, which is based on a series of pre-activation of intracellular pathways including ROS (reactive oxygen species) activation, DM-related RAGE activation, and inhibition of PTPs (protein tyrosine phosphatases) (Tchaikovski, Olieslagers et al. 2009; Waltenberger 2009) (**Figure 1-2**).

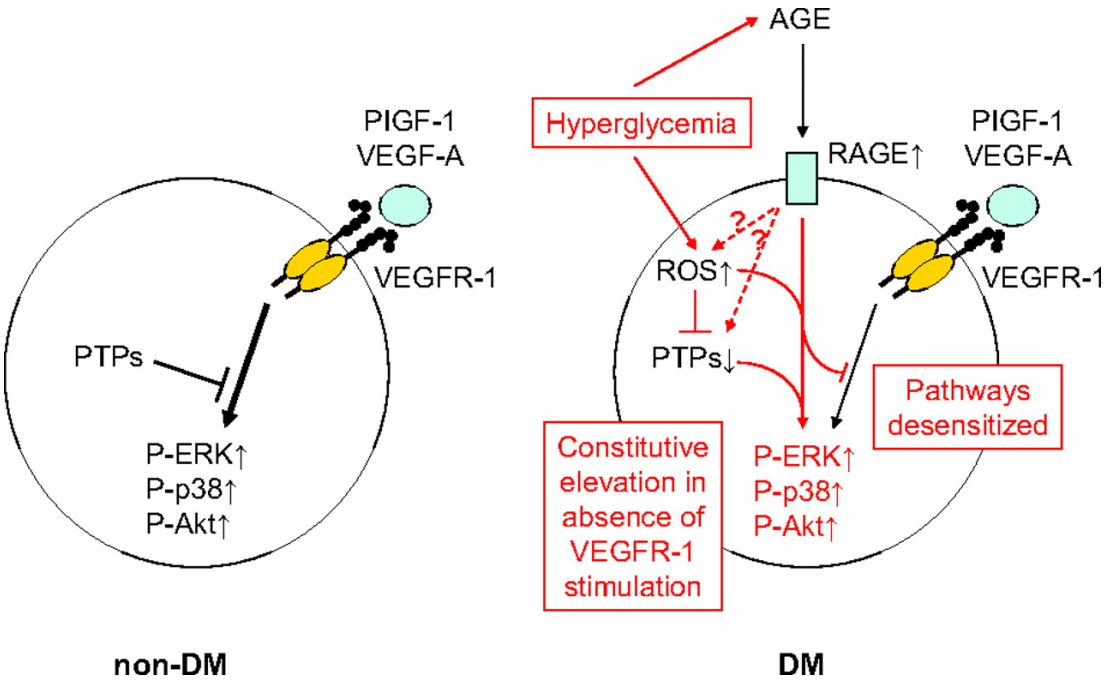

Figure 1-2. The mechanism underlying VEGF-related cellular dysfunction (Tchaikovski, Olieslagers et al. 2009).

Normally, VEGFR-1 participates in monocyte migration mediated by PTPs via signaling pathways, such as the ERK, p38, and AKT pathways. Compared to non-DM, hyperglycemia occurred in DM is associated with increased RAGE and ROS levels. On the one hand, activated RAGE expression leads to altered critical signaling and causes an impaired cellular response to VEGF via VEGFR-1. On the other hand, increased ROS induces activation of kinases via diminished PTPs level. The impaired VEGF response indicates a cellular dysfunction involved in endothelial cell proliferation, migration, and accelerated atherogenesis.

1.3 Homocysteine-induced CV Burdens

Homocysteine (**Figure 1-3**), a homolog α-amino acid of cysteine, is a byproduct formulated during the metabolism of methionine. The normal Hcy level in healthy individuals is 5–15 μmol/L. Hcy at 15–30 μmol/L is considered mildly elevated, 30–60 μmol/L considered moderately elevated, and higher than 60 μmol/L is considered severely elevated (Moll and Varga 2015). The common causes of elevated Hcy level are the deficient uptake of folic acid, vitamin B6, and vitamin B12, as well as metabolic diseases, such as DM, obesity, and chronic renal disease (Moll and Varga 2015).

Hcy has been recognized as an independent CVD risk factor and predictor because of the strong correlation between elevated Hcy level and cardiovascular mortality (McCully 1969; Collaboration 2002). Clinical studies have detected significantly elevated Hcy levels in patients with DM compared to subjects without DM, which is due to a folate and vitamin B12 absorption disorder (Bauman, Shaw et al. 2000; Sahin, Tutuncu et al. 2007; Wile and Toth 2010). Such disorder in DM brings extra risk of CVD and diabetic vascular complications, such as diabetic nephropathy and diabetic foot (Ebesunun and Obajobi 2012; Huang, Asimi et al. 2012; Shaikh, Devrajani et al. 2012). Also, there is a stronger correlation between Hcy level and CVD in diabetic patients than in those without diabetes (Chico, Perez et al. 1998; Emoto, Kanda et al. 2001; Soinio, Marniemi et al. 2004). Consistently, some studies also found that elevated Hcy level has a stronger predictive power than classical CVD risk factors, such as blood pressure, smoking, and electrocardiogram findings (De Ruijter, Westendorp et al. 2009).

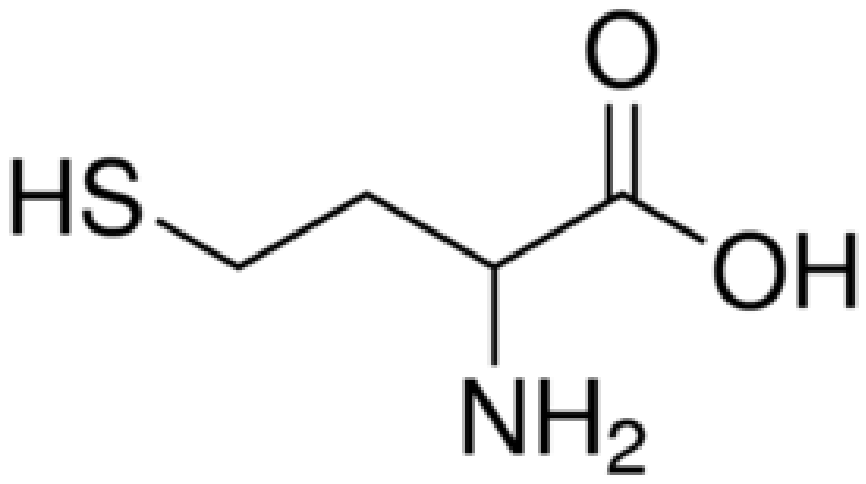

Figure 1-3. The molecular structure of homocysteine.

An elevated Hcy level has been recognized as an independent risk factor for atherosclerosis, which is a significant pathological step leading to myocardial infarction and heart failure (Brazzelli, Grasso et al. 2010). Other than causing heart problem, both *in vivo* and *in vitro* studies have indicated that an elevated Hcy level significantly damages vascular endothelial function via OS triggered by the highly reactive sulfhydryl (-SH) group, reduction of NO production, inflammation, and apoptosis, which are discussed in detail below (Cheng, Yang et al. 2009; Kim, Kim et al. 2011; Lai and Kan 2015). Hcy-induced CVD could be considered a result of altered activities of significant enzymes involved in regulating homocysteine metabolism [e.g., cystathionine b-synthase (CBS) and 5,10-methylenetetrahydrofolate reductase (MTHFR)] (Fonseca, Dicker-Brown et al. 2000).

Homocysteine is metabolized via two main pathways: the remethylation pathway and the trans-sulphuration pathway. The main Hcy metabolism pathways and their relationship with polyphenols (such as Salvianic Acid A) are summarized in the following scheme (Cao, Chai et al. 2009) (**Figure 1-4**).

A: Remethylation pathway

Methionine is given an adenosine group from adenosine triphosphate (ATP) and formulates *S*-adenosyl methionine (SAM), which is catalyzed by S-adenosyl-methionine synthetase. SAM is the source of methyl groups to all methylation reactions in the cell (such as DNA methylation). After this methyl transfer reaction, S-adenosylhomocysteine (SAH) is formulated and is then hydrolyzed by SAH hydrolase and regenerates adenosine and Hcy. In one of the subsequent reactions, Hcy is

remethylated to methionine, catalyzed by methionine synthase (MS) and requiring the cofactors 5-methyltetrahydrofolate and vitamin B12. As part of this process, tetrahydrofolate is converted to 5,10-Methyltetrahydrofolate in a reaction catalyzed by serine hydroxymethyltransferase (SHMT). Then, 5-methyltetrahydrofolate is generated from the reduction of 5,10-Methyltetrahydrofolate by 5,10-methylenetetrahydrofolate reductase (MTHFR). Whereas, in the liver and kidney, Hcy metabolism in the remethylation pathway is catalyzed by betaine homocysteine methyltransferase (BHMT) (Kang 2011).

B: Trans-sulphuration pathway

In this pathway, Hcy is first reacted to cystathionine by cystathionine b-synthase (CBS) and subsequently to cysteine catalyzed by cystathionine g-synthase (CGS), where vitamin B6 (pyridoxine) is an essential cofactor. During these steps, cysteine might be converted to sulfate and excreted in the urine (Finkelstein 1998). However, in the liver, kidney, small intestine, and pancreas, where the entire trans-sulphuration pathway could be present and the cysteine synthesis could serve as a significant endogenous GSH resource (Martinov, Vitvitsky et al. 2000), this Hcy-dependent trans-sulphuration pathway has been implicated in the maintenance of intracellular GSH levels and redox status (Vitvitsky, Mosharov et al. 2003).

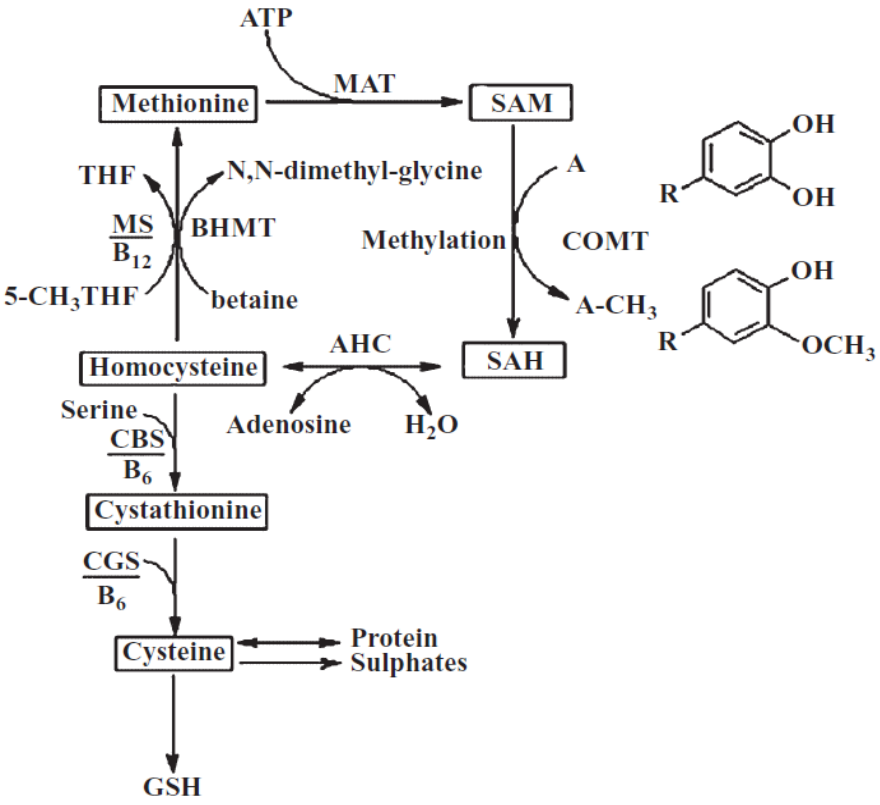

Figure 1-4. Two pathways of homocysteine metabolism involving polyphenol methylation (Cao, Chai et al. 2009)

The metabolism of Hcy was expressed in this figure, in which the R refers to the -CH2CHOHCOOH group; A represents a methylation substrate; A-CH3 refers to a methylated substrate; AHC, AdoHcyase; BHMT, betaine homocysteine methyltransferase; CBS, cystathionine b-synthase; CGS, cystathionine g-synthase; COMT, catechol-O-methyltransferase; MAT, methionine adenosyltransferase; SAM, S-adenosylmethionine; SAH, S-adenosylhomocysteine; and MS, methionine synthase.

Hcy also plays a significant role in the progression of heart disease. A clinical survey indicated that plasma Hcy level mediates morphological and functional cardiac performance (Sundström, Sullivan et al. 2004). In a study with individuals examined by cardiac magnetic resonance imaging, an elevated Hcy level has been reported to correlate with left ventricular dilatation and hypertrophy in cardiomyopathy (Alter, Rupp et al. 2010). Another study found that an elevated Hcy level is correlated with an impaired left ventricular systolic function (Nasir, Tsai et al. 2007). Moreover, the diastolic function of the left ventricle in individuals with elevated an Hcy level was significantly worse than the subjects with a normal Hcy level (Ruhui, Jinfa et al. 2015). Finally, as a mortal result of cardiomyopathy, heart failure could be predicted by the plasma Hcy levels in patients, with or without myocardial infarction (Washio, Nomoto et al. 2011).

How does Hcy affect heart function? A clinical survey has suggested that the involved mechanism could be increased OS in muscle fiber slippage in the heart (Alter, Rupp et al. 2010). In another study, elevated Hcy level and hyperglycemia could induce diabetic cardiomyopathy via activating OS and diminishing peroxisome proliferator-activated receptor gamma (PPARγ), by which endogenous homocysteine triggers endothelial-myocyte uncoupling, leading to diastolic dysfunction (Mishra, Tyagi et al. 2010).

In an animal experiment, myocyte hypertrophy and interstitial fibrosis were detected in rats with an elevated Hcy level induced by methionine administration (Raaf, Noll et al. 2011). On the other hand, transgenic mice carrying a Hcy-lowering gene exhibit an improved infarct healing, ventricular remodeling, and diastolic function (Muthuramu, Jacobs et al. 2013). Further study found that the Hcy-lowering gene significantly

improved the survival rate after receiving transverse aortic constriction, in which the cardiac hypertrophy, interstitial fibrosis, and diastolic function were all positively improved. On the other hand, OS-induced harm and myocytes apoptosis were inhibited compared to the mice without the gene modification (Muthuramu, Singh et al. 2015).

In conclusion, elevated Hcy levels could induce cardiac hypertrophy and diminish diastolic function, in which the involved mechanism could be activated OS, such as auto-oxidation, increased ROS generation, promoted inducible NO synthase, inhibited nitric oxide synthase, activated NADPH-oxidase 2 and NADPH-oxidase 4, and promoted p38 mitogen-activated protein kinase (Sorescu and Griendling 2002; Ungvari, Csiszar et al. 2003; Suematsu, Ojaimi et al. 2007; Wang, Cui et al. 2012). Although there are ever more retrospective and prospective studies focusing on the correlation between Hcy and CVD, the main mechanism of the Hcy-correlated CVD risk remains to be identified, and an effective therapeutic strategy is still poorly defined. Conventional therapies, such as a supplement of folic acid, vitamin B6, and vitamin B12, did not exhibit significant protective effects (Narin, Narin et al. 2002; Huang, Chen et al. 2012). Moreover, as a globally used antidiabetic drug, metformin is considered a factor leading to a deficiency of vitamin B12 and a subsequent elevated Hcy level in patients with DM (de Jager, Kooy et al. 2010; Wile and Toth 2010). Therefore, the identification of an effective treatment or drug that could benefit diabetic patients who have or are likely to have an increased risk of elevated Hcy level and CVD is clinically important.

1.4 Homocysteine-induced CV Burdens in Diabetes

Hcy significantly synergistically contributes to the occurrence of heart disease together with other risk factors such as smoking, high blood pressure, obesity, particularly with DM symptoms hyperglycemia and insulin resistance (Fallon, Elwood et al. 2001; Jeremy, Shukla et al. 2002; Fallon, Virtamo et al. 2003; Fonseca, Fink et al. 2003). It was also reported that an increased Hcy level has a stronger correlation with cardiovascular and macrovascular mortality and the prevalence of nephropathy in DM patients than in subjects without DM (Chico, Perez et al. 1998; Hoogeveen, Kostense et al. 1998). There have also been reports of an increased Hcy level in DM patients than healthy subjects (Emoto, Kanda et al. 2001), possibly due to the adverse effect of high insulin level on the activities of key enzymes in homocysteine metabolism, such as cystathionine b-synthase (CBS) and 5,10-methylenetetrahydrofolate reductase (MTHFR) (Fonseca, Dicker-Brown et al. 2000). Also, a related survey found a significantly increased Hcy level in subjects with insulin resistance, and also suggested the fasting insulin level could be an independent determinant of plasma Hcy level (Giltay, Hoogeveen et al. 1998).

Therefore, the insulin level in diabetic patients could be an independent factor inducing the elevated Hcy level by affecting the enzyme activities of the homocysteine metabolism. Even though the exact mechanisms have not been clarified, and the conclusion about the Hcy level in diabetes has not reached a consistent idea, as an independent risk factor, elevated Hcy level in DM could be aggravated and increase the risk of CVD to diabetic patients relative to those without DM.

Moreover, people with hyperhomocysteinemia were reported to suffer from impaired

vasorelaxation capacity (both endothelial-dependent and endothelial-independent), as well as increased arterial stiffness. The possible involved mechanism could be blunted bioavailability and bioactivity of NO caused by auto-oxidation of Hcy molecule and increased production of ROS (Chousos, Perrea et al. 2010; Doupis, Eleftheriadou et al. 2010). These clinical findings suggest the onset of ED in individuals with elevated Hcy level, which initiates the pathogenesis of CVD via oxidative damage on endothelial cells.

In greater detail, the mechanisms involved in the Hcy-induced endothelial damage are summarized as follows (Chapter 1.4.1 to 1.4.4):

1.4.1 Increased Oxidative Stress

There is a sulfhydryl (-SH) group contained in the Hcy molecule, which is supremely easily self-oxidized and reacted with other spare thiols groups, thus producing a superoxide radical. As a result, most of the Hcy molecules in the plasma were found to have an oxidized status, such as a disposition of the homocysteine disulfide dimer or combined disulfides with proteins (Jacobsen 2000; Sipkens, Hahn et al. 2013) (**Figure 1-5**).

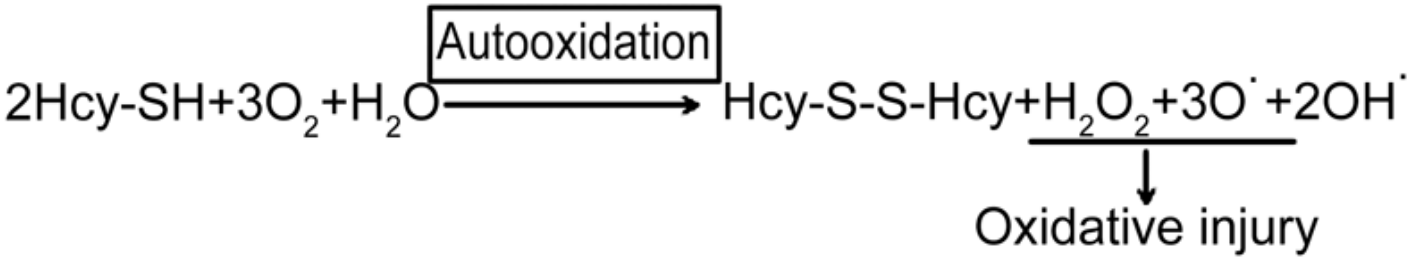

Figure 1-5. The formation of homocysteine autooxidation.

Hcy-SH, free Hcy; Hcy-S-S-Hcy, homocysteine (disulfide); O_2,oxygen; H_2O, water; H_2O_2, hydrogen peroxide; $O^{\cdot}$, singlet oxygen; $OH^{\cdot}$, hydroxyl radical (Yang, Tan et al. 2005).

Secondly, a study on endothelial cells suggested that Hcy could up-regulate the enzyme Nicotinamide adenine dinucleotide phosphate-oxidase (NADPH oxidase) and increase the gene expression of isoforms of NADPH oxidase existed in ECs (NOX2) (Sipkens, Hahn et al. 2013). In contrast, an inhibitor of NADPH oxidase, apocynin, can suppress the generation of ROS induced by Hcy in human umbilical vein endothelial cells (HUVEC) (de Dios, Sobey et al. 2010). These findings suggest that the NADPH oxidase plays a significant role in Hcy-induced OS and subsequent ED and contributes to the OX by superoxide generation via this reaction:

$$\mathbf{NADPH + 2O_2 \leftrightarrow NADP^+ + 2O_2^- + H^+}$$

Thirdly, as mentioned before, the normal NO transformed from eNOS requires L-arginine as a cofactor. Commonly, L-arginine uptake in ECs is regulated by the system y+ cationic amino acid transporter (CAT). However, research on bovine aortic endothelial cells has shown that long-term incubation with Hcy leads to a reduction of CAT-1 (isoform of CAT) expression and a subsequent decrease in trans-membrane L-arginine transportation, thereby leading to a reduction in NO generation (Jin, Caldwell et al. 2007). Consistently, it has been shown that this impeded L-arginine transport is accompanied by an impaired endothelium-dependent relaxation induced by acetylcholine (Ach) (Topal, Brunet et al. 2004).

Furthermore, the insufficient L-arginine supply will lead to an eNOS uncoupling. Normally, as a heterodimer, eNOS contains two reductase domains “coupled” to two separate oxygenase domains. In the reductase domain, NADPH offer electrons to reduce O_2 with cofactor heme, then generated ferrous-dioxygen complex can further oxidize L-arginine to produce NO in the oxygenase domain (Förstermann and Münzel

2006; Bermudez, Bermudez et al. 2008). With insufficient L-arginine, there is an impairment of oxygenase domains used to produce NO, however, the reductase domain continues to reduce oxygen, which will lead to superoxide production. Consequently, eNOS becomes enzymatically uncoupled (Jin, Caldwell et al. 2007).

Subsequently, superoxide resulting from the uncoupled eNOS and increased NADPH oxidase will still suppress the NO function and generate peroxynitrite as an end-product. Peroxynitrite has been shown to oxidize and consume the tetrahydrobiopterin (BH4), which is the key cofactor of the eNOS oxygenase domain. This starts a vicious circle as the depletion of BH4 can further aggravate eNOS uncoupling and destruction of BH4 due to the oxidation (Milstien and Katusic 1999). Consistently, 80% of BH4 availability is lost in ECs treated with Hcy. In contrast, the increased generation of ROS in ECs could be suppressed by 70% using the eNOS inhibitor L-NAME. In addition, either the peroxynitrite blocker or BH4 donor could reinstate the NO generation in ECs treated with Hcy (Topal, Brunet et al. 2004). The process of eNOS uncoupling is described in **Figure 1-6**.

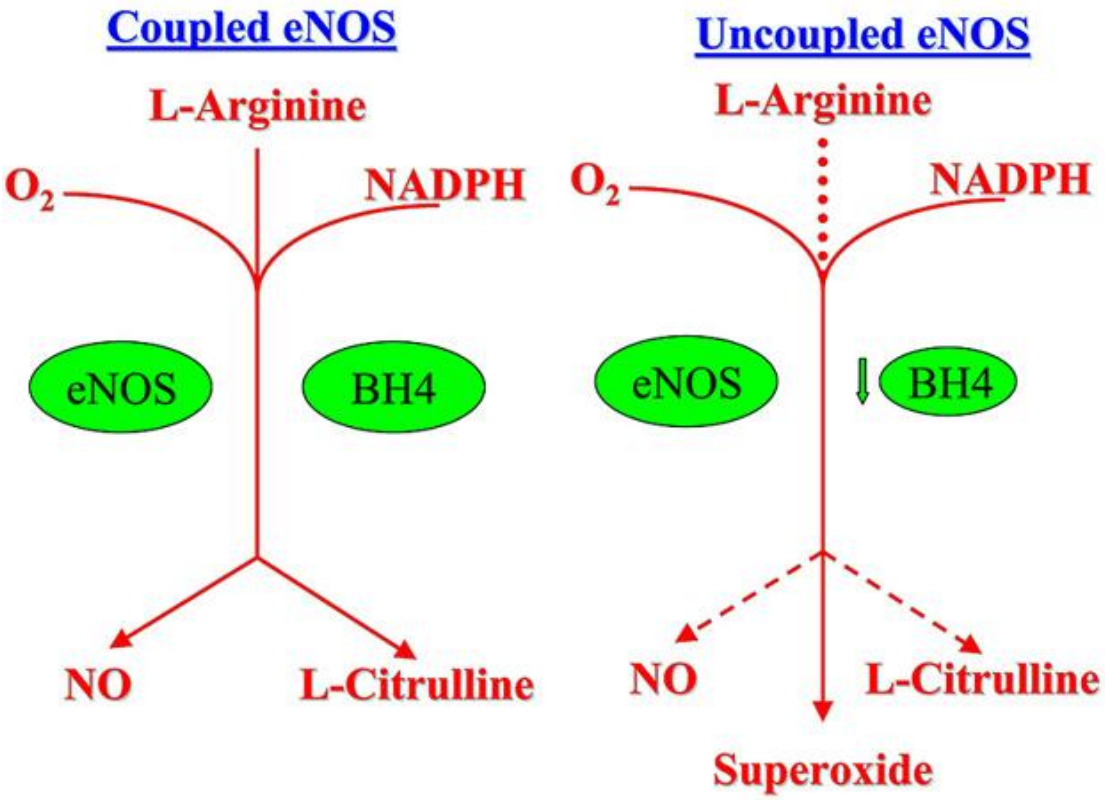

Figure 1-6. The role of coupled and uncoupled eNOS in the increased oxidative stress (Rahangdale, Yeh et al. 2008).

(a) Coupled eNOS utilizes O_2, L-Arginine, and NADPH to produce NO and L-Citrulline; (b) eNOS can be uncoupled by BH_4 deficiency to produce superoxide rather than NO, which might further reduce available NO by combining with it to form peroxynitrite. BH4 tetrahydrobiopterin, NO, nitric oxide; eNOS, endothelial nitric oxide synthesis.

Moreover, Hcy could induce a decrease in the activity and expression of a significant intracellular antioxidant enzyme, glutathione peroxidase-1(GPx1). As a result, the endothelium fails to detoxify hydroxyl radicals and allows further oxidative harm, which means that Hcy might aggravate OS by suppressing endogenous antioxidant capacity (Upchurch, Welch et al. 1997; Jacobsen 2000). Moreover, Hcy has also been proven to inhibit superoxide dismutase, which would permit the increasing of oxidized low-density lipoprotein cholesterol and lipid peroxidation, thereby triggering further oxidative damage on the endothelium (Doshi, McDowell et al. 2001).

The NO generated from the cardiac system significantly regulates the normal contraction and dilation of myocytes, as well as the normal heart rate. In diabetic cardiomyopathy, excessive mitochondrial ROS generation, reduced NO bioactivity, and diminished eNOS expression all contribute to the contractile dysfunction of myocardium and result in myocardial collagen deposition and fibrosis. As mentioned in Section 1.2.1, myocardial fibrosis is an elementary pathogenesis in the progression of the diabetic cardiomyopathy. Moreover, insulin resistance leads to decreased L-arginine and NO generation, and Hcy inhibits the formation of arterial NO. As a result of additive risk, the endothelial nitric oxide metabolism is aggravated (Shukla, Thompson et al. 2002).

Generally, the impaired oxidative defense system leads to not only a vascular dysfunction but also the initiation of cardiomyocyte dysfunction and further contributes to the onset of vascular dysfunction and cardiomyopathy.

1.4.2 Inhibited VEGF Expression

VEGF vascular endothelial growth factor (VEGF) plays a significant role in the regulation of vasculogenesis, angiogenesis, and proliferation (Ferrara 2004). As an endothelial survival factor, *in vitro* investigation indicated that VEGF promotes the growth of endothelial cells via a NO-dependent pathway (Papapetropoulos, García-Cardeña et al. 1997). In that study, VEGF induced an elevated NO generation by increasing the expression of cyclic guanosine monophosphate (cGMP), in which PI3K/eNOS signaling was involved. Consistently, VEGF was indicated to upregulate the activity of eNOS and subsequent release of NO by activation of the PI3K/Akt pathway (Dimmeler, Fleming et al. 1999).

Moreover, VEGF also protects endothelial cells from apoptosis via the PI3/AKT pathway and upregulates the expression of antiapoptotic makers, such as Bcl-2 (Alon, Hemo et al. 1995; Fujio and Walsh 1999). Also, in a mouse model, VEGF was shown to prevent apoptotic changes in the vasculature (Gerber, Hillan et al. 1999).

However, expression of VEGF in endothelial cells has been shown to be inhibited by Hcy, as well as by reduced eNOS expression and NO production (Yan, Li et al. 2010).

Taken together, elevated Hcy levels induce ED by inhibition of VEGF via PI3K/Akt/eNOS signaling, thereby initiating CVD.

1.4.3 Apoptosis

Hcy has also been shown to induce endothelial cell apoptosis. In some studies, Hcy was found to regulate significant genes participating in the progression of cell death in endothelial cells (Hossain, van Thienen et al. 2003). Newly synthesized proteins

normally receive post-translational modifications and are folded into correct conformation in endoplasmic reticulum (ER). Two types of proteins are responsible for the former process, foldase, which regulates the progression of catalyzation of protein folding, and a chaperone, which acts as a protector to withdraw the unexpected intercommunication of unfolded protein domains and neighboring proteins. The accumulation of aggregated and unfolded proteins can lead to ER stress and a cascade of a signaling pathway, which is called Unfolded Protein Response (UPR) (Schröder and Kaufman 2005).

Hcy stimulates ER stress by increasing the UPR molecules in ECs and induces apoptosis mediated by the UPR effector pathway [Inositol-requiring enzyme 1 (IRE1) and RNA activated protein kinase-like ER kinase (PERK)]. At least two apoptotic pathways are involved in this process, overexpression of CHOP/GADD153 (growth arrest- and DNA-damage inducible gene 153) and TDAG51 (T-cell death-associated gene 51). Both of these genes are homocysteine specific and cannot be induced by other similar sulfhydryl amino acids, such as methionine, cysteine or homocysteine (the disulfide dimer form of homocysteine) (Zhang, Cai et al. 2001; Hossain, van Thienen et al. 2003).

1.4.4 Impaired Vasodilatation

As a result of the interfered normal function of the endothelium induced by Hcy, impaired endothelium-dependent vasodilatation capacity has been detected in humans. This process is mediated by the upregulation of asymmetric dimethylarginine (ADMA), which acts as a blocker of eNOS.

ADMA is generated during post-translational protein modification of L-arginine into

proteins, which is methylated by the enzyme protein-arginine methyltransferase (PRMT). Because of its similar chemical structure to L-arginine, ADMA might work as an endogenous competitive inhibitor for eNOS. As evidence for this, a previous study has shown that ADMA is available to reduce the elaboration of endothelial nitrogen oxide species, which could be reversed by administration of L-arginine. Therefore, ADMA has long been recognized as a risk predictor of CVD. Typically, ADMA can be scavenged through metabolism mediated by dimethylarginine dimethylaminohydrolase (DDAH). Now, multiple studies have shown that Hcy can increase the ADMA elaboration, which is associated with impaired endothelial DDAH activity by depleting a significant sulfhydryl group of DDAH. It has been suggested that Hcy could impair NO production by reducing DDAH activity and increasing AMDA accumulation, thus reducing NO elaboration by endothelial cells and aortic segments (Stühlinger, Tsao et al. 2001). The principal relationship between Hcy and ED is shown in **Figure 1-7**.

Impaired vasodilatation contributes to the onset of diabetic cardiomyopathy by impairing endocardial endothelium modulated cardiac function via $CaCl_2$ and the acetylcholine channel. On the other hand, the myocardial contractile response to endothlin-1 is also diminished in the presence of Hcy (Tyagi, Smiley et al. 1999). As a result, the myocardial endothelium dysfunction leads to a disordered cardiac function and a further injured cardiac output outcome, which is correlated with left ventricular dysfunction.

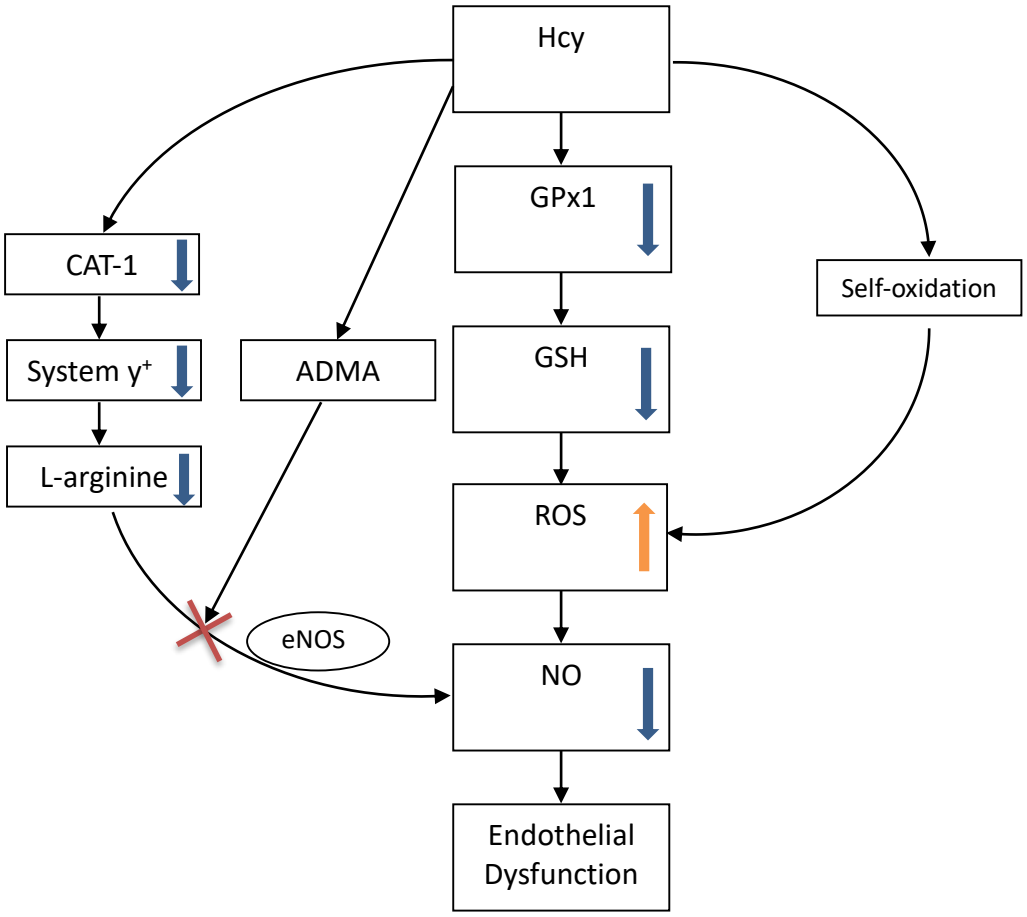

Figure 1-7. Simplified diagram description of the relationship between elevated homocysteine level and the onset of endothelial dysfunction.

Hcy, homocysteine; GPx1, glutathione peroxidase 1; GSH, glutathione; ROS, reactive oxidative species; NO, nitric oxide; ADMA, asymmetric dimethylarginine; CAT-1, cationic amino acid transporter 1.

1.5 Salvianic Acid A

According to the American Heart Association (AHA), smoking, obesity, hypertension, hypercholesterolemia, and no leisure-time, physical activity or exercise are the key risk factors of CVD in diabetic patients (Buse, Ginsberg et al. 2007; Kurian and Cardarelli 2007). Not for the first time, a statement from the AHA and the American Diabetes Association suggested that diagnosis and management should be based on these comprehensive risk factors and lifestyle management. These treatments and management include:

(1) Bodyweight control

(2) Medical nutrition therapy (dietary cholesterol intake limitation to reduce LDL cholesterol; alcohol intake limitation to reduce the risk of aggravating hypertriglyceridemia; sodium intake limitation to maintain blood pressure)

(3) Physical activity (moderate-intensity aerobic physical activity and vigorous aerobic exercise is recommended to improve glycemic control)

(4) Blood pressure therapy, including ACE inhibitors, angiotensin receptor blocker (ARBs), β-blockers, diuretics, and calcium channel blockers.

(5) Lipids control. Statin therapy should be interacted with lifestyle management because of the contribution of dyslipidemia to CVD risk in diabetic patients. However, pharmacological therapy is advised for patients over 40 years old with high CVD risk or those who have a poor response to lifestyle management or elevated cardiovascular risk. Even though there have also been reports showing a correlation between statin use and elevated incident diabetes risk (LDL cholesterol ≤ 100 mg/dl,

should have a low level of risk for the diabetic patients) (Rajpathak, Kumbhani et al. 2009; Sattar, Preiss et al. 2010)

(6) Tobacco avoiding

(7) Antiplatelet agents (aspirin therapy 75–162 mg/day is advised to be a prevention drug for diabetic patients with hypertension, smoking or dyslipidemia). However, the benefit of aspirin has been challenged by the risks of significant bleeding. Consequently, aspirin is not advised for low CVD risk individuals.

(8) Glycemic control, the A1C level should be kept at ＜7%. The recommendations are the same for type 1 and type 2 diabetes (Buse, Ginsberg et al. 2007).

Until now, there is no official guideline or statement available to describe the Hcy level management in the CVD risk prevention strategy, especially for the patients with DM, nor consistently confirmed effective treatments targeting Hcy-induced CVD burden. Therefore, the identification of a new drug that could ameliorate CVD risk imposed by elevated Hcy level in DM is a significant and meaningful research topic.

Danshen, a typical traditional Chinese medicine (TCM), is the dried root of *Salvia Miltiorrhiza*, which has long been used in the treatment of CVD (Cheng 2006). The earliest use of *Danshen* was first recorded in the book "*Shen Nong's Herbal Classic*" (First Century B.C - First century A.D. Eastern Han dynasty). According to the TCM theory, it can remove blood stasis. There are over 35 different formulations and concoctions containing *S. Miltiorrhiza* as the principal or assistant drug and indexed in the Pharmacopoeia of the People's Republic of China (Commission 2010). Both *in vitro* and *in vivo* studies have shown that the active ingredients in *Danshen* can improve

blood circulation, induce vasodilation of coronary artery and inhibit platelet aggregation (Lei and Chiou 1986; Lam, Yeung et al. 2005). During recent decades, TCM has attracted researchers' attention in the treatment of diabetic complications, particularly chronic diabetic cardiovascular disease. Despite these previous studies about the protective properties of *Danshen* on the vasculature, its protective effect on CVD in diabetes, specifically on the ED in diabetic status, has not been well explored. Findings of research addressing this point might affect treatment strategies for diabetic cardiovascular disease and might benefit diabetic CVD patients with a possible mechanism involving ameliorating the endothelial dysfunction. If this effect and its mechanism could be clearly identified, there would be more patients with CVD benefiting from *Danshen* and its active ingredients.

Many active compounds can be extracted from the *S. Miltiorrhiza.* Two major categories of chemically active ingredients isolated from *S. Miltiorrhiza* root have been identified: the water-soluble compounds and the lipophilic diterpenoid quinines (Han, Fan et al. 2008; Jia, Yang et al. 2012; Wang, Xiong et al. 2013). The main extracted ingredients of the water-soluble compounds include:

(1) protocatechuic aldehyde

(2) protocatechuic acid

(3) caffeic acid

(4) salvianic acid A (3, 4-dihydroxyphenyl lactic acid; also named as Danshensu)

(5) salvianolic acid A

(6) salvianolic acid B

In the water-soluble component, the major ingredient is salvianic acid A (SAA). The chemical name for SAA is 3-(3,4-dihydroxyphenyl)-2-hydroxypropanoic acid and its chemical structure is shown in **Figure 1-8**.

On the other hand, the main extracted ingredients of the lipophilic diterpenoid quinines include (Han, Fan et al. 2008; Yin, Guan et al. 2013; Bonaccini, Karioti et al. 2015):

(1) tanshinone I

(2) tanshinone IIATsIIB

(3) tanshinone IIB

(4) cryptotanshinone

(5) tanshindiol C

(6) 15, 16-dihydrotanshinone I

(7) isotanshinone I

(8) isotanshinone II

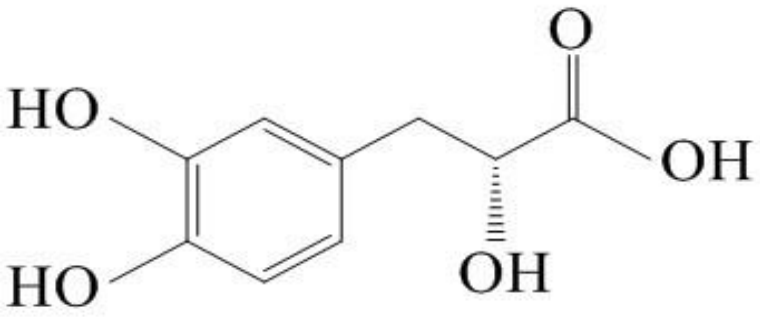

Figure 1-8. The chemical structure of Salvianic Acid A, $C_9H_{10}O_5$.

Conventionally, SAA has been known to have a therapeutic effect on vascular diseases, such as myocardium ischemia, venular thrombosis, and microvascular disturbance (Cheng 2007; Han, Horie et al. 2009; Wang, Liu et al. 2009; Yin, Guan et al. 2013). SAA has been shown to be a powerful and potential drug with multiple beneficial effects. Therefore, in this review, I will summarize the known properties of SAA in the treatment of various diseases, and discuss the potential value of SAA.

1.5.1 Physical and Chemical Properties of SAA

Salvia Miltiorrhiza (*Danshen*) is a well-known TCM and has been applied in the treatment of CVD due to its outstanding promotive effect on blood circulation (Guo 1992; Commission 2010). Drugs consisting of ingredients derived from *Danshen* have also been applied in clinics in Asia and European countries (Zhao, Xiang et al. 2006).

Among the water-soluble components extracted from *Danshen*, the major phenolic acid, salvianic acid A (SAA), also called *Danshen*su, is regarded as the most significant active ingredient for treating CVD due to its antioxidant property (Zhou, Chan et al. 2012). The chemical synonym, chemical, and physical properties of SAA are shown in **Tables 1-2 and 1-3**.

Table 1-2. Chemical synonyms of SAA.

1	3-(3,4-dihydroxyphenyl)-2-hydroxypropanoic acid
2	3,4-dihydroxyphenyllactic acid
3	3,4-dihydroxyphenyllactic acid, (+-)-isomer
4	3,4-dihydroxyphenyllactic acid, (R)-isomer
5	3,4-dihydroxyphenyllactic acid, monosodium salt
6	3,4-dihydroxyphenyllactic acid, monosodium salt, (+-)-isomer
7	3,4-dihydroxyphenyllactic acid, monosodium salt, (R)-isomer
8	Danshensu
9	salvianic acid A sodium

Source Name: MeSH, Source ID: 67035055, Record Name: 3,4-dihydroxyphenyllactic acid, URL: http://www.ncbi.nlm.nih.gov/mesh/67035055

Table 1-3. Chemical and physical properties of SAA.

Item	Value	Source
Water Solubility	6.7 mg/mL	(ALOGPS) http://www.vcclab.org/lab/alogps/
Refractivity	47.42 $m3 \cdot mol^{-1}$	(ChemAxon) http://www.chemaxon.com/products/calculator-plugins/property-calculations/#refractivity
Molecular Weight	198.1727 g/mol	
Molecular Formula	C9H10O5	Source Name: PubChem Source ID: PubChem URL: http://pubchem.ncbi.nlm.nih.gov Description: Data deposited in or computed by PubChem

(URL: http://www.hmdb.ca/metabolites/HMDB03503)

Traditionally, people have extracted useful compounds from *Danshen* herbs using a heat reflux water extraction (HRWE) method. Studies using various extraction methods have verified that more SAA can be extracted from the crude herb using a microwave-assisted extraction with water (WAE-W) method. After three rounds of 2-h heating in a microwave oven at 300W (100℃, 1.01KPa), a relative high yield of SAA (14.20 ± 0.40 mg) could be extracted from 1 g of herb power with MAE, which is almost double the yield obtained using HRWE (Zhou, Chan et al. 2012). It was also found that a greater yield of SAA could be extracted from the herb using a relatively longer hearting time.

The major drugs contain SAA as a main component include Danhong injection (Guan, Yin et al. 2013; Wang, Fan et al. 2013), Xuebijinginjection (Jiang, Zhou et al. 2013), Danshen injection (Guan, Ma et al. 2013), and Danshen Dripping Pills (CDDP) (Ding 2002).

1.5.2 The Known Pharmacological Properties of SAA

1.5.2.1 Antioxidant Effect

In humans, OS can be triggered by excessive accumulation of ROS, such as superoxide anion radical, hydrogen peroxide, and hydroxyl radical. Because of the positive role in blocking OS and defending chronic disease threatening, people started to realize the importance of natural antioxidant substances (Nordberg and Arner 2001; Willcox, Ash et al. 2004). Recently, more and more interest has been focused on antioxidant compounds from natural sources.

As an abundant phenolic acid ingredient extracted from *Danshen* herb, a previous

study has indicated that SAA could be considered as a potential natural antioxidant product. Lipid peroxidation could be initiated by the hydroxyl radical and induce harm to tissue. Moreover, mitochondria are considered the most significant intracellular supplier of ROS. This study tested the effects of SAA on inhibition of lipid peroxidation of the mitochondrial membrane and found that SAA could scavenge lipid free radicals and can protect liver mitochondrial membranes against lipid peroxidation (Wang, Wang et al. 2005). In further experiments involving *in vitro* measurement of hydroxyl free radical (HO.), superoxide anion radical (O2.-), 1,1-diphenyl-2-picryl-hydrazyl (DPPH) radicals, and 2-azino-bis (3-ethylbenzthiazoline-6-sulfonic acid) (ABTS) radicals scavenging activities, SAA exhibits stronger radical scavenging activities than vitamin C (Zhao, Zhang et al. 2008), suggesting an outstanding free radicals scavenging property of SAA. Compared with vitamin C, we found that SAA has a relatively lower efficiency in hydrogen peroxide (H_2O_2) scavenging capacity and iron chelating.

Previous findings suggested that ingredients containing functional groups such as –OH, –SH, –COOH, –NR2, –S–, and –O– are likely to have chelation activity whenever there is a suitable geometrical connection within them (Fennema and Tannenbaum 1996). Nevertheless, huge numbers of flavonoids characterized by phenolic compounds do not chelate copper ions *in vitro* (Miranda, Stevens et al. 2000). This might be because of the structured variety of phenols associating with the iron chelating. Thus, the property of protecting the cell from damage by lipid peroxidation is achieved mainly throughout the property of scavenging free radical, rather than iron chelating or scavenging hydrogen peroxide. It has been noted that, by multiple linear regression analysis in a DPPH assay and ferric reducing/antioxidant potential (FRAP) assay, the concentration of SAA is correlated with the antioxidant capacity of *Danshen*

water-extract (Zhou, Chan et al. 2012). Moreover, in the above-cited *in vitro* study, no significant toxicity was detected.

Taken together, SAA possesses a profound anti-oxidant property, including anti-lipoperoxidant and free radical scavenging activity, without generating significant toxic products. The antioxidant property of SAA is stronger than vitamin C. This function is possibly due to the hydroxyl groups and a carboxyl group in its molecular structure, however, with a weak iron chelating activity. Thus, SAA has been identified and a positive nature antioxidant with a potential food application. However, there is also a limitation. Because of its phenolic hydroxyl groups, SAA becomes unstable and easily self-oxidized. Therefore, some structural modifications needed to stabilize the compound, which will be discussed later in the thesis.

1.5.2.2 Vasorelaxant Effect

An early study demonstrated that SAA shows a bidirectional effect on particular vessels, such as renal, femoral, and mesenteric arteries, indicating a contraction or dilation effect at different concentrations (Lei and Chiou 1986). For example, at a low concentration (10-30 μg/ml), *Danshen* increases vasoconstriction induced by the phenylephrine rat femoral artery, however, at a high concentration (>100 μg/ml), the vasodilation effect was elicited (Lam, Yeung et al. 2005).

Similarly, a recent study using isolated vessels fragments also verified that, at a low concentration (0.59–59 μg/ml), SAA magnifies the vascular contraction induced by phenylephrine on the mesenteric artery (Li, Yang et al. 2015). Whereas, at a higher

concentration, SAA showed a concentration-dependent relaxation effect on rat coronary arteries (20–350 μg/ml)(Lam, Yeung et al. 2007).

However, in *in vivo* studies, *Danshen* or its major active ingredients act as a vasodilator and cause hypotension. Therefore, the vasodilator is generally considered as having a dominant role in the systemic circulation (Lei and Chiou 1986; Li, Yung et al. 1990).

In terms of the mechanisms of dilatory action of SAA, the inhibition of Ca^{2+} influx into the vascular smooth muscle cells is involved as a major factor, and the opening of K^{+} channels is a minor participant (Lam, Yeung et al. 2007). Moreover, no significant difference was found between vessels with or without endothelium, which indicated this effect could be endothelium-independent (Lam, Yeung et al. 2007; Li, Yang et al. 2015). However, another study revealed that SAA could relax the vessel through the endothelium-dependent mechanism and that this is mediated by prostacyclin (PGI2) rather than the eNOS/NO pathway. Thus, whether the endothelium has a role in SAA-induced vasodilation remains a controversy.

1.5.2.3 Homocysteine-normalizing Effect

Homocysteine (Hcy) is a homologueα-amino acid of cysteine. Hcy is not a part of a normal daily diet. Instead, it is a byproduct formulated during the metabolism of methionine by the deduction of the methyl group. Hcy metabolism can be described as two main pathways, the re-methylation and trans-sulphuration pathways.

Normally, Hcy is in a metabolic balance between generation and consumption. However, if this balance is blocked due to enzymatic defects or vitamin deficiencies,

accumulated Hcy could induce an increase in the Hcy level, which is called hyperhomocysteinemia (HHcy). For reference, normal total plasma Hcy level of adults is 5–15 μM (Ueland, Refsum et al. 1993). A total plasma Hcy level > 15 μM is defined as HHcy and can be classified as moderate (15–30 μM), intermediate (30–100 μM) or severe (> 100 μM) (Kang, Wong et al. 1992).

A high Hcy level has been recognized as an independent risk factor of CVD (Ueland, Refsum et al. 1992; Epstein, Welch et al. 1998; Wald, Law et al. 2002), Alzheimer's disease (Seshadri, Beiser et al. 2002), colon cancer (Kato, Dnistrian et al. 1999), osteoporosis (McLean, Jacques et al. 2004), and thrombotic stroke (Li, Sun et al. 2003). For example, it is reported that every 5 μM increase of the Hcy level could lead to a 20% increase in CHD risk. According to a survey in China, many factors are associated with HHcy, including dietary riboflavin deficiency (Jacques, Bostom et al. 2001), high intake of caffeine (Nygård, Refsum et al. 1997), and a lack physical training.

Notably, diabetics are at greater risk of HHcy than the non-diabetic population. Compared to healthy subjects, a higher Hcy level, as well as a stronger correlation between HHcy and CVD, have been reported in subjects with DM (Chico, Perez et al. 1998; Hoogeveen, Kostense et al. 1998; Emoto, Kanda et al. 2001).

Possible reasons for HHcy in DM could be the effect of insulin on the activities of key enzymes involved in homocysteine metabolism [cystathionine b-synthase (CBS) and 5,10-methylenetetrahydrofolate reductase (MTHFR)] (Fonseca, Dicker-Brown et al. 2000). The related survey also found a significantly increased Hcy level in subjects with insulin resistance, and also suggests that the fasting insulin level could be an independent predictor for plasma Hcy level (Giltay, Hoogeveen et al. 1998).

Paradoxically, as a common DM oral therapeutic drug, metformin could also significantly increase the serum Hcy level. After administration of metformin, a decrease of serum folate and vitamin B12 could be observed due to the malabsorption of vitamin B12 (Bauman, Shaw et al. 2000; Sahin, Tutuncu et al. 2007; Wile and Toth 2010). This might be because the biguanides group affects membrane potentials by offering the membrane surface a positive charge, thereby affecting divalent cation membrane functions. Therefore, calcium-dependent activities, such as vitamin B12 absorption, will be blocked (Bauman, Shaw et al. 2000). As a result, insufficient vitamin B12 would cause elevated Hcy level due to a shortage of essential cofactor that participants in the Hcy metabolism. However, relevant to therapeutic strategy, experimental and clinical data have failed to show positive results from B vitamin supplementation (NARIN, Narin et al. 2002; Huang, Chen et al. 2012). Therefore, the search for an effective treatment is becoming increasingly important.

The first study to investigate the effect of SAA on elevated Hcy level was published in 2009 using a methionine-fed rat experimental model of elevated Hcy level. This study verified that SAA could normalize the Hcy level in the rat model with elevated Hcy level by enhancing the trans-sulphuration pathway and up-regulating the activity of essential trans-sulphuration enzymes (Cao, Chai et al. 2009). As a product of the trans-sulphuration pathway metabolism, glutathione, also a significant antioxidant, is increased. This tends to suggest the potential Hcy-lowering property of SAA, as well as providing a beneficial antioxidant. Notably, SAA has a Hcy-lowing effect only in the elevated Hcy rat model, having no significant effect in normal rats (Cao, Chai et al. 2009; Chen, Cao et al. 2009).

In another *in vitro* study, SAA was shown to have a protective effect on endothelial

cells against the Hcy-induced injury (Chan, Chui et al. 2004). As indicated, the elevated Hcy level could trigger OS by generating excessive extracellular ROS and diminishing NO production due to a decreased NO bioavailability and inhibited expression of eNOS (Weissmann, Winterhalder et al. 2001). SAA might produce its anti-toxic effect against elevated Hcy by scavenging extracellular free radicals (Chan, Chui et al. 2004).

In conclusion, SAA is a potentially beneficial drug in protecting against Hcy-induced oxidative injury. Therefore, SAA would likely contribute to CVD therapy, as well as protecting patients who are susceptible to HHcy, such as DM patients with metformin administration. Before clinic application, further study and clinical trials will be necessary, and any side effects caused by lowering Hcy would need to be investigated. Nevertheless, the Hcy-lowering property of SAA likely has a novel beneficial application that requires further exploration (Yin, Guan et al. 2013).

1.5.2.4 Hepatoprotective Effect

In hepatic fibrosis (HF) rat model induced by carbon tetrachloride (CCl4), SAA administration could ameliorate the elevated aspartate transaminase (AST) level, alanine transaminase (ALT) level, and body weight loss, suggesting that SAA could effectively reverse hepatocellular injury and normalize liver dysfunction. Moreover, CCl4-induced hepatotoxicity led to a reduction of SOD and GSH-Px and increased MDA in liver tissue. Whereas, after SAA treatment, the rats were found to have increased intrahepatic SOD and GSH-Px level, and a decreased MDA concentration. This seems to indicate SAA-mediated hepatoprotection via the improvement of its antioxidant capacity and the reduced cytotoxicity induced by MDA (Qu, Huang et al. 2014).

Collagen deposition [e.g., Hydroxyproline, type III procollagen and hyaluronic acid] in scar tissue is an important marker in hepatofibrosis, and alpha-smooth muscle actin acts as an important indicator of the fibrogenic formation. These parameters could also be normalized by SAA, implying an amelioration of metabolic dysfunction and liver fibrosis mediated by SAA. Similar results for collagenic formation were confirmed in pathological observation on a hepatic cell in HF rats with hematoxylin and eosin staining and Masson's Trichrome staining. Further investigation revealed that SAA could activate the JAK/STAT pathway and elevate the expression of a-SMA, p-JAK2, and p-STAT3 in fibrogenic tissue.

Therefore, SAA might exhibit a hepatoprotective effect, in which the mechanism is correlated with improved antioxidant capacity and the regulation of the intrahepatic JAK/STAT pathway.

1.5.2.5 Anti-neurodegeneration Effect

SAA is generally recognized for its antioxidant and cardioprotective properties. Recently, its effect on the central nervous system has also been reported (Kwon, Kim et al. 2014).

Monoamine oxidase (MAO) is an enzyme regulating the degradation of neurotransmitters, such as serotonin (5-HT) and norepinephrine (NE), which contribute to anxiety disorders (Martin, Sainz-Pardo et al. 2007; Legoabe, Kruger et al. 2011). In an *in vitro* test, SAA could inhibit the activity of MAO-A, one of MAO isoforms in a concentration-dependent manner. In the same study, after oral administration of SAA, an anxiolytic-like effect could be elicited in the elevated plus-maze test and the hole-board test, which are widely used to test anxiolytic drugs. This

effect could be blocked by a D1 receptor antagonist, which suggests that this anxiolytic-like effect is partly elicited by up-regulating the dopaminergic neurotransmitter system via D1 receptor signaling. Up to the end of this study, no obvious side effects were observed, although further confirmation is required. Thus, these findings revealed a protective potential of SAA on the central nervous system and provided an expanded therapy strategy of neural disease.

In a Parkinson's disease (PD) zebrafish model induced by 6-hydroxydopamine, which has been suggested as a commonly used selective catecholaminergic neurotoxin of causing neuronal death and injury (Parng, Roy et al. 2007; Blesa, Phani et al. 2012), SAA could significantly inhibit 6-hydroxydopamine-induced oxidative stress of the immunopositive area of neurons. This neuroprotective effect was carried out by inducing the expression of heme oxygenase-1 (HO-1) via activating the nuclear translocation of NF-E2 p45-related Factor 2 (Nrf2), a signaling protein involved in promoting expression of antioxidant enzymes by binding to the antioxidant-response element (ARE) (Satoh, Okamoto et al. 2006; Calabrese, Cornelius et al. 2010). An *in vivo* mechanism study found that SAA could active Nrf2–ARE binding via PI3K/Akt signaling, subsequently, the cellular defense system was enhanced to protect against the cytotoxicity induced by 6-hydroxydopamine. As well as HO-1, SAA-induced ARE activation could also contribute to activation of other antioxidant enzymes, such as glutamate cysteine ligase and glutamylcysteine synthetase. This could promote the generation of endogenous antioxidants, such as GSH, which is an important intracellular antioxidant, to enhance the intracellular redox status and antioxidative ability (Lewerenz and Maher 2011).

Moreover, it has been shown that SAA can cross the blood-brain barrier (Yu, Wang et

al. 2011). Fifteen minutes after Sprague-Dawley rats were administrated with Danshensu (15 mg/kg, intravenously), SAA could be detected in the brain at a relatively high level. Moreover, the concentration of SAA was found significantly higher in the group pretreated with a P-glycoprotein (P-gp) inhibitor, verapamil, which demonstrates an important role of P-gp inhibition in the effluxion of SAA from the brain. As a result, the authors recommended the use of an SAA plus P-gp inhibitor combination for the treatment of CNS disorders.

In conclusion, SAA seems to activate PI3K/Akt pathways and induce Nrf2 accumulation by transporting it from the cytoplasm to the nucleus and binding to the ARE system, and subsequently promoting antioxidative systems mediated by Nrf2 (Chong, Zhou et al. 2013).

Other effects, such as anti-tumor potential, have also detected by both *in vivo* and *in vitro* tests. In B16F10 melanoma cells, although no significant inhibitory effect on cell growth was detected, SAA inhibits cell invasion, migration, tube formation by down-regulating the expression of MMP-2, MMP-9, and VEGF. Using a tumor-bearing mice model, SAA was found to significantly inhibit metastasis on the lung surface, suggesting that SAA has the potential to be developed as an anti-tumor drug because of its ability to inhibit tumor metastasis and angiogenesis.

1.5.3 SAA-induced Toxicity

The toxicity of SAA was assessed in beagle dogs. After intravenous infusion of 150 mg/kg/day for 90 days (5.58 g/70 kg for adults), no obvious mortalities or systemic

toxicity was observed on organ weights, histopathology or hematological (Li, Gao et al. 2009).

Toxicity tests with Kunming mice indicated that, with the acute intravenous administration of SAA, no obvious toxic symptoms were monitored in mice up to 1835 mg/kg. From a dosage of 2000 mg/kg and higher, adverse effects and increased mortality started to be observed. In a subchronic toxicity test with Sprague-Dawley rats via continuously intraperitoneal injections of SAA at a dosage of 450 mg/kg for 90 days, no obvious adverse effects were detected in terms of the toxicological parameters (Gao, Liu et al. 2009).

Based on the above toxicity studies, SAA was considered pharmacologically safe (Yin, Guan et al. 2013).

1.5.4 Conclusion

In conclusion, SAA has multiple beneficial effects in humans. Mainly, it is severing as a CVD treatment drug or effective component, which is made into the various formulations and applied in clinical practice. With the development of techniques and experimental work, ever more beneficial effects have been explored and developed, thus contributing new drugs based on SAA, which might ultimately benefit individuals with DM and CVD. TCM and its active ingredients provide a huge range of natural medicines for human use.

Many previous studies have indicated the improvement in blood circulation, inhibition, the platelet adhesion and aggregation against OS by suppression of ROS production, the protective effect to myocardium ischemia, and amelioration of endothelial cell

dysfunction (Chan, Chui et al. 2004; Cheng 2007; Han, Horie et al. 2009; Wang, Liu et al. 2009; Yin, Guan et al. 2013). Moreover, an *in vivo* study found that, in a hyper-homocysteinemia model, SAA can significantly decrease the Hcy level by increasing the trans-sulphuration pathway and up-regulating the activity of the correlated trans-sulphuration enzymes (Cao, Chai et al. 2009). The increase in the intermediates of the trans-sulphuration pathway (cysteine and glutathione) has been used as evidence for this conclusion. Thus, this suggests that SAA has the capacity to act as a potential Hcy-lowering drug, which can benefit CVD patients by decreasing Hcy level. Also, as a product of trans-sulphuration pathway, GSH is likely to be increased, which has further beneficial potential against CVD by suppressing OS.

Interestingly, this down-regulation effect of Hcy by SAA only exists in the models with elevated Hcy level, and exhibits no significant changes in the models with normal Hcy level (Chen, Cao et al. 2009). Moreover, no research has reported this effect in a diabetic model. Moreover, no study has investigated whether there is a protective effect of SAA on the Hcy metabolism.

It has been revealed that SAA could significantly cause vasorelaxation by blocking the intracellular Ca^{2+} influx in the VSMC (Lam, Yeung et al. 2007). Nevertheless, whether the vasorelaxant effect of SAA is endothelial-dependent and which pathway (PGI or NO) is involved has not been clearly investigated. An *in vitro* study has suggested that SAA works on endothelial cells specifically by activation of NO production via enhancement of the cyclooxygenase cyclooxygenase (COX)-2 pathway, rather than the PGI pathway (Wang, Fan et al. 2013). However, an *ex vivo* experiment (rat aortic ring model) found that SAA induced direct vasorelaxation in an endothelium-independent manner (Zhang, Zou et al. 2010).

In conclusion, there are limited studies addressing the mechanism of SAA-induced vasorelaxation. The vasculature effect of SAA (either in acute administration or chronic consumption) in diabetes remains unclear, with questions remaining about whether this effect is via an endothelial-dependent or independent mechanism. Therefore, research targeting the vasculature effect of SAA in a diabetic model will help to address these questions.

1.6 Research Questions

Recent studies have demonstrated that SAA can lower elevated Hcy levels and stabilized Hcy levels, mediated by the enhancement of the trans-sulphuration pathway (Cao, Chai et al. ; Chen, Cao et al. 2009). In these previous studies, SAA could significantly lower a high methionine diet-induced elevated Hcy level. These findings suggest that SAA can act as a Hcy-lowering drug. The enhanced production of GSH via the trans-sulphuration pathway also partly explains the cardioprotective effect of SAA, in addition to its being a known antioxidant (Cao, Chai et al. 2009). However, whether SAA treatment has a similar effect on Hcy metabolism in the diabetic condition remains unknown.

An elevated Hcy level contributes to the elevated risk and severity of CVD (Wang and Jin 2017), and SAA can normalize the Hcy level in an animal model without DM (Chen, Cao et al. 2009; Yang, Huang et al. 2010). Therefore, can SAA benefit diabetic mice with elevated Hcy level? Will the Hcy-normalizing effect of SAA still be mediated by the enhancement of trans-sulphuration pathway? Can SAA ameliorate the ED induced by Hcy or other pathological factors accompanied by DM? The answers to these questions will be revealed in chapter 2 to 5 of this study.

Chapter 2 Effect of SAA on Cardiomyopathy in Diabetes with Elevated Homocysteine Level

2.1 Introduction

CVD contributes up to 65% of total deaths of diabetics, in which diabetic cardiomyopathy is a significant mortality factor for heart failure as a final event (Tuomilehto and Lindström 2003).

Diabetic cardiomyopathy is a multifactorial diabetic heart complication. The factors involved in the pathogenesis of diabetic cardiomyopathy include increased collagen deposition, cross-linking of collagen fibers, decreased glucose supply and utilization, and increased sensitivity to the ischemia/reperfusion injury. The mechanism underlying pathogenesis of cardiomyopathy could be an excess generation of AGEs; deactivated NO, myocardial inflammation and endothelial dysfunction induced by excessive formation of mitochondrial ROS, impaired calcium Ca^{2+} transient and sensitivity, inhibited expression of GLUT4/GLUT1 or increased free fatty acids (FFA). Moreover, in animal studies, an increase in myocardial mitochondria, apoptosis, intramyocardial lipid accumulation, and fibrosis were also common findings (Gallego, Alday et al. 2009; Deng, Huang et al. 2007; Zieman, Melenovsky et al. 2007; Khullar, Al-Shudiefat et al. 2010).

The most representative morphological changes of diabetic cardiomyopathy are cardiac hypertrophy, especially for the left ventricle, and systolic and diastolic dysfunction. Accordingly, imaging techniques, such as echocardiography or magnetic resonance imaging, are used for the diagnosis and assessment of diabetic cardiomyopathy.

In this study, we use echocardiography to assess the morphological and functional cardiac changes in diabetic mice. Cardiac hypertrophy could be clearly assessed by

echocardiography, even for a small animal model such as mice, as the left ventricle can be located under the probe with suitable size and resolution. Among all symptoms, left ventricle hypertrophy is the most common one, in which the wall thickness and ventricular dimension can be assessed by M-mode, both at the end of the diastole and systole. Another parameter for the assessment of diabetic cardiomyopathy, systolic function, can be calculated based on these collected basic data. The typical histological changes behind the cardiac hypertrophy are suggested as interstitial and perivascular fibrosis, increased collagen deposition, and cross-linking of collagen fibers (Van Hoeven and Factor 1990; Fischer, Barner et al. 1984).

SAA significantly improves the endothelial function and blood circulation and has a protective effect against oxidative harm in the hearts without DM. Theoretically, SAA could be suggested as a potent cardiomyopathy-benefit agent to diabetic hearts. In this study, we investigate the protective potential of chronic oral consumption of SAA on left ventricular hypertrophy and its underlying mechanism in diabetic mice.

The objective of this chapter was to investigate 1) the beneficial effect of long-term administration of SAA on the structural and functional changes in the heart of diabetic mice with elevated homocysteine level, and 2) whether these beneficial potentials are linked with the expression levels of the AKT/eNOS pathway proteins in the heart tissue.

2.2 Methods

2.2.1 Animals and Experiment Design

Female *db/db* and *db/m* mice (10-weeks-old) (**Figure 2-1**) were housed in the Central Animal Facilities, Hong Kong Polytechnic University in a 12-h light/darkness cycle, at 20–25°C and humidity of 50–60%. The mice were allowed regular laboratory chow and tap water ad libitum throughout the experimental period.

The *db/db* (C57BLKsJ strain) mice have long been recognized as an ideal spontaneous diabetic model. *Db/db* mice carry a mutation in the leptin receptor gene that results in hyperglycemia and obesity, which mimics the pathogenesis of DM in humans (Hummel, Dickie et al. 1966). The homozygous *db/db* mice were the diabetic model utilized in this study, whilst the heterozygous *db/m* mice served as a non-diabetic model.

The elevated Hcy level was developed with methionine diet, in which methionine was dissolved in daily tap water as 1% (w/v) and administrated to the DM (Methionine) group as well as the DM (Methionine + SAA) group. SAA was administrated to the DM (SAA) and DM (Methionine + SAA) groups by gastric intubation at a dose of 60 mg/kg/day according to the previous *in vivo* studies with SAA (Gao, Liu et al. 2009; Wang, Ma et al. 2011; Wang, Fu et al. 2012). The DM control group and the non-DM group received daily intragastric tap water as a comparison. The grouping method of mice in Chapter 2 is summarized in **Table 2-1**.

All animal experiments were approved by the Ethical Committee of the Hong Kong Polytechnic University.

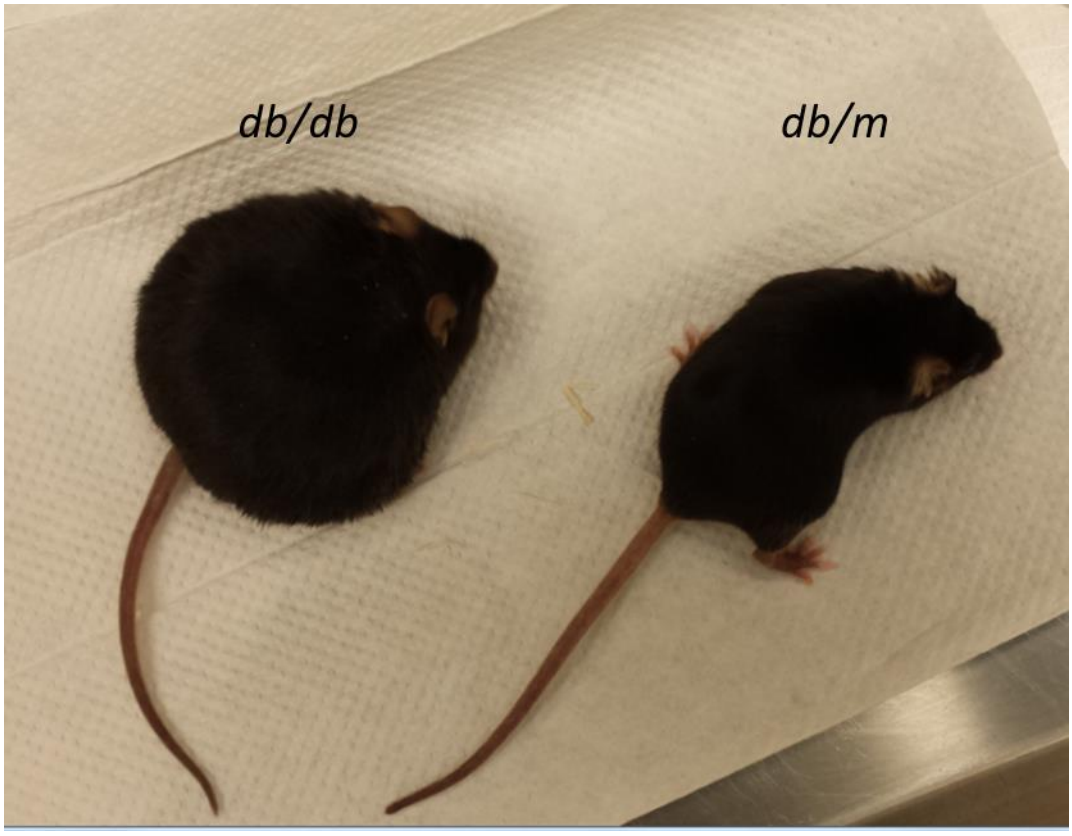

Figure 2-1. The appearance of the *db/db* and *db/m* mice.

Table 2-1. Grouping method of mice used in Chapter 2.

Groups	Mice Strain	Methionine 1%	SAA 60 mg/kg
DM Control (n = 6)	*db/db*	−	−
DM (SAA) (n = 6)	*db/db*	−	+
DM (Methionine) (n = 9)	*db/db*	+	−
DM (Methionine + SAA) (n = 9)	*db/db*	+	+
Non-DM (n = 10)	*db/m*	−	−

2.2.2 Echocardiography

After 1-week acclimation, the intervention was started. At baseline and the end of intervention, all mice were arranged to undergone transthoracic echocardiographic assessment using an ultrasound system (Model: HD11 XE, Philips Medical Systems, Bothell, WA, USA) with a high-resolution broadband compact linear array transducer (Model: L15-7io, Philips Medical Systems, Bothell, WA, USA) according to the protocol of our previous work (Siu, Bae et al. 2007) (**Figure 2-2**). Mice were anesthetized with an intraperitoneal injection of ketamine (80 mg/kg)/xylazine (10 mg/kg) mixture and rested on a heating pad to maintain their body temperature during the whole scanning procedure. Then, the hair on their ventral thorax was carefully shaved. During echocardiography, the mice were positioned in the prone decubitus position, and the cardiac structure in parasternal short-axis view at the papillary level was determined using B-mode. Then, the left ventricular (LV) interventricular septal thicknesses (IVS), LV internal dimensions (LVID), and posterior wall thicknesses (PW) at the diastole and systole were carefully measured using M-mode at the level of the papillary muscles (**Figure 2-3**, **Figure 2-4**). Finally, LV ejection fraction (EF), LV fractional shortening (FS), and LV mass were calculated using the following equation (Gao, Ho et al. 2011):

EF % = $100\times((LVIDd^3 - LVIDs^3)/LVIDd^3)$

FS % = $100\times((LVIDd - LVIDs)/LVIDd)$

LV mass = $1.05\times ((IVSd+LVIDd+PWd)^3 - LVIDd^3)$

(where 1.055 (mg/mm^3) is the density of myocardium)

A

B

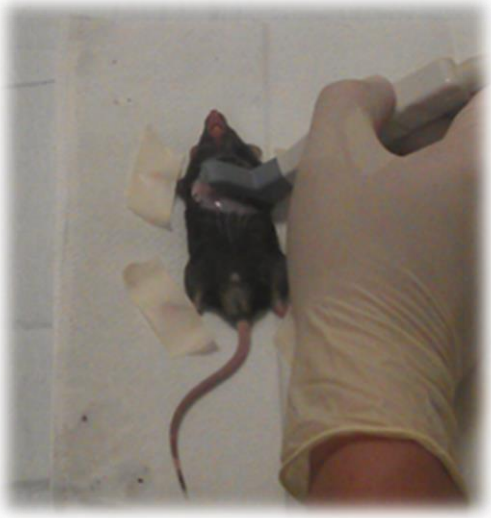

C

Figure 2-2. Equipment and technique used for mouse echocardiography.

A, PHILIPS HD11 XE Ultrasound System used for the echocardiography;
B, L15-7io probe for the assessment of echocardiography as hold by hand in figure C;
C, Echocardiograph on *db/m* mice. The mouse was anesthetized and rested on a heating pad to maintain their body temperature during the whole scanning procedure. The feet were stabilized using sticky tape. The hair on their ventral thorax was carefully shaved, and ultrasound gel was used on the chest region. Then, the image of the cardiac structure in the parasternal short-axis view at the papillary level was captured with the probe.

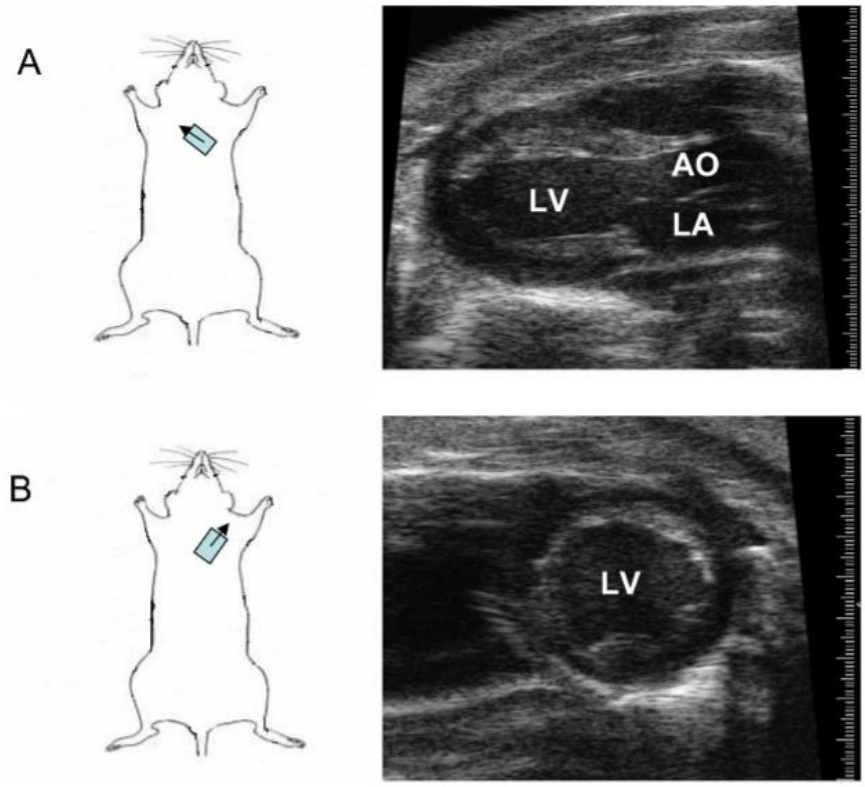

Figure 2-3. Position and direction (small arrow) of the probe when performing mouse echocardiography (Gao, Ho et al. 2011).

A, The position of the probe for the LV long-axis view and the corresponding ultrasound image.

B, The position of the probe for LV short-axis view and the corresponding ultrasound image.

LV = Left ventricle, LA = left atrium, AO = aorta.

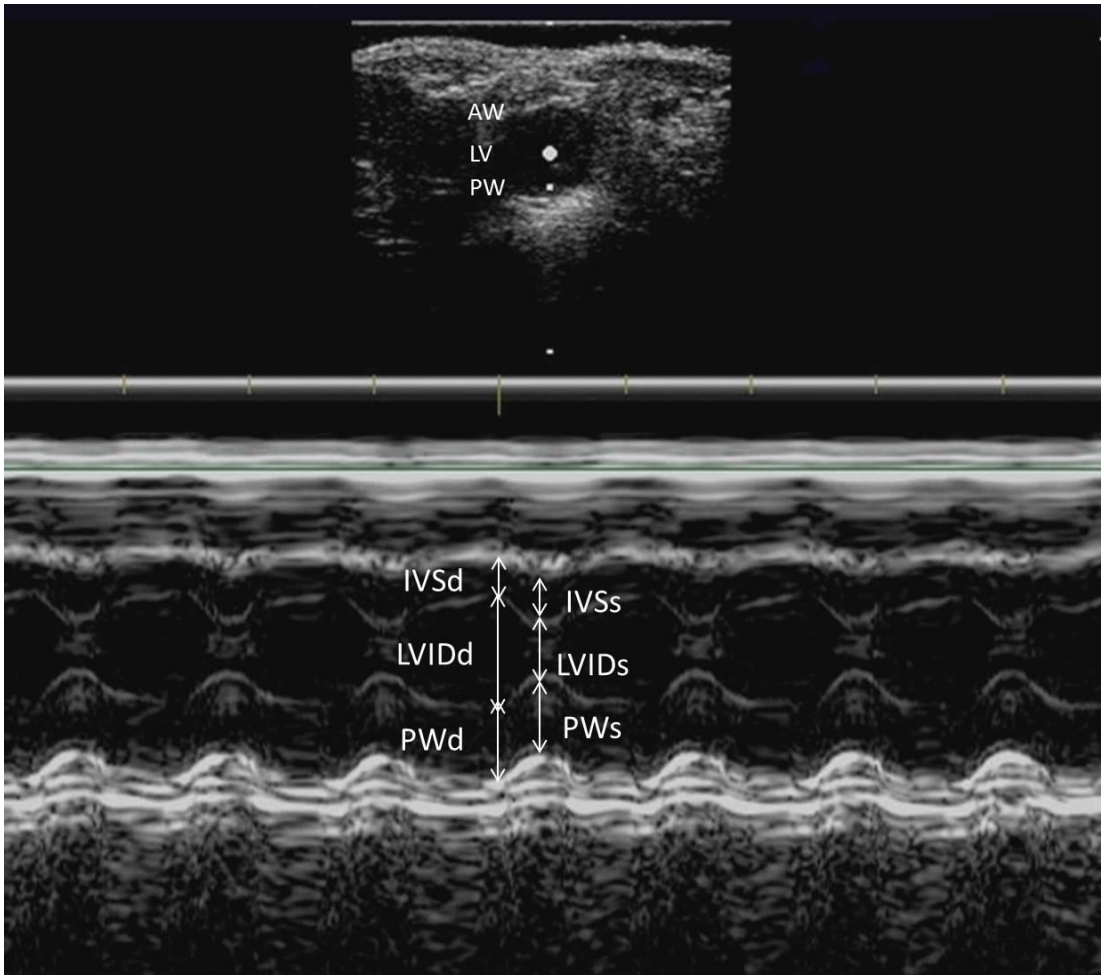

Figure 2-4. A sample echocardiograph showing the measurement of different parameters of the left ventricle of mice (Gao, Siu et al. 2017).

All measurement was performed in M-mode using the parasternal short-axis view and at the papillary level. AW, anterior wall; LV, left ventricle; PW, posterior wall; LVIDd, left ventricular internal dimensions (diastole); LVIDs, left ventricular internal dimensions (systole); PWd, posterior wall thicknesses (diastole); PWs, posterior wall thicknesses (systole); IVSd, interventricular septal thicknesses (diastole); IVSs, interventricular septal thicknesses (systole).

2.2.3 Western Blot

After the echocardiographic assessment, the mice were sacrificed by an overdose of pentobarbital. The heart tissue was collected from dissected mice and washed in ice-cold PBS (Phosphate buffered saline), and then snap frozen by liquid nitrogen, and stored at -80°C for subsequent Western blot analysis. The tissue was immersed in ice-cold RIPA (Radio-Immunoprecipitation Assay buffer) buffer [150 mM sodium chloride; 1.0% NP-40 or Triton X-100; 0.5% sodium deoxycholate; 0.1% SDS (sodium dodecyl sulphate); 50 mM Tris, pH 8.0], and homogenize with an electric homogenizer, then the sample was placed on an orbital shaker at 4°C for 2 h. The homogenate was then centrifuged for 20 min at 12,000 rpm at 4°C, and gently removed from the centrifuge and placed on ice; the supernatant was then transferred to a fresh tube and kept on ice; the pellet was discarded.

To prepare samples for loading into gels, loading buffer was mixed with the samples and vortex. This mixture was then boiled at 95–100°C for 5 min and placed on ice. Then, the running tank and gels were set in place and the tank filled with running buffer (1X Running Buffer; Tris base 3.03 g; Glycine 14.41 g; SDS 1 g; made up to 1 L with distilled water).

Gel loading tips were used to load the protein ladder (molecular weight marker), and samples into the narrow wells and the gel was run at 90V for about 2 h. When the dye molecule had reached the bottom of the gel, the electrophoresis was stopped and the gel prepared for the transfer process. The proteins were transferred and staining on the PVDF membrane as follows. First, the PVDF membrane was soaked in absolute methanol for 1–2 min, then incubated in ice cold transfer buffer for 5 min. The stacking

gel and dye front were removed from the gel. Then, the gel was left to equilibrate for 3–5 min in ice cold transfer buffer. Failure to do so would cause shrinking while transferring, and a distorted pattern of transfer. During the next step of protein transfer, the PVDF membrane was sandwiched between the gel, sponge, and filter paper. The whole set was pressed hard and stabilized together to make sure no air bubble existed between the gel and membrane layers (Eslami and Lujan 2010).

The wet transfer was performed at 80V for about 2 h at 4°C. Afterwards, the membrane was incubated in 5% non-fat milk for 1 h under agitation, then rinsed for 5 s in TBST [TBS 10× (concentrated TBS), for 1 L: Tris base (24.23 g) and NaCl (80.06 g) dissolve in 800 mL distilled water; adjusted to pH to 7.6 with pure HCl and made up to 1 L using ultra-pure water; Tween20 (1% v/v) was then added to TBS 1× to make TBST]. To incubate with the primary antibody, the antibody is diluted at the suggested dilution in 5% non-fat milk and incubated overnight at 4°C under agitation. For the incubation with the secondary antibody, the membrane was washed in TBST while agitating for three times, 5 min per wash.

The antibody was diluted to the suggested dilution in 5% non-fat milk for 1–2 h at room temperature with agitation. The membrane was washed in TBST while agitating (three times, 5 min per wash). Using the ECL detection kit, the chemiluminescent signals were captured using the Bio-Rad imager. The total protein concentration was determined using the Bradford protein assay (Bio-Rad, Catalog No. 500-0002). Finally, the band intensity of the target protein was quantitatively analyzed with ImageJ software. The list of antibodies used in this study is summarized in Appendix A. All data were analyzed using IBM SPSS Statistics (version 21.0, IBM SPSS Inc., Chicago, IL, USA), and represented as the mean ± SEM. Comparison among multiple groups

was conducted by one-way ANOVA followed by *post hoc* Bonferroni test. A p value of less than 0.05 was considered significant. All figures were generated using GraphPad Prism software (version 5.01, GraphPad Software Inc., San Diego, CA, USA).

2.3 Results

The fasting blood glucose level and body weight at the beginning and end of the experiment can be found in **Table 2-2**. The two groups without taking SAA treatment [DM (control) and DM Methionine)] had increased PWd (58.5%, $p < 0.01$; 58.2%, $p < 0.05$), PWs (31.6%, $p < 0.05$; 32.5%, $p < 0.05$), LVSd (38.1%, $p < 0.05$; 25.4%, $p < 0.001$) and LV mass (49.0%, $p < 0.001$; 31.7%, $p < 0.01$) at the end of intervention period, when compared to their baseline values. In the non-DM group, the only observable morphological change was an increase in IVSs (decrease 6.5%, $p < 0.05$) after 8 weeks. Moreover, the progressions of LV mass in the two SAA treatment groups [DM (SAA) (2.9%, $p > 0.05$) and DM (SAA+ Methionine) (4.3%, $p > 0.05$)] were not significantly change compared with baseline, suggesting a delay in the progression of LVH in these diabetic mice treated with SAA. However, the cardiac function among different groups, as represented by EF and DS, were similar, suggesting that SAA might have a limited effect on diabetic cardiac function (**Table 2-3**).

Table 2-2. Fasting blood glucose level and body weight at the beginning and end of the experiment (Gao, Siu et al. 2017).

	DM (Control)	DM (SAA)	DM (Methionine)	DM (Methionine + SAA)	Non-DM
Baseline					
Fasting blood glucose (mmol/L)	27.73±2.08*	22.72±1.50*	27.72±2.14*	23.99±1.71*	5.94±0.50
Body weight (g)	42.95 ±2.33*	44.63±1.22*	44.76 ±1.43*	48.42±1.39*	22.14±0.58
After 8 weeks					
Fasting blood glucose (mmol/L)	29.18±1.67*	27.08±1.23*	25.77±0.75*	25.64±1.65*	5.43±0.45
Body weight (g)	49.56±4.83*	56.82±2.68*	49.06±3.16*	53.12±2.78*	25.36±0.53

* $p < 0.001$ when compared to the **non-DM** group.

Table 2-3. Results of echocardiography (Gao, Siu et al. 2017).

Echocardiography parameters	DM (Control)		DM (SAA)		DM (Methionine)		DM (Methionine + SAA)		Non-DM	
	Baseline	Post	Baseline	Post	Baseline	Post	Baseline	Post	Baseline	Post
HR (bpm)	265.78±14.22	249.93±14.23	257.65±12.47	263.32±5.81	263.77±14.00	241.28±7.96	261.90±9.85	238.63±4.75	242.75±6.53	242.26±5.32
Morphological changes										
LVIDd (mm)	3.79±0.12	3.54±0.20	3.96±0.12	4.04±0.11	3.80±0.07	3.45±0.22	3.90±0.06	3.75±0.10	3.70±0.07	3.46±0.78*
LVIDs (mm)	2.08±0.05	2.13±0.16	2.34±0.11	2.25±0.11	2.03±0.08	1.97±0.22	2.15±0.09	2.01±0.10	2.16±0.09	2.07±0.09
PWd (mm)	0.53±0.10	0.84±0.09 **	0.49±0.01	0.53±0.02	0.55±0.04	0.87±0.10*	0.56±0.02	0.67±0.05	0.57±0.03	0.60±0.02
PWs (mm)	0.79±0.04	1.04±0.08*	0.80±0.02	0.87±0.03	0.83±0.04	1.10±0.09*	0.94±0.03	1.03±0.06	0.87±0.04	0.88±0.03
IVSd (mm)	0.63±0.06	0.87±0.07*	0.62±0.02	0.58±0.03	0.67±0.02	0.84±0.04***	0.65±0.04	0.65±0.03	0.60±0.02	0.65±0.03
IVSs (mm)	1.08±0.05	1.16±0.09	1.06±0.06	1.02±0.05	1.02±0.03	1.16±0.07	1.02±0.04	1.10±0.05	0.96±0.03	1.07±0.04*
LV mass (mg)	69.98±2.54	104.29±4.63***	71.54±2.27	73.63±2.86	75.66±2.40	99.64±5.30**	78.27±2.07	81.65±3.82	67.91±2.07	65.74±1.85
Functional changes										
LV EF (%)	83.11±1.29	78.02±2.10	78.77±2.00	82.33±1.42	84.25±1.50	80.68±3.26	83.04±1.35	84.10±1.97	79.72±1.72	78.04±1.89

LV FS (%)	45.11±1.45	40.08±1.86	40.77±2.03	44.30±1.57	46.67±1.71	44.34±3.70	45.08±1.49	46.53±2.08	41.93±1.83	40.23±1.84

HR, heart rate; LVIDd, left ventricular internal dimensions (diastole); **LVIDs**, left ventricular internal dimensions (systole);

PWd, posterior wall thicknesses (diastole); **PWs**, posterior wall thicknesses (systole); **IVSd**, interventricular septal thicknesses (diastole);

IVSs, interventricular septal thicknesses (systole); **EF**, left ventricular ejection fraction; **FS**, left ventricular fractional shortening;

LV mass, left ventricular mass.

* $p \leq 0.05$, ** $p \leq 0.01$, *** $p \leq 0.001$ when compared to its corresponding baseline values.

The Western blotting results are shown in **Figure 2-5**, **Figure 2-6**, **Figure 2-7** and **Figure 2-8**. As shown in **Figure 2-5** and **Figure 2-7**, the expression level of phosphorylating eNOS/ total eNOS in the heart tissue of mice in the DM (SAA) group was higher than in the DM (Methionine) and DM (SAA + Methionine) groups. Also, the expression level of phosphorylating eNOS/total eNOS in the heart tissue of mice in the DM (Methionine) group was lower than in the DM (control) group. Moreover, the expression level of eNOS/total eNOS in the DM (SAA + Methionine) group was elevated compared to the DM group (Methionine). Finally, the phosphorylating eNOS/total eNOS expression trends across the different groups were similar to the p-Akt/total Akt ratios.

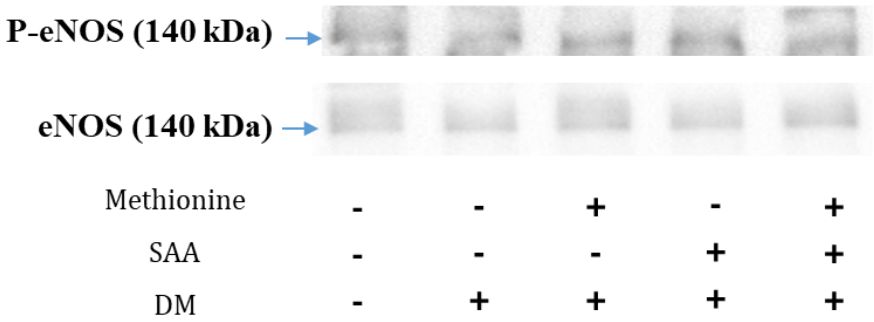

Figure 2-5. Expression of phosphorylating eNOS and t-eNOS and in heart tissue of mice by Western blot.

In the Western blot, from left to right, the samples are the Non-DM group, DM Control group, DM (Methionine) group, DM (SAA) group and DM (Methionine + SAA) group.

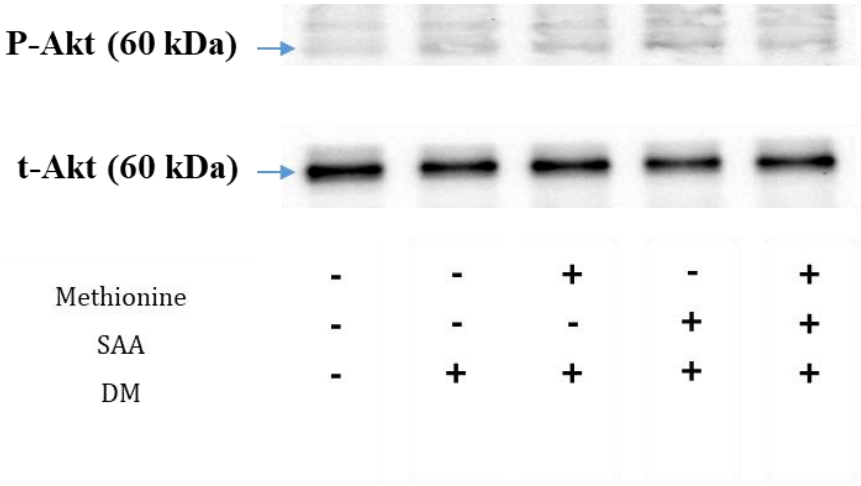

Figure 2-6. The expression level of phosphorylating Akt and t-Akt in the heart tissue of mice, determined by Western blotting.

In the Western blot, from left to right, the samples are Non-DM group, DM Control group, DM (Methionine) group, DM (SAA) group and DM (Methionine + SAA), group.

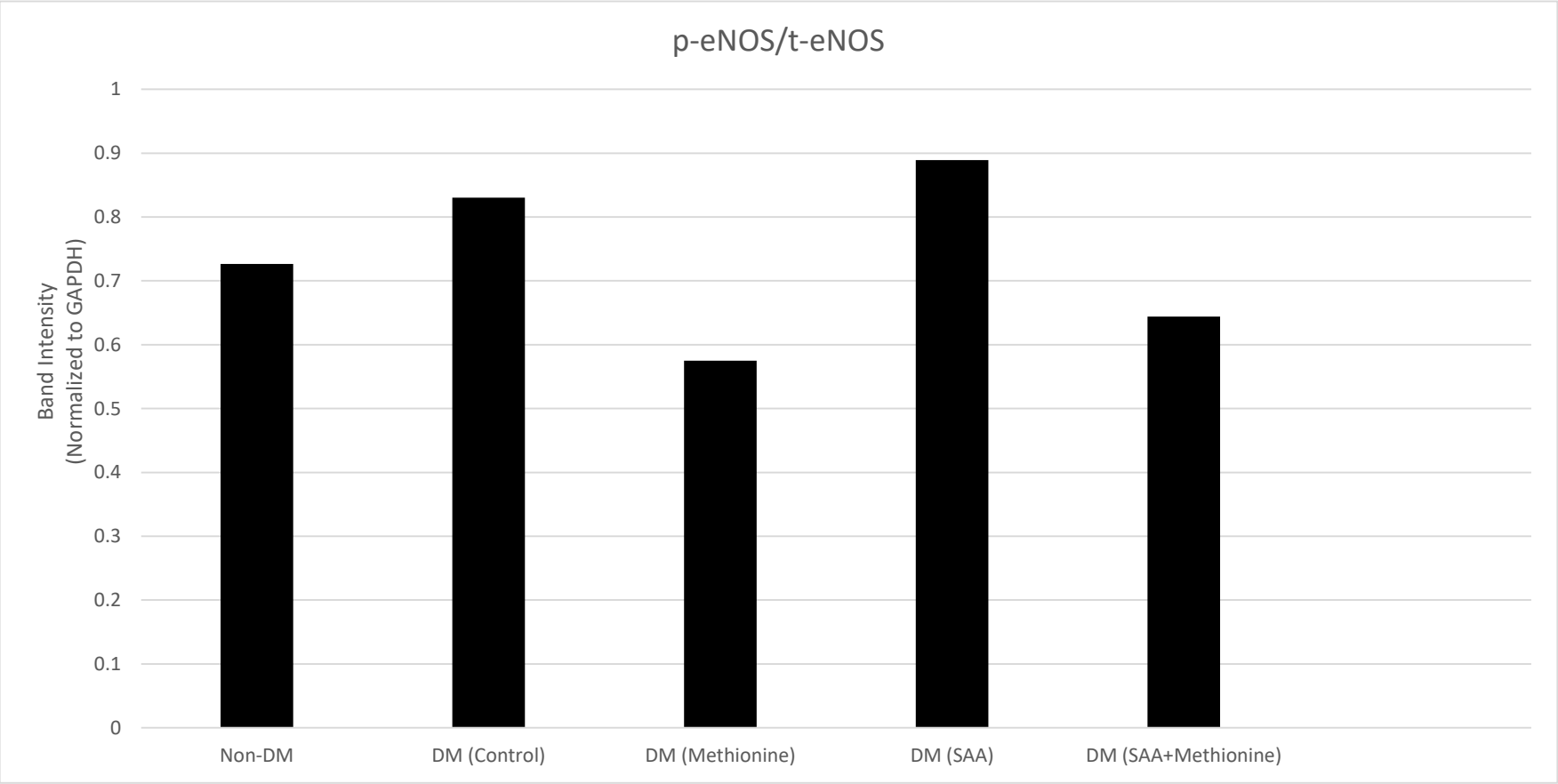

Figure 2-7. Quantified expression level of phosphorylating eNOS to total eNOS ratio in the heart tissue of mice.

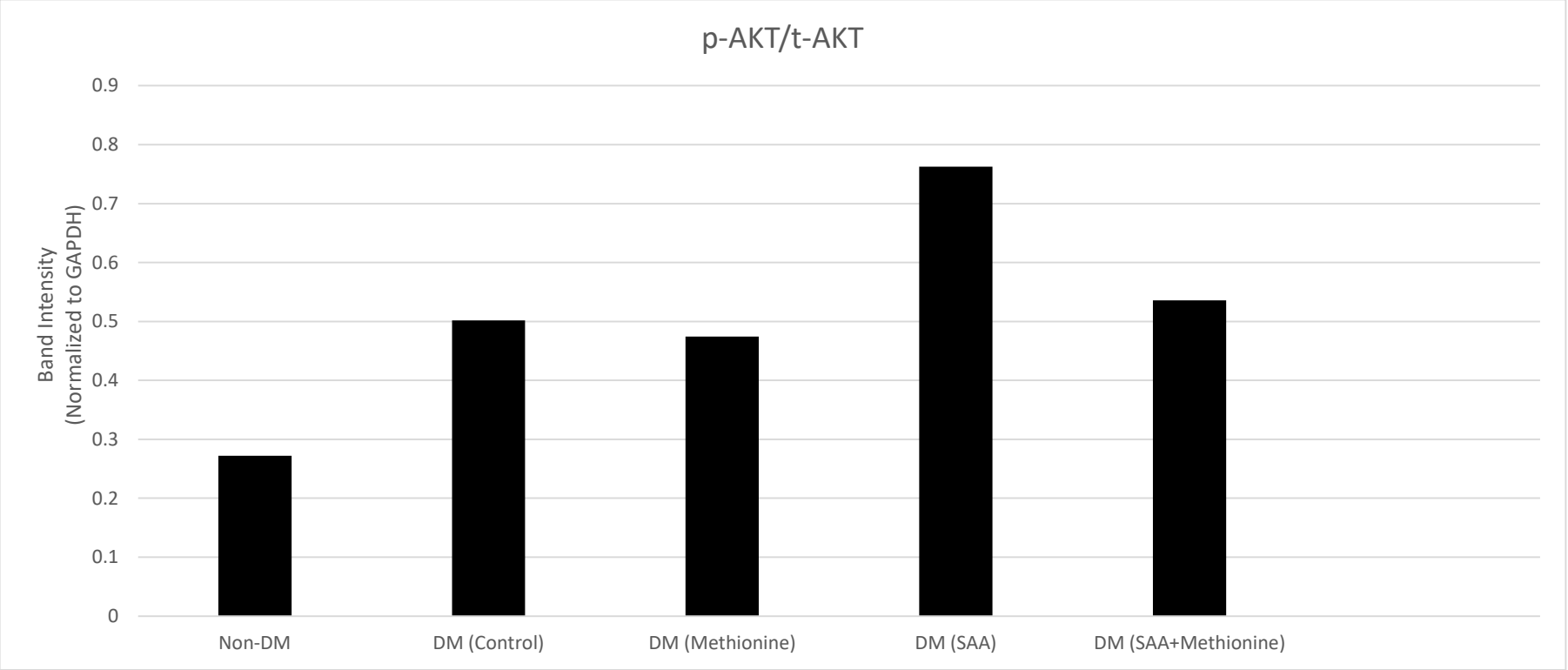

Figure 2-8. The quantified expression level of phosphorylating Akt to total Akt ratio in the heart tissue of mice.

2.4 Discussion

In this study, SAA significantly slowed the progression of left ventricular hypertrophy, possibly via increased eNOS/Akt signaling.

Our findings are consistent with previous research, in which SAA significantly protected cardiomyocytes from apoptosis and ischemic injury by upregulation of the phosphorylation of Akt and extracellular signal-related kinase 1/2 *in vivo* and *in vitro* (Yin, Guan et al. 2013). Moreover, in the myocardial hypertrophy rat model induced by ischemia/reperfusion, the treatment of SAA significantly improved the expression of eNOS, as well as the production of NO (Xiao-Yong, Chun-Lin et al. 2008).

It has been recognized that the activation of AKt and eNOS significantly contribute to normal glucose regulation, and disordered insulin-glucose homeostasis can lead to insufficient ATP storage and further trigger the onset of cardiomyopathy (Nikolaidis, Sturzu et al. 2004). As mentioned above, a decrease in eNOS expression leads to a depletion of NO production, which induces further myocardial apoptosis and dysfunction. The oxidative damage induced by increased ROS production and self-oxidation could accelerate this progression, especially in DM patients with elevated Hcy levels (Neilan, Blake et al. 2007). Similarly, Akt signaling also protects the myocyte from apoptosis and cardiomyopathy against OS-induced cardiac and endothelial dysfunction (Taniyama and Walsh 2002). As important therapeutic signals, the upregulated Akt and eNOS have been suggested to improve glucose uptake in the diabetic myocardium (Penumathsa, Thirunavukkarasu et al. 2008).

Diabetic cardiomyopathy is a critical heart disease that occurs independently of hypertension and coronary artery disease (Letonja and Petrovič 2014). Diabetic

cardiomyopathy is a unique disease characterized by abnormal structural and functional changes that ultimately lead to heart failure (Boudina and Abel 2010). Diabetic cardiomyopathy can be triggered by cardiac remodeling and fibrosis, which is initiated by apoptosis of cardiomyocytes and endothelial cells induced by the oxidative stresses occurring under diabetic status (Garg, Narula et al. 2005). In the cardiomyocytes of diabetic mice, elevated reactive oxygen and reactive nitrogen species have been detected (Ye, Metreveli et al. 2003; Fiordaliso, Bianchi et al. 2004), and increased ROS production might lead to activation of initiator caspases, such as apoptosis-like caspase-9 and caspase-3 (Green and Kroemer 2004), subsequently causing oxidative injury and cardiac cell death that is correlated with a significant decline of GSH (Ghosh, Pulinilkunnil et al. 2005). In other words, cardiac cell death is the critical cause of diabetic cardiomyopathy and is significantly correlated with increased oxidative stress damage induced by diminished GSH (Cai, Wang et al. 2006). Therefore, the therapeutic options aiming at ameliorating such oxidative injury, such as GSH supplementation for scavenging oxidative species, have been used as a prevention or treatment of diabetic cardiomyopathy (Muntean, Sturza et al. 2016).

Elevated Hcy level was shown to be associated with increased ROS production, decreased NO production, and an impaired Akt pathway, leading to a damaged redox status and increased apoptosis risk (Sood, Hunt et al. 2003). Normally, NO derived from the endocardial endothelium participates in the homeostasis of myocyte contraction and dilation function. Whilst, impaired NO production lead to a imbalance between contraction and relaxation of myocardium, which initiates cardiomyopathy (Tyagi, Rodriguez et al. 2005). Moreover, Hcy-triggered OS increased matrix metalloproteinase activity and decreased peroxisome proliferator-activated receptor expression, which contribute to the fibrosis of endothelium and smooth muscle and

induce endothelial-myocyte disconnection and uncoupling (Bissonnette, Treacy et al. 2001).

SAA has been reported to be capable of improving blood circulation by inhibiting platelet adhesion and aggregation and acting against OS by suppressing the production of ROS, thereby protecting myocardium ischemia, and ameliorating endothelial cells dysfunction via Akt and ERK1/2 phosphorylation (Cheng 2007; Yin, Guan et al. 2013). In DM, excessive ROS generation due to hyperglycemia and autoxidation (Jay, Hitomi et al. 2006) has been indicated associated with increased cell death and apoptosis in the heart of *db/db* mice (Barouch, Berkowitz et al. 2003), leading to pathological cardiac remodeling and fibrosis (Cai, Wang et al. 2006) and subsequent abnormal cardiac morphological and functional change (Boudina and Abel 2007). In this regard, SAA possess significant *in vitro* potential for scavenging free radicals and lipid such as hydroxyl and anion radicals in endothelial cells, thus having a similar effect as vitamin E. In a vitamin C equivalent antioxidant capacity test, SAA was shown to produce a better antioxidant value than vitamin C (Kim, Lee et al. 2002), as well as double the antioxidant activity compared to caffeic acid in a 2,20-azino-di-3-ethylbenzthiazoline sulphonate (ABTS) radical assay (Zhao, Zhang et al. 2008). The free radical scavenging capacity of SAA might be contributed to by the two hydroxyl groups in the SAA structure, which make SAA a hydrophilic molecule, thus allowing SAA to approach and react with the free radicals. With this potent antioxidant efficacy, SAA not only acts as a single antioxidant but also as an alternate intracellular oxidative stress status, which suggests multiple effects in terms of triggering intracellular defenses against different diseases.

In the present study, the presence of LVH was found in the DM (control) group, as

evidenced by the increased LV mass and wall thickness after 8 weeks, which was inconsistent with a previous study (Yue, Arai et al. 2007). As a comparison, the LV mass and wall thickness did not show significant changes in the non-DM group, except for LVIDd and IVs, or for the systolic function, which was not significantly changed after 8 weeks. As expected, the cardiac hypertrophy was especially developed in the left ventricle of the diabetic mice. As the most representative and significant morphological changes of diabetic cardiomyopathy, left ventricle hypertrophy commonly takes place during the advanced pathological progress because of cardiomyocytes apoptosis and necrotic loss (Letonja and Petrovič 2014). Although the underlying mechanism has not been clearly recognized, it was reported that, in diabetic animals, hyperglycemia and hyperinsulinemia, among others, have a role in the development of cardiac hypertrophy via the alternation of apoptosis and fibrosis of myocardiocytes (Karason, Sjöström et al. 2003). Moreover, experimental studies have also revealed the several marker hypertrophic genes are overexpressed in the early diabetic stage, such as an atrial natriuretic peptide, brain natriuretic peptide, and β-myosin heavy chain (Rosenkranz, Hood et al. 2003; Nunes, Soares et al. 2013).

In the groups treated with SAA [DM (SAA) and DM (Methionine + SAA) groups], we found that the progression of LV mass was similar to the non-DM group, suggesting the SAA treatment could prevent or slow the progression of diabetic LVH. Also, the mechanism underlying these effects might be the antioxidant property of SAA, the protective effect of endothelial cell, and the promotion of intracellular GSH production, as described above.

To conclude, in the *db/db* mice with elevated Hcy level, SAA could significantly slow the progression of left ventricular hypertrophy after 8 weeks of administration,

although the systolic function was not significantly improved by SAA treatment. Also, the improvement in LVH by SAA treatment might be linked with the upregulation of eNOS/AKT pathway. Further study on the detailed mechanism involved in the effect of SAA on myocyte hypertrophy will be required to determine the specific cardiac benefit of SAA.

Chapter 3 Effect of SAA on Endothelial Dysfunction in Diabetes with Elevated Homocysteine Level

3.1 Introduction

Endothelial dysfunction is the dominant pathological characteristic of CVD progression in DM, having a significant role in the maintenance of vascular homeostasis (Schalkwijk and Stehouwer 2005; Van den Oever, Raterman et al. 2010). As mentioned in Chapter 1, there is a fine balance between the dilation and contraction factors regulated by the endothelium. This is the dynamic balance that will be alternated when ED occurs, thereby initiating the onset of CVD (Tan, Chow et al. 2002).

It has been shown that ED is correlated with the progression of DM due to hyperglycaemia, oxidative stress, insulin resistance, obesity, and hyperlipidaemia, which alter the proliferation and adhesion of circulation cells, and apoptosis of endothelial cells (Favaro, Miceli et al. 2008; Van den Oever, Raterman et al. 2010). Although the exact underlying mechanism has not been fully understood, the triggered OS, apoptosis of endothelial cells, and a decrease in important antioxidants and vasodilators, such as NO, have significant roles in the progression of endothelial dysfunction in DM, as we introduced in Chapter 1.

Hcy, as mentioned above, is a byproduct of the metabolism of methionine, in which the sulfur group of methionine will be terminated by the generation of the thiol group of Hcy as a final result of the trans-sulphuration pathway (Stipanuk and Ueki 2011). An elevated Hcy level was shown to contribute to the onset of CVD by injuring endothelial function, causing auto-oxidation, increasing the ROS production, and decreasing the levels of important antioxidants, such as glutathione (Handy, Zhang et al. 2005).

As reported in a previous study, Hcy injured the endothelial function by diminishing NO production and bioavailability by decrease the cellular source of L-arginine, which leads to further elevated ROS production (Jin, Caldwell et al. 2007).

A methionine-rich diet administration will significantly increase the blood Hcy level, with which we stimulate the elevated Hcy level in diabetic mice (Velez-Carrasco, Merkel et al. 2008). The mechanism underlying the increased CVD risk in the comorbid hyperhomocysteinemia and diabetes patients involves various pathogenic factors, such as endothelial dysfunction, vascular lesions, and smooth muscle cell proliferation. Among these pathogenic factors, ED seems to play a dominant role (McCully 1969; Groot, Willems et al. 1983; McCully 1993; Tawakol, Omland et al. 1997). Therefore, in this study, to induce an elevated homocysteine condition in mice, 1% methionine (w/v) was added into the daily drinking water of mice. I anticipated that the increased Hcy level would cause harm to endothelial function.

To sum up, Hcy aggravates the redox imbalance under DM status and doubles the risk of the onset of endothelial dysfunction. However, the effect of elevated Hcy level on the endothelial function of diabetic mice remains unknown and its potential beneficial protection is unclear. Therefore, in this study, I proposed to investigate the protective effect of SAA on the endothelial dysfunction in *db/db* mice with elevated Hcy (i.e., whether it is endothelial-dependent or independent). The overall aims of this study are to investigate 1) whether SAA has an acute vasorelaxant effect, 2) whether this vasorelaxant effect is endothelial-dependent (NO-pathway or PGI2 pathway), and 3) whether chronic SAA consumption might improve vascular endothelial function in

diabetic mice with elevated Hcy levels.

3.2 Methods

As mentioned previously, both Hcy and DM promote endothelial damage, and SAA treatment is expected to preserve the endothelial function of non-diabetic rodents. The protective effect from SAA on endothelial dysfunction was assessed by both chronic oral consumption and acute experimental conditions using myograph. The chronic administration of SAA in mice was used to investigate the long-term therapeutic effect of SAA on the endothelial function, and the direct effect of SAA condition was used to investigate the direct vasorelaxant effect of SAA.

To collect the aortic rings to be used in the endothelial function tests, mice received an overdose of pentobarbital and the chest region was then dissected. Fresh aortic tissue was cut down immediately and washed with PBS (phosphate-buffered saline) buffer. The aortic tissue was then stabilized using two pins at each of its ends and immersed in Kreb's buffer, as shown in **Figure3-1 C**. The adhesive tissue was carefully removed using microsurgical tools under a microscope. Subsequently, the clean aorta tissue was cut into the aortic ring to a length of 2–3 mm. Then, the aortic ring was hung by the two L-shape hooks in the organ chamber, as shown in **Figure 3-1 B**. The operation and equipment are shown in **Figure 3-1**.

A myograph is a sensitive and efficient device used to detect the contraction and dilatation of tubular samples, such as vascular tissue from mice. In our experiment, the isolated aortic tissue segment (about 2-mm long) was cannulated at both ends of L-shape hooks, which are connected to a sensitive force transducer. The collected data was recorded and displayed by a computer program. By this approach, the force changes of the vessel can be visualized and quantified by the program in real-time, in which an increasing force indicates a contraction of the vessel and a decreasing forced

indicates a dilation.

The whole aortic tissue was immersed in Kreb's buffer at 37°C, and an oxygen and carbon dioxide mixture was supplied to maintain the bioactivity of the tissue. As mentioned above, the dominate vasodilator derived by the endothelium was recognized as NO (Cohen 1995). The endothelium-dependent vasodilator acetylcholine was used to induce dilation, specifically mediated by the endothelium, and the dilation range reflects the endothelial function. The equipment and an example curve are shown in **Figure 3-1**.

A

B

C

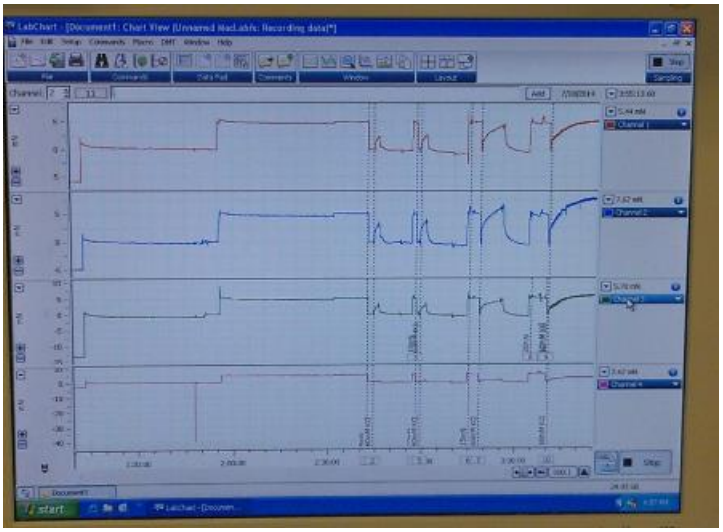

D

Figure 3-1. Equipment used in the endothelial function assessment.

A, ADInstruments/DMT 610m Wire Myograph System; (Danish Myo Technology, Aarhus, Denmark)

B, Organ chamber;

C, Aortic ring dissection;

D, Real-time tension monitoring. After freshly collected from the mice, the aortic tissue was stabilized by two pins at both ends of it and immersed in Kreb's buffer in the plate as shown in figure C. The adhesive tissue was carefully removed, and the clean aorta tissue was cut into the aortic ring (2–3 mm long). Then the aortic ring was hung using the two L-shape hooks in the organ chamber, as shown in Figure B, and then placed in the myograph system, as shown in Figure A. During the whole experiment, the tension changes were monitored and recorded by the real-time program, LabChart, for later analysis.

3.2.1 Direct Effect of SAA on Endothelial Function

C57BL/6 mice (12–16-weeks-old) were used in this test. After being anesthetized, the mice were dissected, and aortic tissues were collected. Then the thoracic aortas were freshly collected from dissected mice, and adhesive tissues were carefully removed under a microscope. Next, the aorta was cut into 2–3 mm long rings, which were each held by an L-shape hook in myograph chamber containing 5 ml of Krebs' buffer (126 mM NaCl, 2.5 mM KCl; 25 mM $NaHCO_3$, 1.2 mM NaH_2PO_4, 1.2 mM $MgCl_2$, 2.5 mM $CaCl_2$, pH to 7.2).

Then, the aortic ring was stabilized in an organ chamber, and the tension was maintained at 0.5 g for 60 min for equilibration. The temperature of the buffer was maintained at 37°C, and an oxygen (95%) and carbon dioxide (5%) mixture was supplied. Next, 100 mM KCL was used to challenge the aortic tissue and confirm its integrity. The aortic ring was then washed clean with Kreb's buffer (three washes). After the final wash, 10^{-6} M PE is used to induce pre-contraction, where the maximum tension was set as 100% of contraction before the tested compounded was added.

To search for SAA-like compounds, I inputted the chemical structure of SAA into the National Center for Biotechnology Information Structure Database (Kim, Thiessen et al. 2015) and identified five compounds that exhibit very high similarity to SAA. These five SAA-like compounds are:

1. Caffeic acid
2. 2,4-dihydroxy- cinnamic acid (Cinnamic Acid)
3. 4-coumaric acid (Coumaric Acid)
4. Salvianolic Acid A (SalA)

5. Salvianolic Acid B (SalB)

The chemical structures and sources of all six tested compounds (including SAA) are listed in **Table 3-1**.

Table 3-1. Those compounds that are structurally similar to SAA.

	Name	Structure	Plant Source
1	**Salvianic Acid A (SAA)**	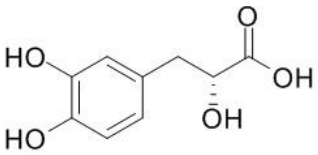	*Salvia Miltiorrhiza (Danshen)*
2	**Caffeic acid**	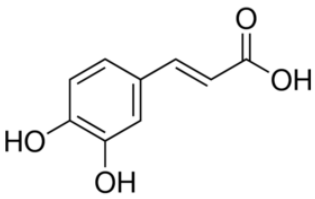	*Salvia Miltiorrhiza & Rz. Chuanxiong etc.*
3	**2,4-dihydroxy-cinnamic acid (Cinnamic Acid)**	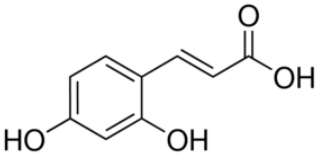	*Cinnamon*
4	**4-Coumaric acid (Coumaric acid)**	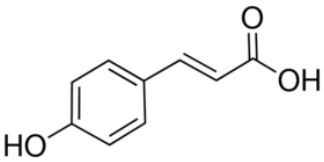	-
5	**Salvianolic Acid A (SalA)**	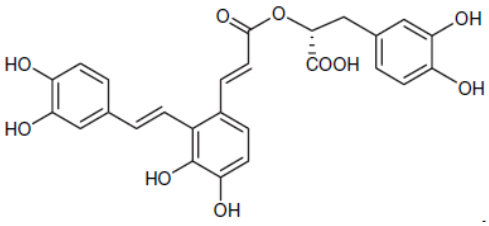	*Salvia Miltiorrhiza (Danshen)*
6	**Salvianolic Acid B (SalB)**	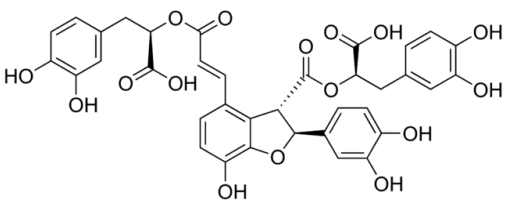	*Salvia Miltiorrhiza (Danshen)*

3.2.1.1 Time Control Test

This test was to assess the response of the aortic tissue to the direct administration of SAA with only one concentration. In the time control, 1 mg/mL of SAA of was directly administrated into the organ chamber, and the tension response from the aortic ring was found to define its acute vasorelaxant effect.

3.2.1.2 Time-Response Test on Vasodilation with Endothelial Pathway Inhibitors

In this part, endothelial pathway inhibitors were added to investigate whether the vasorelaxant effect was mediated through the endothelial-dependent pathway. SAA (1 mg/mL) was also added together with each of the tested inhibitors: indomethacin (INDO) as COX inhibitor; Nω-nitro-L-arginine (LNNA) as nitric oxide synthase inhibitor; and 1H-[1,2,4]oxadiazolo[4,3-a]quinoxalin-1-one (ODQ) as guanylate cyclase inhibitor, respectively. All samples were grouped as follows:

Group1: Control (with no treatment after PE precontraction);

Group2: L-NNA (treated with SAA in the presence of 200 μM L-NNA);

Group3: Indomethacin group (treated with SAA in the presence of 10 μM Indomethacin);

Group4: ODQ group (treated with SAA in the presence of 100 μM ODQ)

3.2.1.3 Calcium Channel Test

In this test, the role of calcium channels in the vasodilation induced by SAA is investigated. All samples were immersed in Ca2+-free Kreb's buffer in organ chambers and divided into two groups. The **+SAA group** contained SAA (1 mg/ml) in the buffer; the **- SAA group** did not contain SAA as a control. After pre-contraction induced by PE, $CaCl_2$ was added into both of the two groups at an accumulative concentration of between 1.56×10^{-4} M and 5.00×10^{-3} M.

3.2.1.4 Dose-Response Test with Endothelial Pathway Inhibitors

Dose-response tests were used to investigate the vascular response to the administration of SAA at a different concentration, as well as the relationship between the vasodilation extent and the concentration of SAA. We also tested whether this effect involves the endothelium. In this test, SAA was added at an accumulative concentration of up to 10 mM after PE pre-contraction. The samples were divided into four groups, and each sing group was treated with SAA in the presence of one endothelial pathway inhibitor:

Group1: Control (with no treatment);

Group2: L-NNA group (treated with SAA in the presence of 200 μM L-NNA);

Group3: Indomethacin group (treated with SAA in the presence of 10 μM Indomethacin);

Group4: ODQ group (treated with SAA in the presence of 100 μM ODQ)

In addition to SAA, other SAA-alike compounds (SalA, SalB, Coumaric Acid, Caffeic Acid and Cinnamic Acid) were also included in this test. All of the real-time dynamic vasomotor tone changes captured from the test described in Section 3.2.1 were recorded by the LabChart Pro software (AD Instruments) and saved for later analysis.

3.2.2 Chronic Effect of SAA Consumption on Endothelial Function

All of the aorta samples of used in this study were collected from the mice used in Chapter 2. The grouping and mice treatments are shown in **Table 2-1** of Chapter 2.1.1. In brief, after 1-week acclimation, the intervention was started. Methionine was prepared daily by dissolving in tap water as 1% (w/v); SAA was administrated by gastric intubation at a dose of 60 mg/kg/day, and the intervention period was 8 weeks. At the end of the intervention, mice received an overdose of pentobarbital and were dissected.

At the end of the 8-week intervention, mice were sacrificed by an overdose of pentobarbital. The aortas were freshly collected from dissected mice and immediately placed in ice-cold PBS (phosphate buffered saline). Aortic tissue was then carefully isolated from adhesive tissue under a microscope, and an aortic ring segment (2 mm length) was prepared and stabilized in the myograph system. This procedure was the same as described in Section 3.2.1. The temperature of buffer was maintained at 37°C, and an oxygen 95% and carbon dioxide (5%) mixture was supplied. After 1-h of equilibrium, the prepared aortic ring was challenged with 60 mM KCL to confirm its

bioactivity. For this, I conducted two sets of experiments to check for endothelium-dependent vasodilation and endothelium-independent vasodilation capacity on each of the collected aorta samples (collection described in Chapter 2).

3.2.2.1 Endothelium-dependent Vasorelaxation Test

Acetylcholine (Ach) was used as an endothelial-dependent vasodilator (Ach stimulates the vessel endothelium to release the NO). After KCl was washed out from the organ chambers, aorta rings were then challenged by phenylephrine (10^{-6} M) for pre-contraction until stabilized, in which the maximum tension was set as full contraction (0% of relaxation). Ach at an accumulative concentration from 10^{-9} to 10^{-6} M was then added to the buffer to determine the endothelial-dependent vasodilation.

3.2.2.2 Endothelium-independent Vasorelaxation Test

On the other hand, sodium nitroprusside (SNP) serves as a NO donor and works directly on smooth muscle cells to induce endothelium-independent vasodilation. The major process in this test was the same as 3.2.2.1, in which Ach was repeated by SNP at an accumulative concentration from 10^{-10} to 10^{-5} M for endothelial-independent dilation assessment.

After pre-contraction by PE, full contraction (0% dilation) was set at the point of maximum tension. The changes in isometric tension of the dissected aortic ring were monitored and recorded using a real-time force acquisition program, LabChart Pro

software (AD Instruments). All of the data were analyzed by LabChart Reader and statistic program SPSS 21.0 (IBM SPSS Inc., Chicago, IL, USA), and represented as mean ± SEM. Comparison among multiple groups was conducted by one-way ANOVA followed by *post hoc* Bonferroni testing. A p value of less than 0.05 was considered significant. All figures were generated using GraphPad Prism software (version 5.01, GraphPad Software Inc., San Diego, CA, USA).

3.3 Results

3.3.1 Direct Effect of SAA on Endothelial Function

3.3.1.1 Time Control Test

In the time control test, the results are expressed as a percentage of the starting tension against time. The starting point tension (100%) was set as the maximum pre-contraction induced by PE. After that, SAA (1 mg/ml) was added, and the tension change against time curve (min) was plotted (**Figure 3-2**).

After the first 5 min, the tension had increased from the starting tension (100%) to 120%. Subsequently, the aortic tissue started to relax with the presence of SAA, and the tension dropped to below 20% after 30 min of treatment. Thus, the SAA first causes a brief contraction of the aorta, followed by a strong vasodilation effect. Also, the 1 mg/ml of SAA could relax the aortic tissue by more than 80% of the PE-induced pre-contraction.

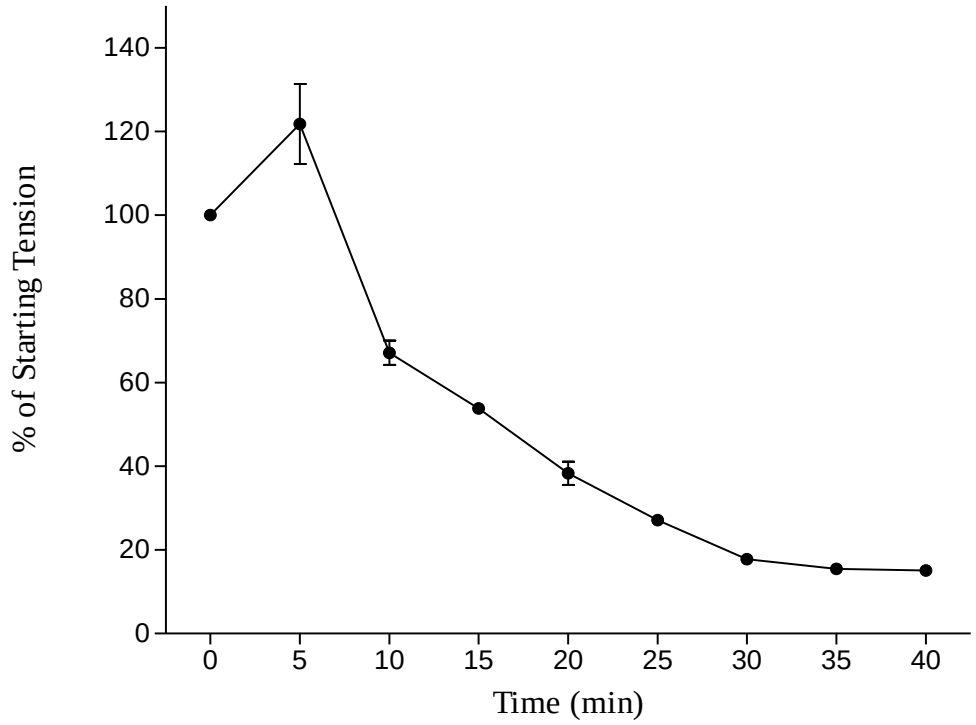

Figure 3-2. Time-response curve of the vasorelaxant test of SAA (1 mg/mL) (n = 3).

The direct vasorelaxant effect of SAA on the aortic ring. The maximum tension of PE-induced pre-contraction was set at 100% (the starting point), and the curve is blotted by tension against time.

3.3.1.2 Time-Response Test with Endothelial Pathway Inhibitors

In the time-response test, there were four groups: Group 1, control group with SAA treatment and without inhibitor; Group 2, treated with SAA plus L-NNA; Group 3, treated with SAA plus Indo; and Group 4, treated with SAA plus ODQ. The maximum tension point pre-contracted by PE was set at 100% (the starting tension), and the time-response tension changes were then observed after SAA had been added. The results are shown in **Figure 3-3**, and there were no significant differences among the tested groups up to the 40 min time point. Therefore, the vasodilation effect of SAA at 1 mg/ml could not be blocked by either NO pathway or PGI pathway inhibitors.

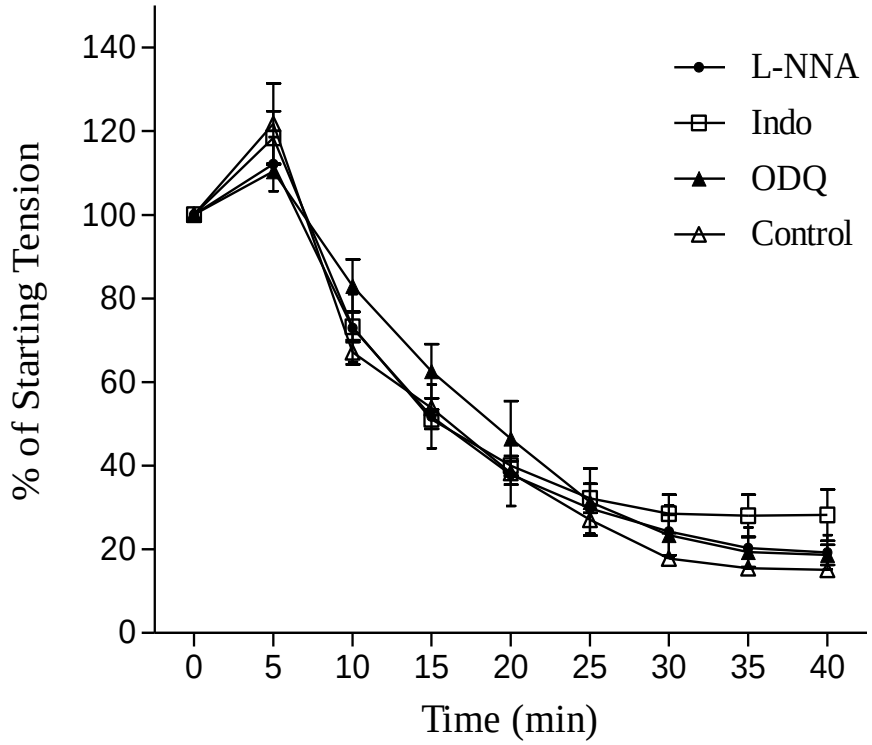

Figure 3-3. Time-response curve of the vasorelaxant test of SAA (1 mg/mL) in the presence of inhibitors (n = 3).

This time-response cure was used to express the direct vasorelaxant effect of SAA in the presence of various inhibitors (L-NNA, Indo, and ODQ). We detected no significant difference between the inhibitor-treated samples and the control.

3.3.1.3 Calcium Channel Test

There were two groups included in this test: the **+SAA group**, treated with 1 mg/ml of SAA; and the **-SAA group**, with no treatment. Samples from both two groups were incubated in a Ca^{2+}-free buffer.

At the beginning, 1 mg/ml of SAA was administrated to the **+SAA group**. Next, 10^{-6} M PE was added to the Ca^{2+}-free buffer. Up to this point, there had been no vasocontraction because of the lack of Ca^{2+}, and the stabilized tension was regarded as a baseline.

Next, $CaCl_2$ (1.56×10^{-4} M to 5.00×10^{-3} M) was added to the buffer, step-wise. Then, because of the Ca^{2+} supply, vasoconstriction could be detected, and an increase in tension (△ tension = current tension – baseline tension) was recorded. The curve of △ tension against the concentration of $CaCl_2$ was expressed (**Figure 3-4**).

As the Ca^{2+} concentration increased, the tension increased in both groups. When the $CaCl_2$ concentration reached 1.25×10^{-3} M, there was a significant difference of △ tension detected between the two groups ($p < 0.05$, 90% higher in the -SAA group than the +SAA group). This difference persisted up to the $CaCl_2$ concentration of 5.00×10^{-3} M (166.7% higher for the +SAA group compared to the -SAA group, $p < 0.001$). Therefore, the vasocontraction of the SAA containing samples was significantly inhibited compared to the without SAA group (**Figure 3-4**).

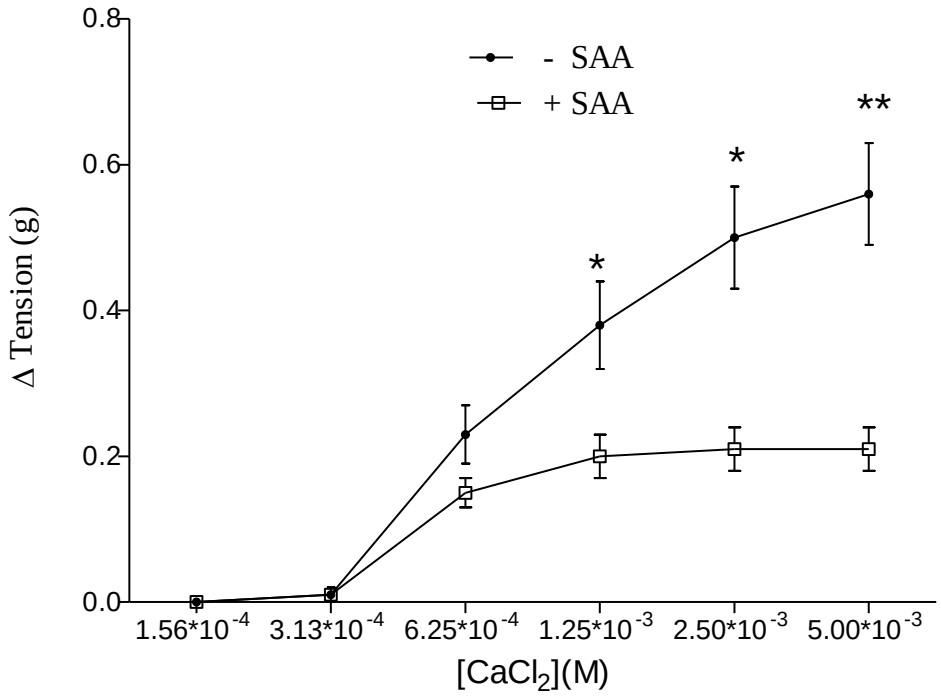

Figure 3-4. Dose-response curve of the vasoconstriction test induced by $CaCl_2$ with or without the presence of SAA (1 mg/mL) in the Ca^{2+}-free buffer (n = 9).

$CaCl_2$ was added at the accumulated concentration shown by the horizontal bar, and the change of tension was recorded against the $CaCl_2$ concentration.

*, $p > 0.05$ when comparing the +SAA and –SAA groups.

3.3.1.4 Dose-Response Test with Endothelial Pathway Inhibitors

After PE had induced full-contraction, the maximum tension point was set at 100% (the starting tension). In the control group, as the concentration of SAA increased from 0 to 0.3 mM, the aortic tissue was constricted up to 108.62 ± 5.21% (at the concentration of 0.3 mM) of the starting tension (pre-contracted by PE). At concentrations between 0.3 and 10 mM, the vasorelaxant effect of SAA started to dominate, and the isometric tension began to drop. At the final accumulated concentration (10 mM), the control group sample was dilated to 12.39 ± 0.31% of the starting tension. Compared to control group, there was no significant difference detected in the endothelial pathway inhibitor-treated groups. Therefore, it seems that neither the NO or PGI pathway significantly block the vasorelaxant effect of SAA. Finally, according to the generated control curve, the EC 50 was calculated as 2.730 mM (**Figure 3-5**).

The vasodilation effect of SalA is shown in **Figure 3-6**. The vascular tone was decreased from the top to approximately 20% of full contraction. Similar to SAA, at a lower concentration (0–0.1 mM), the preliminary effect of SalA was found to be contractive; whereas when the concentration increased, SalA starts to exhibit a vasorelaxant effect. The EC50 (median effect concentration) for SalA was 0.2942 mM (**Table 3-2**).

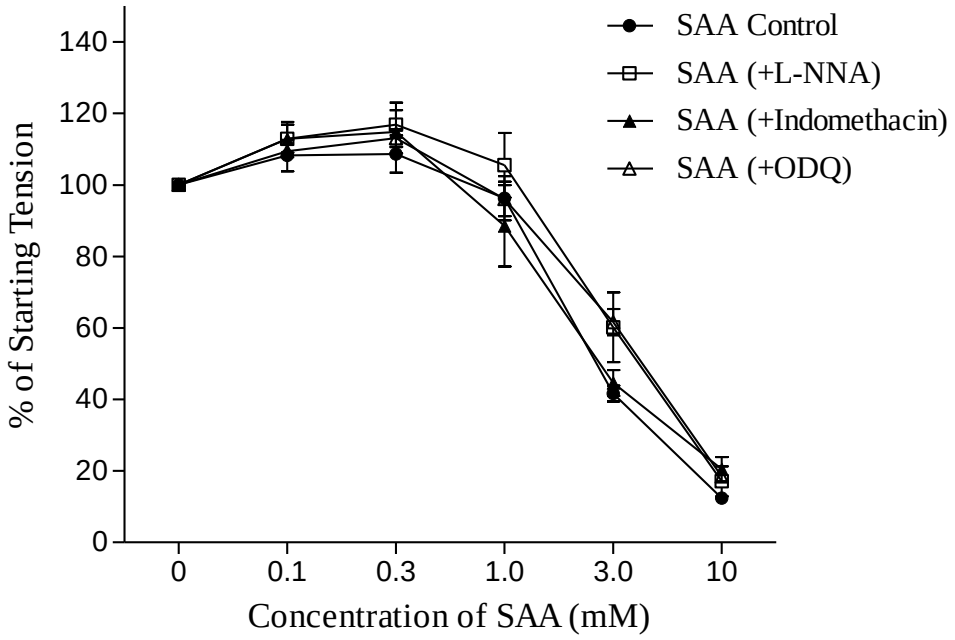

Figure 3-5. Dose-response curve of the vasorelaxant test of SAA with endothelial pathway inhibitors.

Compared to control group, we detected no significant difference ($p > 0.05$) for the groups treated with inhibitors.

In the vasodilation effect test of SalB (**Figure 3-6**), at the beginning (0–0.1 mM SalB), the vascular tone remained above 80% of the starting tension. However, as the concentration increased, SalB began to induce vasorelaxation (up to ~20%). Among the inhibitors, ODQ inhibited the SalB induced-relaxation most compared to the control groups, but this did not reach statistical significance ($p > 0.05$). Finally, the calculated EC50 was 0.4725 mM and is summarized in **Table 3-2**.

In the vasodilation effect test of Coumaric Acid (**Figure 3-6**), at the highest concentration (3 mM), Coumaric Acid -induced vasorelaxation reach just 80% of the starting tension. We detected no significant differences between the inhibitor-treated and control groups. The EC50 of Coumaric Acid was 47.04 mM (**Table 3-2**).

In the vasodilation effect test of Caffeic Acid (**Figure 3-6**), up to the highest concentration (3 mM), Caffeic Acid-induced vasorelaxation remained above 80% of the starting tension. This indicates that the vasorelaxant efficiency of Caffeic Acid was very low, and the EC50 was estimated to be > 2000 mM (**Table 3-2**). Moreover, there was no significant difference found between the inhibitor and control groups. The Cinnamic Acid data were similar to those of Caffeic Acid (**Figure 3-6** and **Table 3-2**).

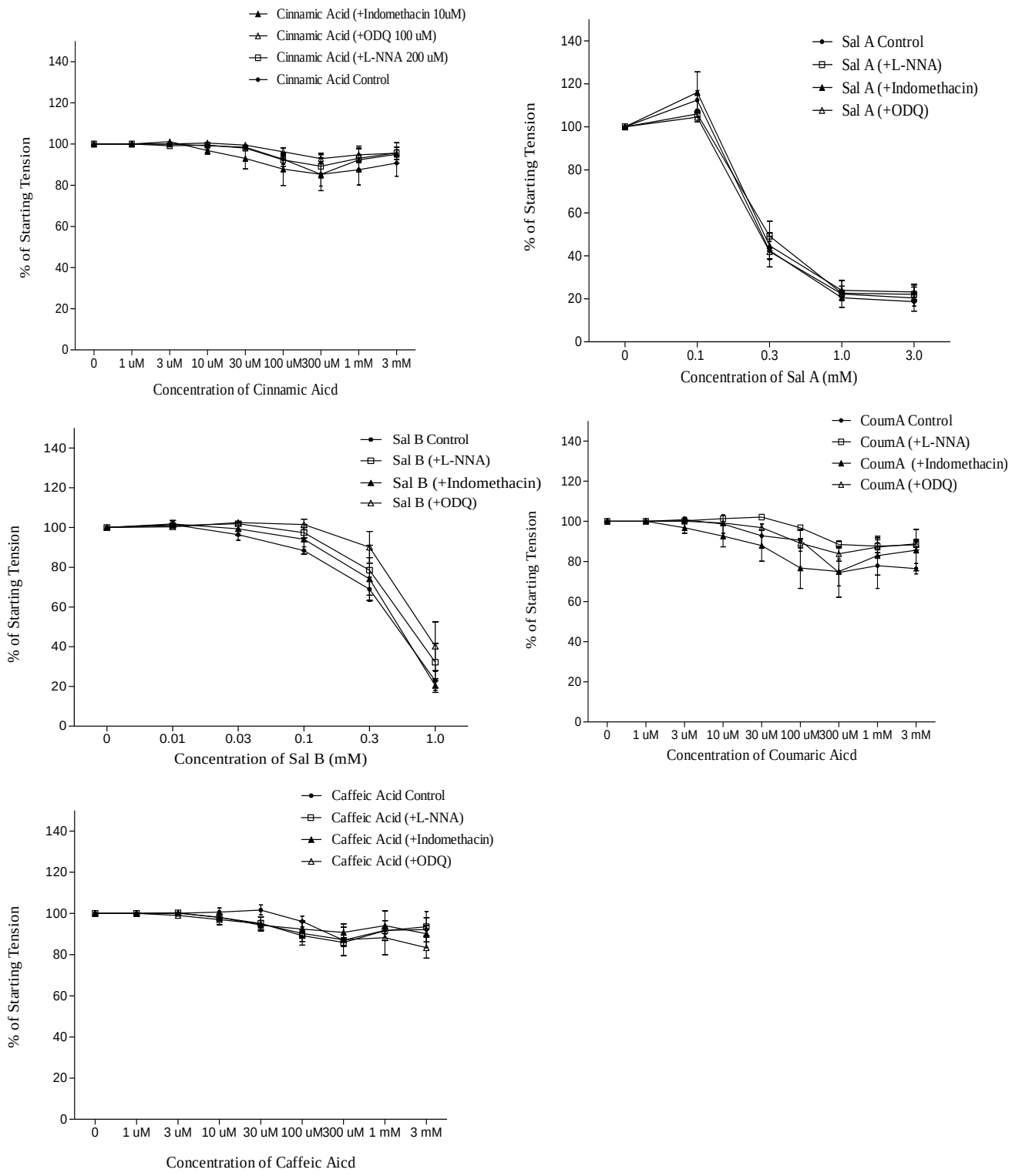

Figure 3-6. Dose-response curve of the vasorelaxant test of SalA, SalB, Coumaric Acid, Cinnamic Acid and Caffeic Acid in the presence of endothelial pathway inhibitors.

Comparing samples with inhibitors to the control, the *p* value was > 0.05 for all tested compounds.

Table 3-2. EC50 of the dose-response curve of all tested compounds in this study.

Compound	EC50
Salvianolic Acid A	0.2942mM
Salvianolic Acid B	0.4725mM
SAA	2.730mM
Coumaric Acid	47.04mM
Caffeic Acid	>2000mM
Cinnamic Acid	>3000mM

The EC50 value indicates the median effect concentration point of the selected compounds when the vasorelaxation range arrived at 50% of full pre-contraction, as calculated from the dose-response curve.

3.3.2 Chronic Effect of SAA Consumption on Endothelial Function

The result of endothelium-dependent vasodilation and endothelium-independent vasodilation capacity on each dissected aorta sample (collection described in Chapter 2) were summarized using concentration-dependent relaxation curves and expressed in **Figure 3-7** and **Figure 3-8** respectively. At the concentration of 10^{-9}–10^{-7} M of Ach, a significant reduction in the percentage of Ach-induced relaxations was observed in all diabetic groups compared to the non-DM group ($p < 0.05$ for all diabetic groups). From $10^{-6.5}$ to 10^{-6} M, this significant decline of endothelial-dependent relaxations of DM (control) and DM (SAA) was gradually attenuated ($p > 0.05$), whereas the DM (Methionine) group has a continuously impaired Ach-induced vasorelaxation compared to the non-DM group ($p < 0.001$, except for the starting point at $p < 0.05$). Compared to the DM (Methionine) group, the percentage of relaxation induced by Ach in DM (SAA + Methionine) group was not improved until the Ach reach a concentration of 10^{-6} M ($p < 0.05$). Conversely, the percentage of relaxation induced by SNP in all groups were similar, except at the concentrations between 10^{-9} and 10^{-7} M, where a significantly diminished relaxation was observed in the DM (Methionine) group compared to the non-DM group ($p < 0.05$).

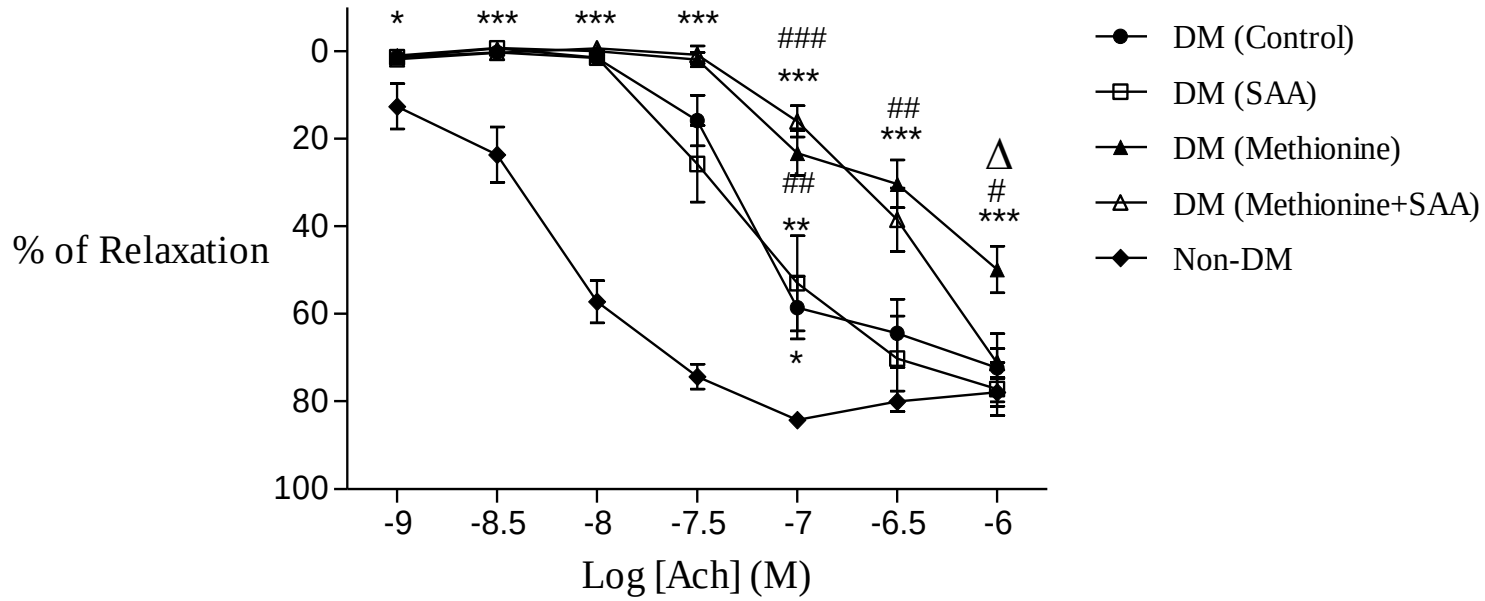

Figure 3-7. Endothelium dependent vasorelaxation test induced by acetylcholine (Ach) (Gao, Siu et al. 2017).

*, $p < 0.05$; **, $p < 0.01$; ***, $p < 0.001$ compared with **non-DM** group;

#, $p < 0.05$; ##, $p < 0.01$; ###, $p < 0.001$ compared with **DM (control)** group;

△, $p < 0.05$ compared with **DM (SAA)** group.

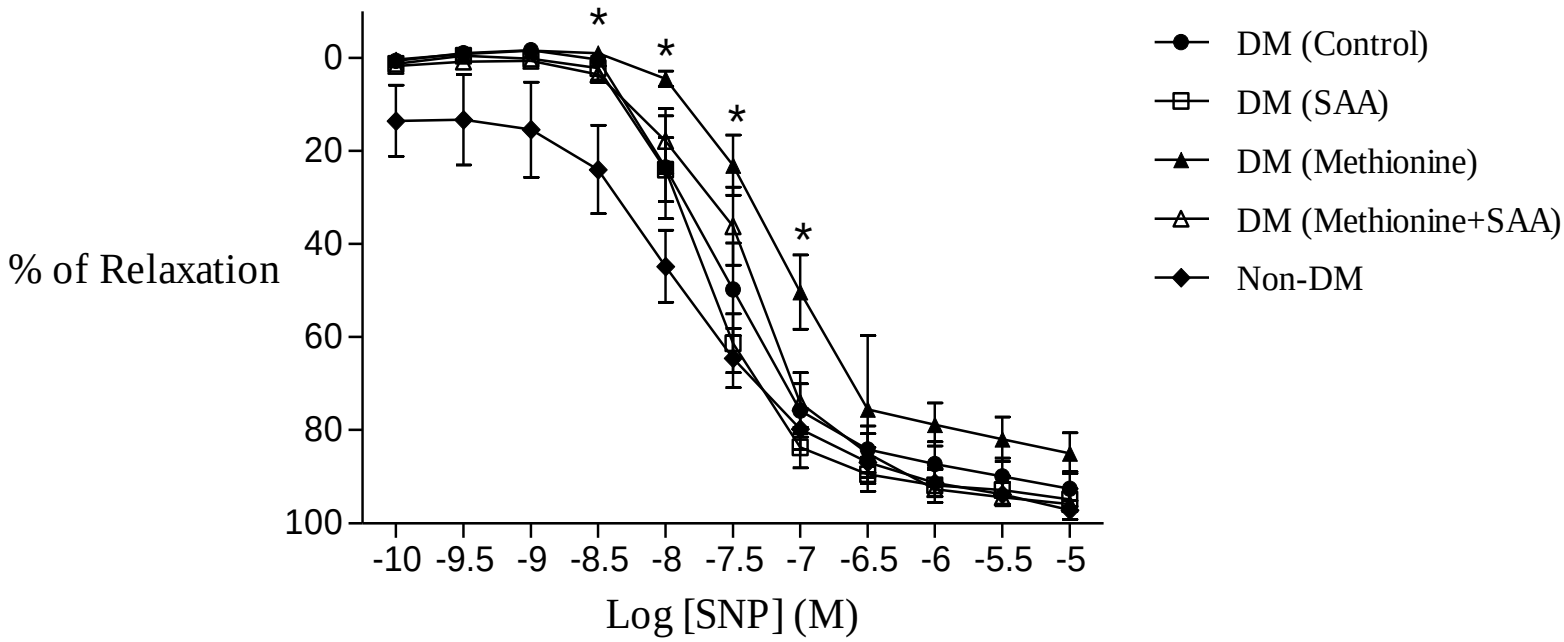

Figure 3-8. Endothelium-independent vasorelaxation test induced by sodium nitroprusside (SNP) (Gao, Siu et al. 2017).

*, $p < 0.05$, compared with the **non-DM** group.

3.4 Discussion

Testing the direct vasorelaxant effect of SAA, we found that acute administration of SAA has a vasorelaxant effect, which is consistent with previous studies (Lam, Yeung et al. 2007; Zhang, Zou et al. 2010).

In our study, a biphasic effect on the vascular tone was detected in the test with direct administration of SAA. At low SAA concentrations, some vasocontraction was detected, which is in line with the findings of a previous study with rat femoral arteries (Wang, Fan et al. 2013). It has been suggested that the vasocontraction induced by low concentration of SAA is mediated by the transient enhancement of Ca^{2+} influx, which might be inhibited in Ca^{2+}-free buffer (Zhang, Zou et al. 2010).

However, in our later experiments, as the concentration of SAA increased, a dominant vasorelaxation effect was observed, and the remaining tests indicated this effect was time-dependent and dose-dependent. Consistently, in previous *in vivo* studies, the origin herb *Danshen* has been shown to induce hypotension in a rat model (Li, Yung et al. 1990), in which the vasorelaxant effect also overwhelmed the vasocontraction effect. As a major ingredient of *Danshen* extract, SAA was shown to exert a similar biphasic effect on vascular tone.

In the Ca^{2+} channel test, SAA could significantly inhibit the Ca^{2+}-induced vasocontraction compared to the sample without SAA treatment. This result shows that SAA can regulate vascular activity in a Ca^{2+} channel-dependent manner, which is in line with previous studies. In a very similar way, in previous experiments with rat thoracic aorta, the authors reported that SAA could block intracellular Ca^{2+} influx, thereby inhibiting the vasocontraction induced by $CaCl_2$ in the Ca^{2+}-free buffer (Zhang,

Zou et al. 2010).

In the later test, endothelial pathway inhibitors were added together with SAA. As a significant mediator in the generation of NO, soluble guanylyl cyclase (sGC) works through upregulation of the cGMP level. As a specific inhibitor of sGC, 1H-[1,2,4] oxadiazolo[4,3,-a]quinoxalin-1-one (ODQ) was utilized in this test. Indomethacin (INDO) served as COX inhibitor and Nω-nitro-L-arginine (LNNA) as nitric oxide synthase inhibitor. We found that the direct vasorelaxant effect of SAA cannot be significantly inhibited by endothelial pathway inhibitors, suggesting that the SAA-induced vasorelaxation is endothelium-independent, which is in line with a previous study (Lam, Yeung et al. 2007).

In contrast, in another test with SAA injection for the treatment of CVD, the injection induced a significant acute vasorelaxation in an endothelium-dependent pathway (Wang, Fan et al. 2013) via upregulation of COX-2 gene expression and prostacyclin production, rather than via the NO/eNOS pathway. Therefore, there seems to be an inconsistent conclusion between the *in vitro* and *ex vivo* experiments in terms of the mechanism involved in the SAA-induced vasorelaxation.

From the result of the vasorelaxation test with compounds such as SalA and SalB, SAA can reach a maximum range of vasorelaxation at around 20% of the starting tension at their final tested concentrations. However, the Coumaric Acid, Caffeic Acid and Cinnamic Acid remain above 80% of the precontraction at their final concentration. Notably, when compared to the sample treated with a NO pathway blocker (Indo, ODQ or L-NNA), there is no significant difference between the treated groups and the control group for all tested compounds. This phenomenon seems to reveal that, none

of these compounds is exhibiting the vasorelaxation effect via a NO-mediated or PGI-mediated pathway. Therefore, the vasorelaxation effect of these compounds worked through an endothelium-independent pathway in the acute administration condition.

As a comparison, Coumaric Acid, Caffeic Acid, and Cinnamic Acid did not exhibit any observable vasorelaxation effect even though the concentration reached up to 3 mM. Our EC50 result suggests that, among all of the tested compounds, SalA is the most efficient, followed by SalB, whilst the caffeic Acid and Cinnamic Acid-induced almost no vasodilation by the acute administration. In contrast, the family-source chemical SalA and SalB, which contained one or more SAA molecules, could induce even greater vasorelaxation than SAA. However, the chemical structure responsible for this effect could not be clearly determined, and further investigation with more derivates with similar structures will be needed to address this.

In the present study, after the 8-week administration, SAA was shown to be able to ameliorate the detrimental effect by hyperglycemia and/or elevated Hcy level in the endothelium-dependent vasorelaxation test induced by Ach. The endothelium-independent vasorelaxation induced by SNP indicates that the impaired vasorelaxation caused by hyperglycemia and/or elevated Hcy level is due to nitric oxide (NO) bioavailability (i.e., proper function of the endothelial cells), rather than NO insensitive (i.e., with adequate NO provided by SNP, the vessel can be expanded to the full extent). Moreover, the additive detrimental effects of hyperglycemia and elevated Hcy level on endothelial function in the DM (Methionine) group were evidenced by a relatively lower percentage of Ach-induced vasorelaxation at any concentration compared to the DM (control) group. Consistently, this endothelial protective effect of SAA has also been indicated in a previous *in vitro* study, and SAA has even been shown

to reverse the oxidative harm induced by high Hcy level incubation.

Generally, both the chronic and direct administration of SAA exhibit a protective effect on vasorelaxation capacity. In the direct administration condition, SAA induces vasorelaxation in a dose-dependent and time-dependent manner. The underlying mechanism for this might be the inhibition of the intracellular influx of Ca^{2+} and is endothelium-independent. Interestingly, the chronic administration of SAA significantly improves the vasorelaxation capacity via an endothelium-dependent manner.

To conclude, in the direct administration of SAA condition, SAA mainly served as a Ca^{2+} antagonist working on the smooth muscle cell to inhibit vasoconstriction. However, in the chronic treatment condition, SAA might protect the endothelium from oxidative damage induced by DM status and elevated Hcy status via activation of signaling pathways related to NO and/or PGI2. Further studies in terms of the detailed mechanism are required.

Chapter 4 The Hcy-lowering Effect of SAA in Diabetes with Elevated Homocysteine Level

4.1 Introduction

Homocysteine (Hcy) has been recognized as an independent CVD risk factor and predictor because of the strong correlation between elevated Hcy level and cardiovascular mortality (McCully 1969; Collaboration 2002). Elevated Hcy level has a stronger predictive power than classic CVD risk factors such as blood pressure, smoking, and electrocardiogram (De Ruijter, Westendorp et al. 2009). Additionally, the Hcy level has been reported to be higher in people with DM than people without DM (Emoto, Kanda et al. 2001). Reasons for this could be the altered activities of significant enzymes involved in regulating Hcy metabolism [e.g., cystathionine b-synthase (CBS) and 5,10-methylenetetrahydrofolate reductase (MTHFR)] (Fonseca, Dicker-Brown et al. 2000). Besides, diabetic patients are suffering from an extra risk of developing elevated Hcy level because of folate and vitamin B12 absorption disorder induced by metformin administration (Bauman, Shaw et al. 2000; Sahin, Tutuncu et al. 2007; Wile and Toth 2010).

Hcy is metabolized in two pathways, the trans-sulphuration, and remethylation pathways. Under the remethylation pathway, methionine is given an adenosine group from ATP and formulates S-adenosyl methionine (SAM). Following the methyl transfer reaction, S-adenosylhomocysteine (SAH) is formed and then rehydrolyzed by SAH hydrolase to regenerate adenosine and Hcy. The Hcy formed is then remethylated to methionine, which is catalyzed by methionine synthase. On the other hand, cysteine is generated with vitamin B6 as an essential cofactor if the Hcy is metabolized through the trans-sulphuration pathway. It is important to note that the cysteine synthesis could serve as a significant endogenous glutathione resource, which provides a significant

source for redox balance.

However, up to now, there has been no consistent conclusion about the therapeutic effect of treatment of elevated Hcy level, such as vitamin or folic acid supplement (NARIN, Narin et al. 2002; Huang, Chen et al. 2012). In a previous rat experiment, SAA exhibited a beneficial effect on elevated Hcy level (Cao, Chai et al. 2009), suggesting the Hcy-lowering potential. Therefore, the aim of study in this chapter is to investigate any Hcy-normalizing effect induced by SAA treatment and whether this effect is associated with the upregulation of the trans-sulphuration pathway.

4.2 Methods

4.2.1 Animals and Experiment Design

All analyzed samples in this chapter were collected from the mice used in Chapter 2. The grouping and treatment protocols were the same as shown in **Table 2-1**. In brief, after 1-week of acclimation, the intervention was started. Methionine (1% w/v) was dissolved in tap water; SAA was administrated by gastric intubation at a dose of 60 mg/kg/day, and the intervention period was 8 weeks.

At the end of the intervention, all mice received an overdose of pentobarbital and were dissected, and the blood was collected from the heart and placed on ice. Then, the whole blood was centrifuged at 13000 rpm (4°C) for 15 min. The serum was then moved to new tubes, snap frozen by liquid nitrogen, and stored at -80°C for later high-performance liquid chromatography (HPLC) analysis.

4.2.2 Serum Homocysteine Analysis

The serum Hcy levels were measured by HPLC, as described previously with minor modification (Nolin, McMenamin et al. 2007). The materials used are listed in **Appendix B** (**Figure 4-1**).

Figure 4-1. Equipment used to measure serum Hcy levels by HPLC.

A Waters 2695 Module (right), which was used to separate the serum sample. A Waters 474 Detector (left) was used to capture fluorescent signal of Hcy and thus determine the serum Hcy level.

Mobile phases A was a 50 mM KH_2PO_4 water solution (pH 5.0); mobile phases B was 50% (v/v) Methanol in 50 mM aqueous KH_2PO_4 (pH 5.0); the detector was adjusted for detection by fluorescence at an excitation wavelength of 385 nm; emission wavelength of 515 nm; autosampler temperature of 4°C; gradient program for elution; and 10 min per run for each injection. To equilibrate the columns before sample running, mobile phase A only was injected for the first two injections. The running program is given in **Table 4-1**, and a sample HPLC chromatogram of homocysteine was shown in **Figure 4-2**.

Table 4-1. Flow speed and duration of mobile phase A and B in the HPLC running program for the assessment of serum Hcy level.

Time (min)	**Flow (mL/min)**	A%	B%
-	**1.2**	97	3
5.0	**1.2**	97	3
5.1	**1.2**	45	55
8.0	**1.2**	45	55
8.1	**1.2**	100	0
9.0	**1.2**	100	0
9.1	**1.2**	97	3
10.0	**1.2**	97	3

A%, the percentage of mobile phase A, which is a 50 mM KH_2PO_4 water solution (pH 5.0); B%, the percentage of mobile phases B, which is a 50% (v/v) Methanol solution in 50 mM aqueous KH_2PO_4 (pH 5.0).

4.2.3 Liver SAM, SAH, GSSG and GSH Analysis

SAM and SAH levels in the liver tissues were determined following the instructions of a commercial ELISA kits (item no. IK00202S and IK00302S, Arthus Biosystems, LLC, Richmond, CA, USA). The glutathione (GSH) and glutathione disulfide (GSSG) levels in the liver were determined using a glutathione assay kit (item no. 703002, Cayman Chemical, Ann Arbor, Michigan, USA).

4.3 Results

Elevated SAM level in the liver was observed in the DM (Methionine) group compared to the non-DM (114.5%, $p < 0.05$) and DM (SAA) (160.8%, $p < 0.05$) groups, while the liver SAH level in the DM (SAA+ Methionine) group was increased compared to the DM (SAA) (112.0%, $p < 0.05$) and non-DM (116.3%, $p < 0.001$) groups. Moreover, the SAM/SAH ratio in the DM (SAA+ Methionine) group was significantly lower when compared to DM (control) (70.7%, $p < 0.01$). A reduced GSH level in the liver was observed in the DM (Methionine) (28.5%, $p < 0.001$) and DM (control) (29.0, $p < 0.001$) groups when compared to the non-DM groups. An elevated GSH level was also observed in the DM (Methionine + SAA) group when compared to the DM (Methionine) (23.2%, $p < 0.05$) group. In addition, a reduced GSSG level in liver was observed in both the DM (SAA) (45.6%, $p < 0.05$) and DM (Methionine) (50.0%, $p < 0.05$) groups when compared to the non-DM group. Interestingly, the GSH/GSSG level was significantly improved and elevated in the DM (SAA) group when compared to the DM (control) (125.4%, $p < 0.05$) and non-DM (122.1%, $p < 0.05$) groups. All results are summarized in **Figure 4-3**, **Table 4-2**, and **Table 4-3**.

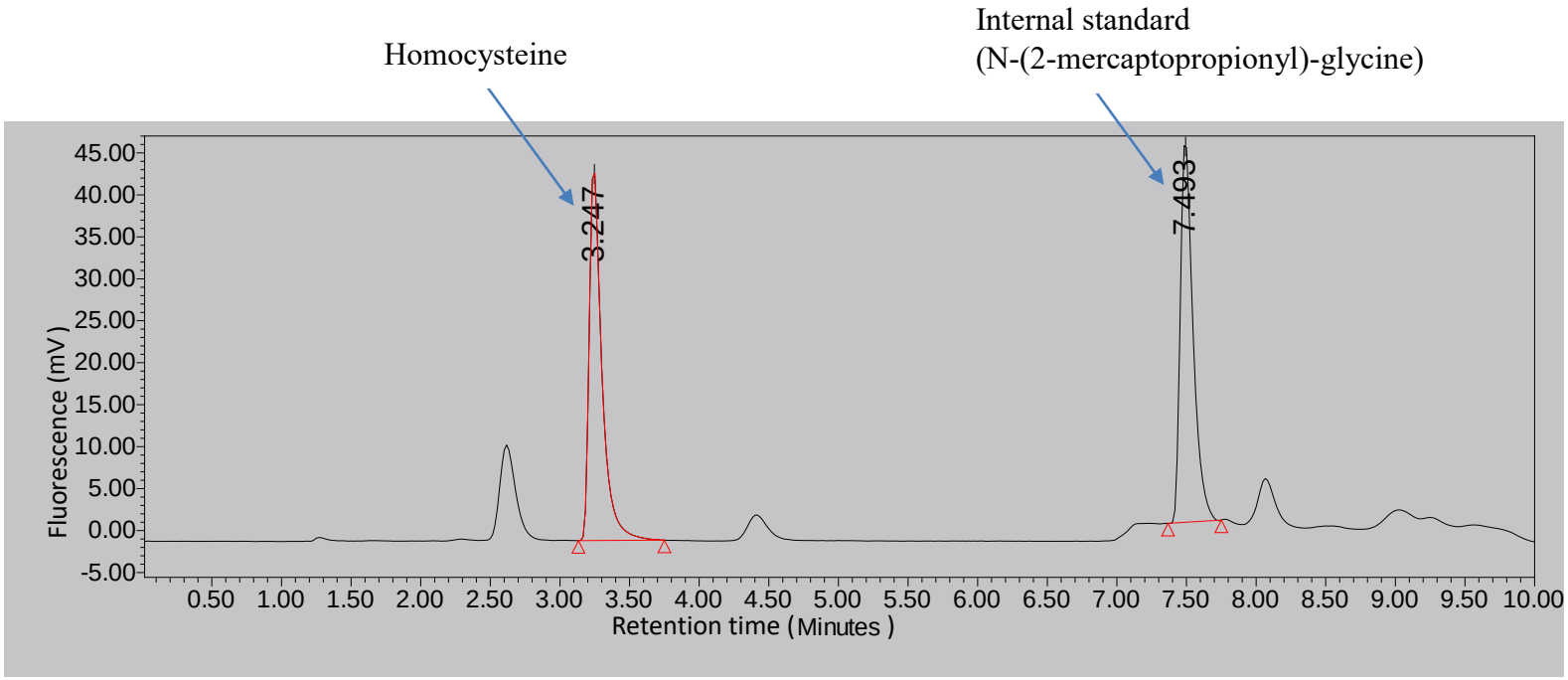

Figure 4-2. Sample HPLC chromatogram of homocysteine.

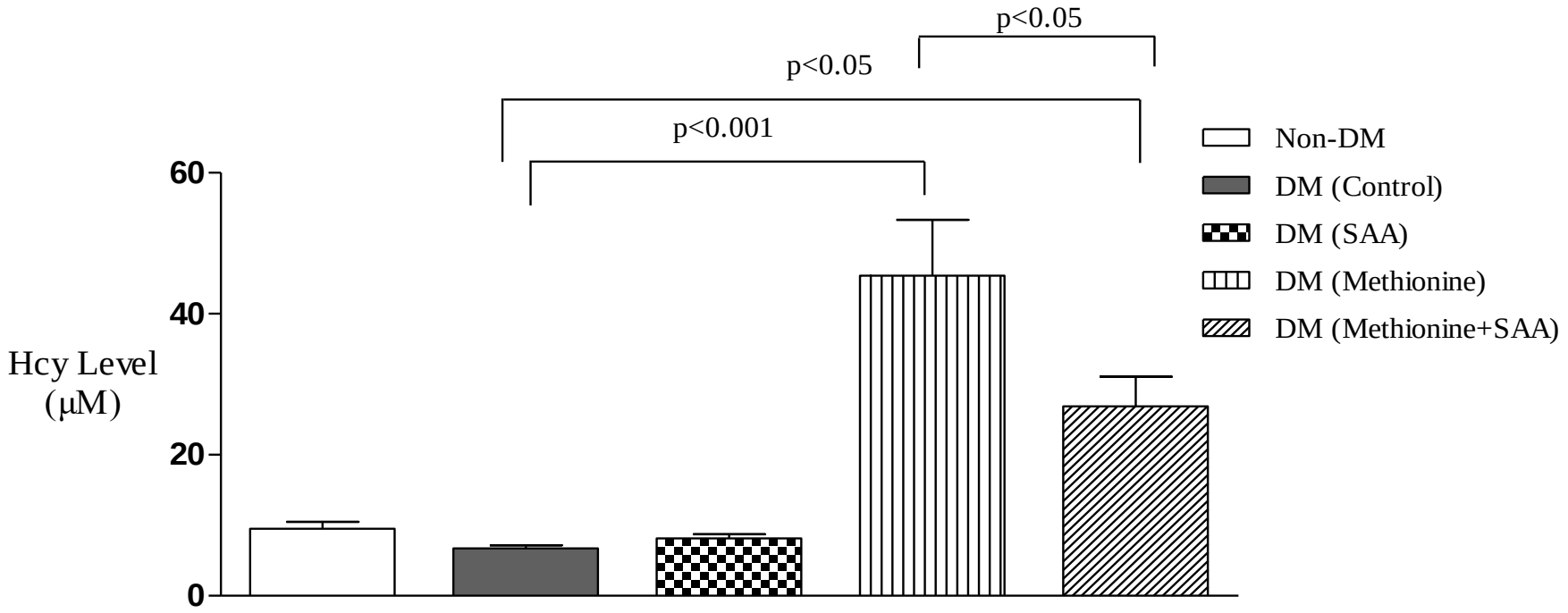

Figure 4-3. Serum homocysteine (Hcy) level at the end of the experiment (Gao, Siu et al. 2017).

$p < 0.05$ when comparing the DM (Methionine + SAA) and DM (Methionine) groups; $p < 0.05$ when comparing the DM (Methionine + SAA) and DM (control) groups; $p < 0.001$ when comparing the DM (Methionine + SAA) and DM (control) groups.

Both the **DM (Methionine) and DM (Methionine+ SAA)** groups exhibit a significantly higher Hcy level than the **DM (control)** group. Moreover, the Hcy level in the **DM (Methionine+ SAA)** group was reduced to a level significantly lower than in the **DM (Methionine)** group, likely due to the Hcy-lowering effect induced by the 8-week SAA treatment.

Table 4-2. The liver methylation status of mice at the end of the experiment (Gao, Siu et al. 2017).

	DM (Control)	DM (SAA)	DM (Methionine)	DM (Methionine +SAA)	Non-DM
SAM(μg/g)	0.101±0.01	0.051±0.003	0.133±0.021*	0.089±0.011	0.062±0.007
SAH(μg/g)	0.112±0.027	0.100±0.027**	0.156±0.010	0.212±0.024	0.098±0.025***
SAM/SAH Ratio	1.57±0.75***	0.94±0.37	0.86±0.13	0.46±0.08	0.93±0.19

SAM, S-adenosyl-L-methionine; **SAH**, S-Adenosyl-L-homocysteine.

All values are expressed as concentration (μg/g) per 1 g of liver tissue.

* $p = 0.01$ versus the **Non-DM** and **DM (SAA)** groups.

** $p < 0.05$ versus the **DM (Methionine +SAA)** group.

*** $p < 0.01$ versus the **DM (Methionine +SAA)** group.

Table 4-3. GSH, GSSG, and oxidative stress (GSH/GSSH ratio) in the liver tissue of mice at the end of the experiment (Gao, Siu et al. 2017).

	DM (Control)	DM (SAA)	DM (Methionine)	DM (Methionine +SAA)	Non-DM
GSH (mg/g)	3.04±0.13[a,c]	3.53±0.17[b]	3.06±0.17[a,c]	3.77±0.10	4.28±0.18
GSSG (mg/g)	0.85±0.17	0.62±0.21*	0.57±0.06*	0.78±0.07	1.14±0.12
Oxidative stress (GSH/GSSG ratio)	4.05±0.47[**]	9.13±2.24	5.60±0.47	5.20±0.58	4.11±0.45[**]

GSH, glutathione; **GSSG**, oxidized glutathione.

[a]$p < 0.001$ versus the **Non-DM** group

[b]$p < 0.05$ versus the **Non-DM** group.

[c]$p < 0.05$ versus the **DM (Methionine +SAA)** group.

[*]$p < 0.05$ versus the **Non-DM** group.

[**]$p < 0.05$ versus the **DM (SAA)** group.

4.4 Discussion

In the present study, elevated Hcy level in *db/db* mice was successfully induced using 1% (w/v) methionine in water for 8 weeks and was evidenced by a nearly 3-fold increase relative to those not given methionine (**Figure 4-3**). Moreover, our results indicate that SAA does not affect the plasma Hcy level in diabetic mice with a normal level of Hcy, while clearly lowering the plasma Hcy level in the diabetic mice with elevated Hcy level. This observation suggests that the beneficial effect of SAA in lowering Hcy level is largely dependent on the baseline initial value of the plasma Hcy level in *db/db* mice. A previous study reported a similar bi-directional effect of SAA on the Hcy-lowering effect in a rat model (Cao, Chai et al. 2009).

The SAH levels were elevated in the two groups with elevated Hcy level. The SAH level is usually high in subjects with elevated Hcy level because the process of re-methylation is a reversible process that is catalyzed by SAM and is always at equilibrium due to the high activity of SAH (Martinov, Vitvitsky et al. 2000). As a powerful catechol-O-methyltransferase inhibitor, SAH specifically dominates the methylation of polyphenols, such as SAA (Rivett and Roth 1982; Cao, Chai et al. 2009). Moreover, a high expression of SAH and low methylation potential would inhibit methylation and thus limit the Hcy-lowering capability. In the **DM (SAA+ Methionine)** group, the Hcy level was half that of the **DM (Methionine)** group. At the same time, the SAM/SAH ratio or methylation potential was lower in the groups treated with SAA, suggesting that, after SAA treatment, the methylation capacity became lower. Therefore, it is likely that re-methylation of Hcy by SAA treatment has been largely inhibited by the elevated SAH level in the **DM (SAA+ Methionine)** group, suggesting that the observed Hcy-lowering effect by SAA treatment in diabetic

mice with elevated Hcy level is most likely through the trans-sulphuration pathway. A previous study reported a similar finding, where SAA markedly attenuated elevated Hcy level through enhanced production of cysteine and GSH via the trans-sulphuration pathway in rats (Cao, Chai et al. 2009). In addition to being a potent antioxidant, the enhanced production of GSH via the trans-sulphuration pathway under the bidirectional effect of SAA treatment (i.e., only effective under elevated Hcy level status but not normal Hcy status) partly explains the observed higher degree of cardiovascular protective effects against LVH and ED in the diabetic mice with elevated Hcy level.

The GSH level in the **DM (SAA+ Methionine)** group was higher than that of the **DM (Methionine)** group after 8 weeks of intervention. This observation further supports our postulation that SAA can normalize the Hcy level in the diabetic mice with elevated Hcy level, predominately by activation of the trans-sulphuration pathway and production of more GSH. The significance of the trans-sulphuration pathway in the maintenance of the redox homeostasis has been mooted (Mosharov, Cranford et al. 2000; Deplancke and Gaskins 2002) based on the finding that it provides an endogenous pathway for Hcy conversion into GSH, a potent antioxidant (Martinov, Vitvitsky et al. 2000; Vitvitsky, Mosharov et al. 2003). As an important intracellular antioxidant, GSH plays a significant role in redox balance and cell apoptosis (Cho, Lee et al. 2001; Dickinson and Forman 2002; Franco and Cidlowski 2009; Marí, Morales et al. 2009). GSSG is the oxidized form of glutathione, and the ratio between GSH and GSSG is fundamental for maintaining a balanced redox status (Jones, Carlson et al. 2000; Noctor, Gomez et al. 2002). I found that oxidative stress was greatly improved in the **DM (SAA)** group compared to the **DM (control)** and **non-DM** groups. An imbalance in the redox status leads to the onset and progression of many

cardiovascular diseases, including LVH and ED. Therefore, the ability of SAA treatment to enhance production of GSH via the trans-sulphuration pathway in diabetic mice with elevated Hcy level, as well as to improve oxidative stress in diabetic mice with normal Hcy levels, likely promotes the cardiovascular protection via redox regulation.

In this study, greater oxidative stress was noted in diabetes, as indicated by the lower GSH pool size in the DM (control) group compared to the **non-DM** group. In the setting of diabetes, GSH depletion caused by disturbed trans-sulphuration could lead to an oxidant/antioxidant imbalance, and impaired trans-sulphuration could cause the loss of the compensatory GSH synthesis in response to oxidative stress, which would lead to further oxidative stress (Mosharov, Cranford et al. 2000; Vitvitsky, Mosharov et al. 2003). From our observation, the trans-sulphuration pathway activated by SAA treatment is likely to be a potential target for Hcy-lowering and redox rebalancing in both hyperglycemic and hyperhomocysteinemic settings. Although the key players in the trans-sulphuration pathway, such as cystathionine and cysteine levels, were not identified in our experiments, the relatively higher GSH levels in the liver of our diabetic mice with elevated Hcy level after SAA treatment suggest that SAA can increase the activity of the trans-sulphuration pathway as a means of lowering the Hcy level.

GSH reduction was reported as a crucial cause of cardiac cell apoptotic death in diabetic rats, and supplement of GSH could prevent the diabetic rat from heart disease by reversing cell apoptosis and mitochondrial oxidative stress (Ghosh, Pulinilkunnil et al. 2005). In the present study, the increased intracellular GSH production by SAA treatment contributed to the reversal of the redox imbalance, normalizing the NO

bioactivity and protecting the endothelial cell from free radical harm. Taken together, SAA is an important endogenous antioxidant, works as an exogenous antioxidant against ROS-induced harm, and promotes the endothelial function in the heart. Therefore, SAA intervention is able to protect the heart from cardiac hypertrophy in diabetic cardiomyopathy. Moreover, the elevated GSH level after SAA treatment provides another explanation for the overall improved antioxidant activity of SAA in protecting against LVH and ED. Further studies should now address the key players in the trans-sulphuration pathway, as well as the underlying mechanism/signaling pathway of cardiovascular protective effects by SAA treatment in DM with elevated Hcy level.

Chapter 5 Antidiabetic Effect of SAA

5.1 Introduction

Researchers have been reporting an overt cardioprotective effect of SAA for decades. However, compared to its outstanding improvement property on the vascular system, researchers have rarely investigated the antidiabetic effect of SAA. The α-glucosidase inhibitory assay is a classical test to investigate the antidiabetic effect of compounds from natural plants (Önal, Timur et al. 2005). α-glucosidase, or α-D-glucoside glucohydrolase, is an exo-type carbohydrase widely existing in animal tissue and plants, which catalyzes the release of a-glucose by hydrolyzing terminal non-reducing (1,4) linked α -D-Glucose (Kimura, Lee et al. 2004). Therefore, inhibitors of α-D-glucoside could attenuate this reaction, thus decrease the amount of α-D-Glucose in the blood, especially after a high-carbohydrate meal (Lebovitz 1997). The structure of the α-glucosidase substrate and reaction formula are shown in **Figure 5-1**.

In humans, α-glucosidase is found in the brush border of the small intestine and breaks down starch and disaccharides to α-D-Glucose. There are two subunits within molecule with different substrate specificities, in which the N-terminal catalytic domain has high activity against maltose, while the C-terminal catalytic domain has high activity against glucose oligomers. This assay is performed with the substrate p-nitrophenol-D-glucopyranoside (*p*NPG), which reacts with the enzyme and generates a yellow product, p-nitrophenol (*p*NP), which can be detected at 405 nm using a microplate reader.

Acarbose, as a typical antidiabetic drug, acts as a glucosidase inhibitor via prohibition of the intestinal absorption of glucose, thereby decreasing the postprandial glucose peak in the plasma (Hakamata, Kurihara et al. 2009).

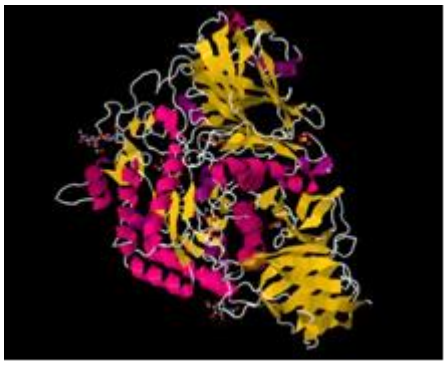

A

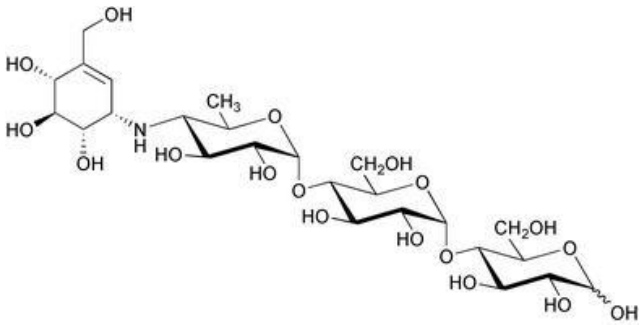

B

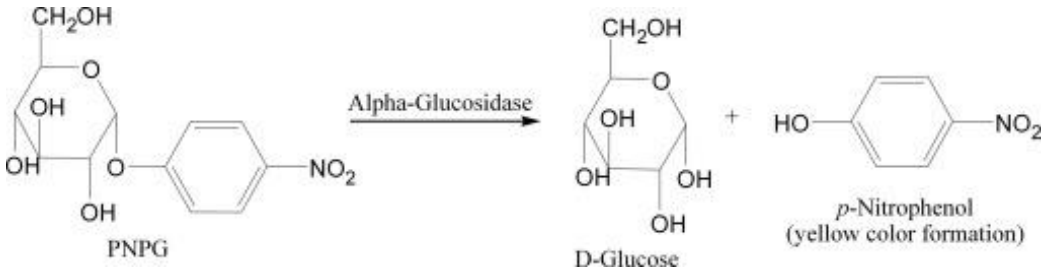

C

Figure 5-1. A structural explanation of the α-glucosidase inhibitory assay (Srianta, Kusumawati et al. 2013).

A, A 3D-view of human α-glucosidase;

B, The chemical structure of acarbose;

C, The reaction formula of the hydrolysis of p-nitrophenyl alpha-D-glucopyranoside by α-glucosidase

In Chapters 2 and 3, it was shown that SAA has cardioprotective potential that can protect diabetic mice from CVD, in which I have addressed the antioxidant, endothelial-protective, heart-protective, and Hcy-lowing effects. Subsequently, in this chapter, I discuss the *in vitro* antidiabetic effect of SAA. The aim of this chapter was, therefore, to investigate whether there is any direct antidiabetic effect could be induced by SAA using an α-glucosidase inhibitory assay, and to detect the α-glucosidase inhibitory activity of some additional compounds that have a similar chemical structure to that of SAA. To my knowledge, this is the first time that SAA has been tested with this method for the investigation of its antidiabetic potential.

5.2 Methods

The α-glucosidase inhibitory assay was done as previously reported with minor modifications (Dej-adisai and Pitakbut 2015). To search for SAA-like compounds, its chemical structure was submitted to the National Center for Biotechnology Information Structure Database (Kim, Thiessen et al. 2015), returning compounds with a highly similar chemical structure to SAA. Considering the solubility and stability of the required solvent of the α-glucosidase inhibitory assay, four SAA-like compounds were selected for testing:

1. Caffeic acid
2. 4-coumaric acid (Coumaric Acid)
3. Salvianolic Acid A (SalA)
4. Salvianolic Acid B (SalB)

The chemical structures and source of all five tested compounds (including SAA) and the positive control (Acarbose) used in this study are summarized in **Table 3-1**.

5.2.1 α-glucosidase Inhibitory Assay Test

Phosphate buffer solution (PBS, 10 mM, pH = 7.0) was prepared from a 0.02 M solution of Na_2HPO_4 and a 0.02M solution of NaH_2PO_4 and diluted 1:1 (v/v) with distilled water. Then, 21.6 mg of bovine serum albumin and 2.16 mg of sodium azide were mixed with 10.8 ml of PBS buffer. An enzyme solution of 1 Unit/ml was prepared by α-Glucosidase from lyophilized *Saccharomyces cerevisiae* (Type I). The substrate

solution consisted of 4 mM of 4-Nitrophenyl α-D-glucopyranoside in PBS solution. All tested compounds were singly dissolved in 20% DMSO solution, among which acarbose (4 mg/ml) was used as a positive control dissolved in 20% DMSO solution. The material sources are listed in detail in **Table 5-1**.

The test was performed in 96-well plate. In the vails that used for *p*NG determination, 50 μl of the sample solution, 50 μl of PBS buffer and 50 μl of enzyme solution were added and mixed in a single vail, respectively. There were three groups, in which the sample solution for the **Control group** was 20% DMSO solution (sample solvent); the sample solution for the **Standard group** was acarbose (4 g/ml) solution; and the sample solution for the **Sample group** was the compound solution (4 g/ml) (six compounds tested in this experiment). For each group, blank vails (no enzyme) were made up to establish the background signal. All tested vails were tested in triplicate (**Table 5-2**).

Table 5-1. Names and suppliers of reagents used in the α-glucosidase inhibitory assay.

Reagents	Cat No.	Supplier
Acarbose ≥ 95%	A8980	Sigma-Aldrich
Sodium Azide NaN3, ReagentPlus®, ≥99.5%	S2002	Sigma-Aldrich
Albumin from bovine serum,	A7906	Sigma-Aldrich
4-Nitrophenyl α-D-glucopyranoside ≥ 99%	N1377	Sigma-Aldrich
α-glucosidase from Saccharomyces cerevisiae,	G5003	Sigma-Aldrich
Dimethylsulfoxide ≥ 99.8%	4720.3	Carl Roth GmbH

Table 5-2. The chemical added into the different groups of the α-glucosidase inhibitory assay in a 96-well plate format.

	Control	Standard	Sample
*p*NG Determination	50 µl 20% DMSO 50 µl PBS 50 µl enzyme solution	50 µl Acarbose solution 50 µl PBS 50 µl enzyme solution	50 µl compound solution 50 µl PBS 50 µl enzyme solution
Background	50 µl 20% DMSO 100 µl PBS	50 µl standard solution 100 µl PBS	50 µl sample 100 µl PBS

The control group contained no enzyme. Therefore, this group serves as a blank control with a theoretically 100% reaction velocity. The standard group contained positive control, acarbose, in which there should be a high inhibition of the reaction velocity. The sample group contained one compound solution (either Caffeic acid, Coumaric Acid, SalA, SalB or SAA). *p*NG was generated as a product of the reaction between α-glucosidase and substrate, and its concentration was detected to assess the velocity of reaction. Blank vials were also set as references.

Then, the 96-well plate was placed at 37°C for 2 min in an incubator. After removing the plate, 50 µl of the substrate solution was added into each well and immediately placed into the microplate reader. Measurement of the absorbance at 405 nm was conducted every 30 s for 10 min at 37°C.

The velocity of the *p*NP formation was calculated, and the linear relationship between absorbance and time was plotted using **equation A**:

$$\text{Velocity} = \frac{\triangle \text{Absorbance at 405 nm}}{\triangle \text{Time}}$$

The highest velocity of the initial reaction of each sample was determined. Then, the percentage of inhibition was calculated by **equation B** (V=Velocity):

$$\%\text{Inhibition} = \frac{\text{V(Control)} - \text{V(Sample)}}{\text{V(Control)}} \times 100$$

In this assay, the compound with a better antidiabetic effect exhibits a stronger inhibition of the reaction progression (i.e., a lower reaction velocity in equation A). As expressed by **equation B**, a lower velocity of sample group [V(Sample)] will result in a higher inhibition percentage, indicating a stronger α-glucosidase inhibitory activity.

Once a compound had been serially diluted (e.g., 8 concentrations), a linear curve was generated by plotting the inhibition percentage against concentration, as shown in **Figure 5-4**. Then, the IC50 of the compound was calculated from the equation

generated by the linear cure. The IC50 value represents the concentration of the inhibitor (compound) at which the α-glucosidase activity is inhibited by half.

5.3 Results

5.3.1 The α-glucosidase Inhibitory Activity of Acarbose

As a classic α-glucosidase inhibitor, acarbose was used as a positive control in this study. The reaction velocity of acarbose (1 mg/ml, 2 mg/ml) in the α-glucosidase inhibitory assay is shown in **Figure 5-2**.

5.3.2 The α-glucosidase Inhibitory Activity of SAA

The α-glucosidase inhibitory assay results for SAA, Caffeic Acid, Coumaric Acid, and SalA and SalB are represented by absorbance changes at 405 nm (OD 405 nm) against time changes (△Time) as plotted in **Figure 5-3**.

The reaction velocity of the α-glucosidase inhibitory assay from the sample was expressed by plotting the absorbance (OD 450 nm) against the reaction duration, in which a higher slop refers to a higher reaction velocity and vice versa.

In the α-glucosidase inhibitory assay with SAA, the slop of the linear cure of SAA is much higher than acarbose and close to that of the blank control, which indicates a much weaker α-glucosidase inhibitory activity for SAA (18.28 ± 6.88%) than acarbose.

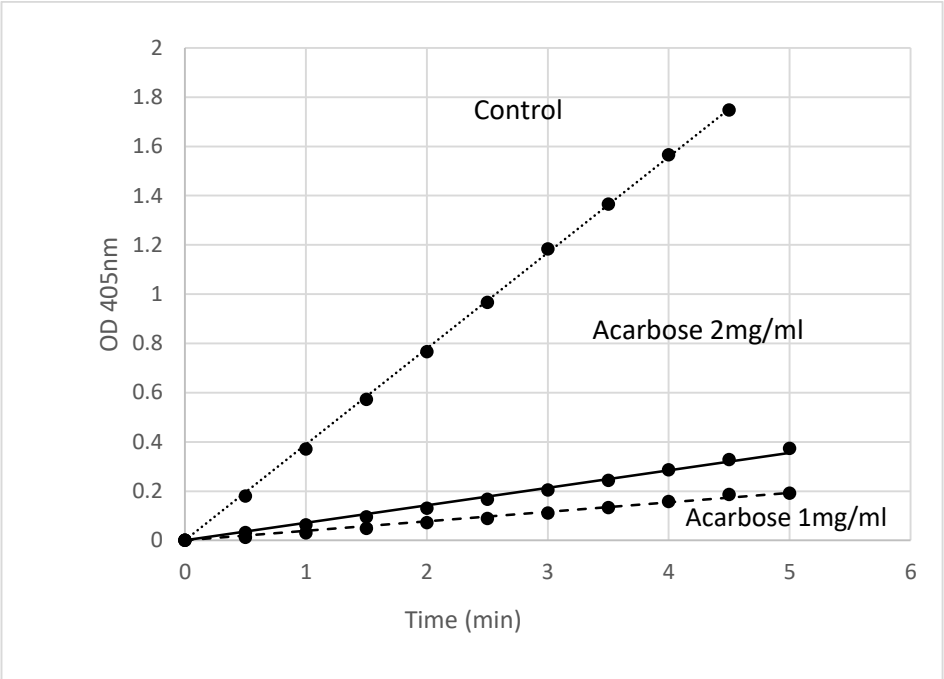

Figure 5-2. α-glucosidase inhibitory assay result of acarbose (positive control) at concentrations of 2 mg/ml and 1 mg/ml.

Reaction velocity of the α-glucosidase inhibitory assay from acarbose was expressed by plotting absorbance (OD 450 nm) against reaction duration.

5.3.3 The α-glucosidase Inhibitory Activities of the Four SAA-alike Compounds

5.3.3.1 The α-glucosidase Inhibitory Activity of Caffeic Acid

The α-glucosidase inhibitory activity assay slop for caffeic acid was lower than that of the positive control, acarbose, which indicates a very strong α-glucosidase inhibitory activity for caffeic acid (99.34±0.02%) – even stronger than that of acarbose (**Figure 5-3**).

5.3.3.2 The α-glucosidase Inhibitory Activity of Coumaric Acid

The velocity of the α-glucosidase inhibitory assay for Coumaric Acid, the control sample, and acarbose is represented by absorbance changes at 405 nm against time and plotted in **Figure 5-3**. We found that the slop of Coumaric Acid is even lower than the positive control, acarbose, which indicates a very strong α-glucosidase inhibitory activity (99.64 ± 0.02%), which is similar to that of Caffeic Acid.

5.3.3.3 The α-glucosidase Inhibitory Activity of Salvianolic Acid A (SalA)

As shown in **Figure 5-3**, the velocity of the α-glucosidase inhibitory assay of SalA was also lower than the positive control, acarbose, indicating a strong α-glucosidase inhibitory activity (97.71 ± 0.42%).

5.3.3.4 The α-glucosidase Inhibitory Activity of Salvianolic Acid B (SalB)

As shown in **Figure 5-3**, the velocity of the α-glucosidase inhibitory assay of SalB was a little higher than acarbose, indicating a slightly lower α-glucosidase inhibitory activity for SalB (76.83 ± 0.74%) than acarbose.

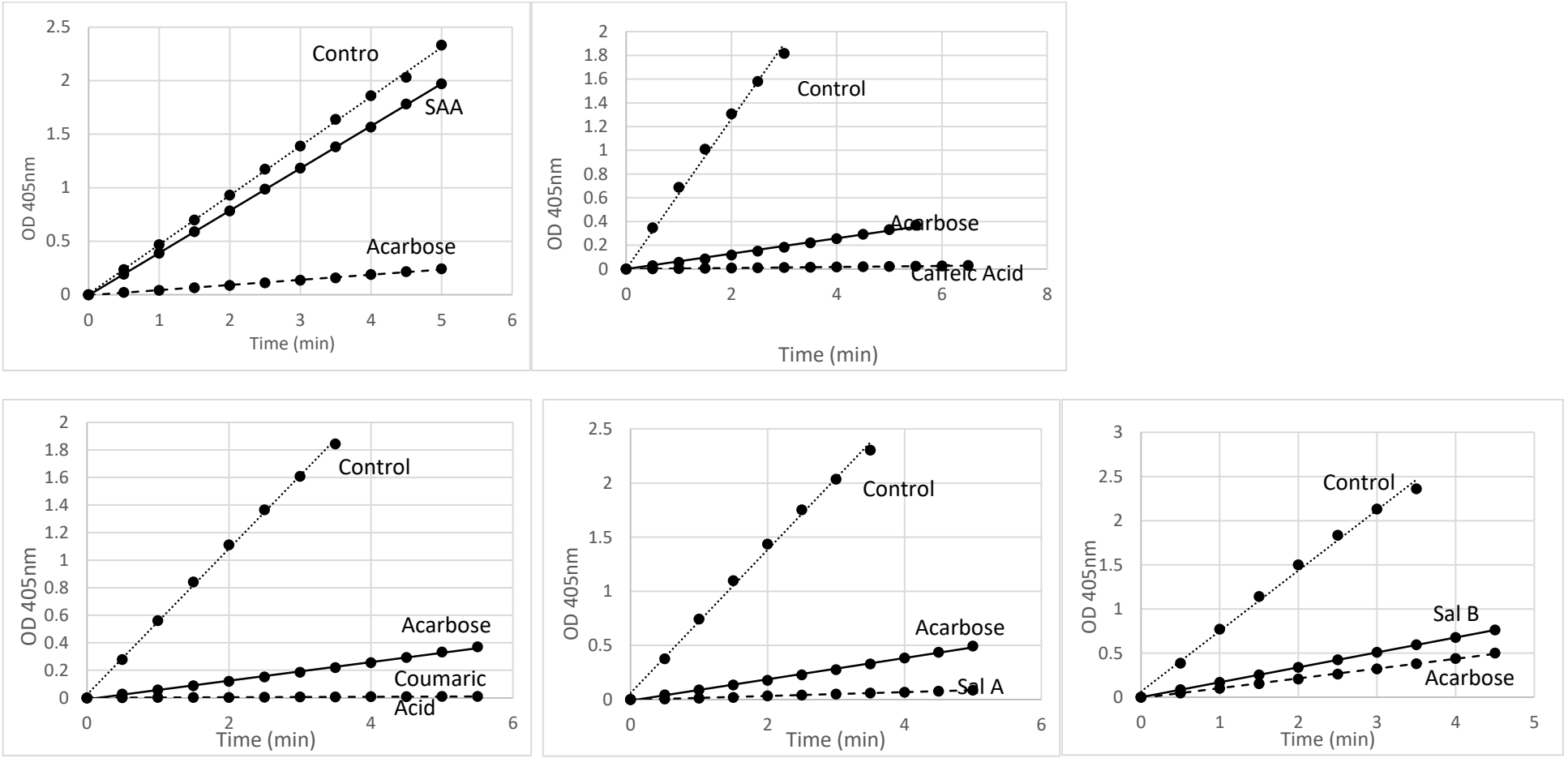

Figure 5-3. The α-glucosidase inhibitory assay results for SAA, Caffeic Acid, Coumaric Acid, SalA and SalB.

Reaction velocity of the α-glucosidase inhibitory assay from the sample was expressed by plotting absorbance (OD 450nm) against reaction duration.

5.3.4 IC50 of α-glucosidase Inhibitory Activities of All Selected Compounds

The IC50 of the α-glucosidase inhibitory activities of all compounds are summarized in **Table 5-3**, which were calculated from the linear curve of the percent inhibition plotted against concentration (**Figure 5-4**).

Among the tested compounds, I found that Caffeic Acid has the highest inhibitory activity at a concentration of 1 mg/ml, followed by Coumaric Acid and SalA. Salvianic Acid A had the lowest inhibitory activity among the tested compounds. According to the calculated IC50, acarbose was the most efficient agent in the α-glucosidase inhibitory assay. SalA and Coumaric Acid were also potent inhibitors, only a little weaker than acarbose. However, SAA was not as strong of a α-glucosidase inhibitor as acarbose, which is even weaker than the other natural compounds extracted from *Danshen* (SalA and SalB).

Table 5-3. IC50 (median effect concentration) of α-glucosidase inhibitory activity for all tested compounds.

Compounds	Inhibitory activity	IC50 (µg/ml)
Caffeic Acid	99.34 ± 0.02%	422.76
Coumaric Acid	99.64 ± 0.02%	290.92
Salvianolic Acid A	97.71 ± 0.42%	268.65
Acarbose	81.88 ± 0.80%	228.74
Salvianolic Acid B	76.83 ± 0.74%	303.64
Salvianic Acid A	18.28 ± 6.88%	>1000

The value of IC50 in the α-glucosidase inhibitory assay indicated the median effective concentration point of the selected compounds when the *p*NG reaction velocity was inhibited by 50% compared to the full reaction velocity (reaction velocity of the control group in each sample as shown in Table 5-2).

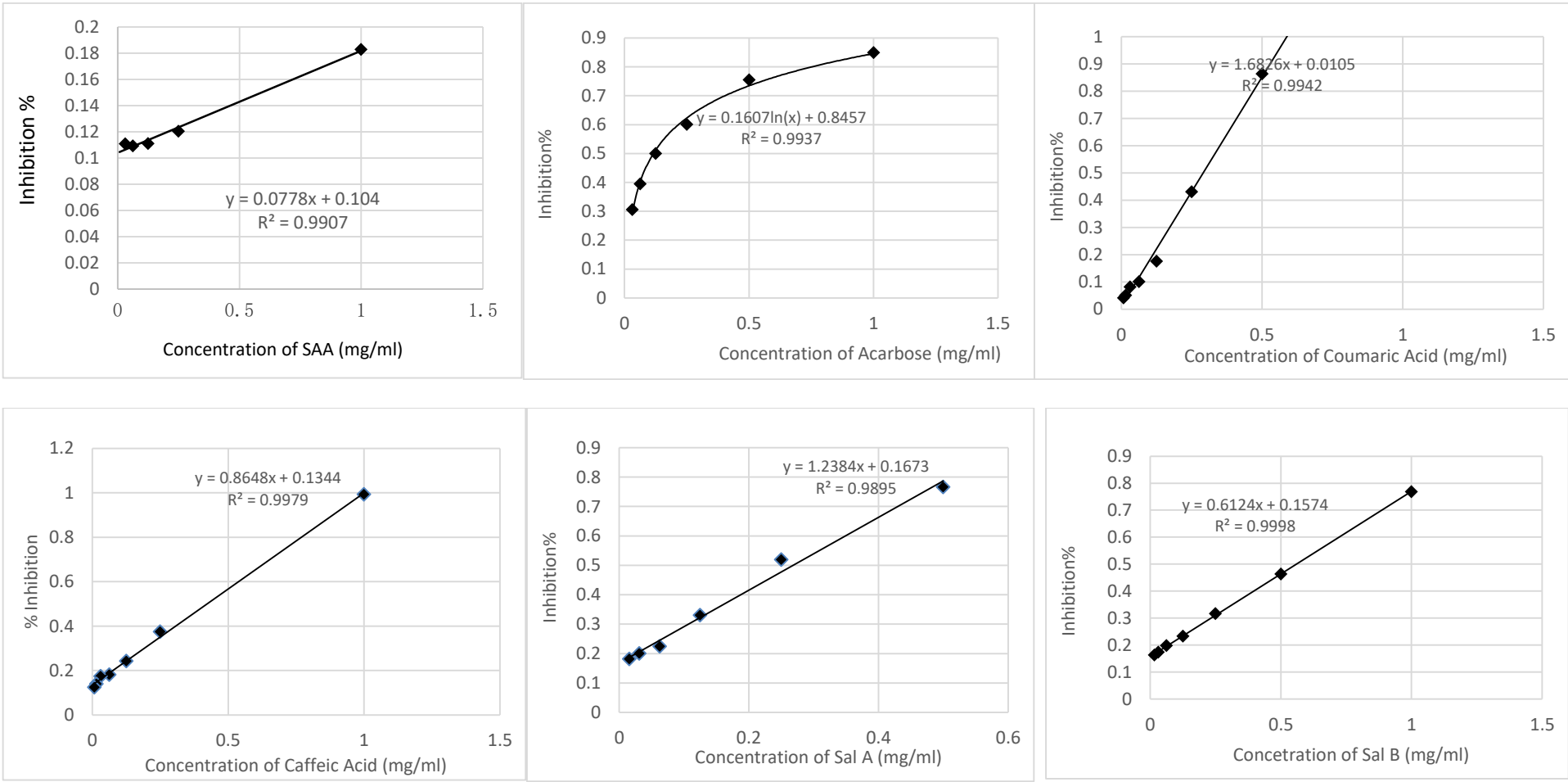

Figure 5-4. The linear curve of percentage inhibition against concentration for all tested compounds.
These are the secondary replots of the α-glucosidase inhibitory activity, where %Inhibition is calculated using the equation described in the methods section, and the horizontal axis is the concentration of the tested sample.

5.4 Discussion

Over thousands of years, TCM has been regarded as a potent natural plant source for the prevention or therapy of various chronic diseases, in which DM was known as "Xiao Ke". This ancient name of DM in TCM theory described the major symptoms of DM, such as an increased feeling of thirst and hunger, extreme fatigue, urinating often, and unplanned weight loss. Faced with these typical DM symptoms, many TCM formulations were recommended as therapeutic strategies (Guan, Sun et al. 2000; Jia, Gao et al. 2003). For example, some herbs have been proposed as being able to modulate carbohydrate and fat metabolism, thereby improving microcirculation and the blood glucose level in diabetics, among which *Danshen* (*Salvia Miltiorrhiza*) has been listed (Chang, Jia et al. 2015).

As a major ingredient extracted from *S. Miltiorrhiza*, the beneficial effect of SAA for the vascular system has been reported by multiple studies (see Chapter 1). However, the antidiabetic or α-glucosidase inhibitory effect was not investigated clearly enough. Therefore, in this study, to investigate the antidiabetic effect of SAA, I performed the α-glucosidase inhibitory assay on SAA and five other structurally similar compounds.

I found that, among all tested compounds, Coumaric Acid exhibits the highest α-glucosidase inhibitory activity, followed by Caffeic Acid, Coumaric Acid, and Salvianolic Acid A. Surprisingly, Caffeic Acid, Coumaric Acid, and Salvianolic Acid A had higher α-glucosidase inhibitory activities than acarbose. Besides, Salvianolic Acid B has an α-glucosidase inhibitory activity of around 76%, whilst SAA has an α-glucosidase inhibitory activity of just 18.28 ± 6.88%, indicating a relatively weak α-glucosidase inhibitory activity.

The IC50 was calculated for those compounds with an α-glucosidase inhibitory activity greater than 70% (acarbose, SalA, SalB, Coumaric Acid). By this approach, it was shown that acarbose, as the standard drug, has the best efficiency among all tested samples, with IC50 of 228.74 μg/ml. Salvianolic Acid A and Coumaric Acid had efficiency close to that of acarbose (~268 and 290 μg/ml respectively). On the other hand, Salvianolic Acid B and Caffeic Acid were found to have relatively low IC50s (303 and 422 μg/ml respectively). Not surprisingly, the IC50 for the α-glucosidase inhibitory activity of SAA was the lowest among the tested compounds.

From these results, I postulated that *Salvia Miltiorrhiza* does consist of active ingredients that have antidiabetic effect potential, such as Salvianolic Acid A and Salvianolic Acid B, even though SAA has a limited antidiabetic effect compared to the positive control-acarbose. Caffeic Acid and Coumaric Acid both share similar structures with SAA (just one hydroxyl group difference between compounds), but have much higher α-glucosidase inhibitory activities compared to SAA, which was not expected. On the other hand, the α-glucosidase inhibitory activities of Sal A and Sal B suggest antidiabetic potentials of these two compounds.

In conclusion, even there are similar chemical structures contained in the molecules of the compounds involved in this test, the antidiabetic potentials of them are diverse. Thus, further structure analysis and prediction by computation techniques are required to uncover the structure-related mechanism of the antidiabetic effect of these compounds.

Chapter 6 General Discussion, Limitation and Future Perspective

6.1 General Discussion

In this project, I performed a series of experiments to investigate the cardiovascular protective effect of SAA in our elevated-Hcy-level diabetic mice model.

The beneficial effect of SAA or *Salvia Miltiorrhiza* has been recognized in previous studies (see Chapter 1). However, to our knowledge, the cardioprotective effect of SAA in *db/db* mice with elevated Hcy has not been addressed by other studies. Therefore, the first contribution of this project was to set-up a valid spontaneous diabetic mice model with diet-induced elevated Hcy levels. Both the elevated glucose and Hcy levels is an ideal simulation of the pathological progression of human diabetes, which can be referenced in future related studies.

A more solid conclusion about the mechanism underlying the direct effect of SAA on the vasomotor is needed and should be addressed in future studies. However, in our current study, the chronic administration of SAA could protect the vascular function in an endothelial-dependent manner in *db/db* mice with an elevated Hcy level, and acute pure SAA administration induced a vasorelaxation effect in an endothelial-independent manner via a calcium channel-dependent pathway.

To diabetics, cardiomyopathy plays a significant role in cardiovascular disorders. However, there is currently a lack of effective therapeutic strategies targeting this antioxidant damage to the heart and aggressive left ventricular hypertrophy. As a significant antioxidant, SAA could improve microcirculation, thereby improving the *in vivo* redox status and protecting the cardiovascular system. In our test, chronic administration of SAA slowed the progression of left ventricular hypertrophy, even though it did not improve the left ventricular systolic function. This might be due to

the intervention period or the starting point of the intervention, which might be not sufficiently early or long. However, the morphological improvement might be mediated by its antioxidant effect and the blood circulation improvement effect. By Western blotting, we found that the eNOS/AKT pathway might be upregulated. Consistent with a recent study, in an experiment with Wistar rat cardiac hypertrophy model that received injections containing SAA, the left ventricle mass, and wall thickness were significantly reduced compared to the group without treatment. A further experiment using H9c2 cells revealed that this cardioprotective effect is possibly mediated by p38 and the NF-κb pathway (Mao, Wang et al. 2016). To my knowledge, this thesis is the first study to investigate the anti-hypertrophic effect of SAA on diabetic cardiomyopathy in the *db/db* mice with elevated Hcy level. However, further detailed and more comprehensive research on cardiomyopathies, such as its protective effect on systolic dysfunction and ventricular hypertrophy is required to address this knowledge gap.

An elevated Hcy level has long been realized as an independent CVD risk factor. Unfortunately, effective therapy or prevention remains controversial and requires further study. This is the first investigation to look into the Hcy-normalizing effect of SAA in diabetic mice with an elevated Hcy level. In this project, the chronic oral administration of SAA significantly reduced the Hcy level. Besides, the GSH level in the liver of diabetic mice was found significantly lower than in non-diabetic mice, which is possibly because of the triggered oxidative stress status in diabetic mice. Notably, in the SAA-treated mice, the GSH level was found significantly higher compared to the mice without SAA treatment. Meanwhile, the levels of SAM, SAH and SAM/SAH ratio remained no significant change. As introduced, SAM and SAH were important intermediates generated in re-methylation pathway of Hcy metabolism.

Therefore, the elevated GSH level in the liver indicates that SAA could normalize the Hcy level by activating the trans-sulphuration pathway of Hcy metabolism, rather than the re-methylation pathway.

Finally, although, the antiglycemic effect of SAA was not detected in this study after an 8-week intervention, to investigate the glucose-lowering potential of SAA, I performed a more specific antidiabetic assay, the α-glucosidase inhibitory assay. By this approach, I found that the α-glucosidase inhibitory activity is weaker compared to the positive control, acarbose. However, I was able to identify other compounds, such as caffeic acid, SalA, SalB, which shows strong α-glucosidase inhibitory activities, thereby providing useful information for SAA derivate development.

To conclude, SAA can ameliorate endothelial dysfunction, slow the progression of left ventricular hypertrophy, normalize elevated Hcy level, and reduce oxidative stress, suggesting that SAA can protect the cardiovascular system of diabetics from multiple aspects, especially to those with an elevated Hcy level.

6.2 Overall Significance of the Study

Because of the high CVD risk for patients with DM and the additional threats from high Hcy levels, the findings of the current study will be particularly relevant to future efforts to address CVD in diabetic patients, especially in those with comorbid elevated Hcy levels. Future studies might identify an efficient drug that reduces the Hcy level by increasing the trans-sulphuration pathway and ameliorating the ventricular hypertrophy and endothelial dysfunction. Such a drug would benefit DM patients with elevated Hcy levels and improve their cardiovascular function.

Firstly, rare studies have focused on endothelial dysfunction in a diabetic model accompanied by elevated Hcy level, not to mention the mechanisms underlying these pathological changes. Moreover, clinical studies have reported controversial results about the pharmacological therapy effect. A reliable consequence of a specific therapy on ED in a diabetic model accompanied by elevated Hcy level and the exact mechanism is still lacking.

Secondly, as our selected transgenic diabetic animal model, *db/db* mouse is a mutation diabetes model accompanied by persistent hyperphagia and obesity, with consequent, naturally-developed high leptin and insulin levels (Hummel, Dickie et al. 1966), which simulate the human chronic process. These features make this mouse an excellent model for research addressing DM and diabetic complications, especially for cardiovascular complications, which are poorly simulated by acute drug-induced models, such as streptozotocin (STZ) or alloxan model. I successfully developed a diabetic model with elevated Hcy level model based on the *db/db* mouse, which is extremely close to the status of humans. However, related studies and results which

could be referenced are rare, and also the vessel tissues and organ tissues have extremely small, which is a challenge in handling in the later complex steps involved in the aortic ring assay, more so than for other animal models, such as STZ-induced rats. After overcoming these difficulties, I finally collected the experimental data from this reliable and ideal diabetic animal model.

Finally, in clinical practice, there are numerous patients with diabetes being treated with metformin. These patients are at greater risk of CVD and are likely to develop elevated Hcy levels, which is highly similar to the model in this experiment but is often ignored. By studying about this disease, the treatment effects, and the involved mechanisms will impact future research addressing diabetic CVD. Therefore, these studies will be meaningful and could be referenced by both further experimental research and clinical practice. Furthermore, if a series of exact, reliable results are generated, these findings could have profound significance and will probably benefit patients with DM globally.

6.3 Overall Limitation of the Study

Here we have revealed the beneficial effect of SAA on the elevated Hcy level and endothelial dysfunction of the diabetic animal model. However, the underlying mechanism for this requires further exploration, such as the relationship between the endothelial protective effect of SAA and the AKT/eNOS pathway.

In a mice study, the amount of aortic tissue is too limited to conduct multiple tests. After myograph testing, the left tissue is insufficient to extract protein; therefore, further tests addressing protein expression levels could not be conducted. Consequently, it may necessary to use a different model to achieve such objectives. In our case, based on the acute test and chronic consumption test with aortic tissue, human umbilical vein endothelial cells or human aortic endothelial cells could be used to further investigate the mechanisms involved.

Apart from the chronic effects of normalizing the Hcy level and improving endothelial function, SAA might also have an acute protective effect. The elevated Hcy level model used in this study is induced by methionine administration with daily diet. To achieve a comprehensive conclusion about the beneficial effect of SAA on the elevated Hcy level, an acute elevated Hcy level model could be designed. Similarly, the endothelial protective effect of SAA, which is also detected in chronic-style studies, might also possess an acute or direct vascular dilation effect, which could be tested with a direct vessel dilation test.

In addition to the cardiovascular beneficial effect, SAA has also been proposed to have a protective effect on other systems, such as the nervous system, many of which are also involved in major diabetic complications. Therefore, those potential beneficial

effects might also be discovered in future relevant studies, which would no doubt enhance efforts to develop an effective drug to apply clinically for diabetics.

6.4 Future Perspective

SAA is an elementary and powerful active ingredient extracted from a renowned TCM, *Danshen*. As an effective compound, SAA has long been applied in the treatment of CVD. However, the detailed mechanisms of its multiple protective potentials in the cardiovascular system, as well as other systems, have not yet been clearly understood and remain a hot topic due to its natural source and relative clinical safety.

In previous studies, the comprehensive cardioprotective effect of the SAA has been addressed in multiple ways with various models. The mechanism also involves multiple aspects, mainly involving antioxidant and anti-apoptosis pathways. Pharmacological research has also uncovered the detailed pharmacokinetics and pharmacological properties of SAA. Its safety makes SAA a popular ingredient which is included in many drugs applied in clinical practice. However, further drugs are still in the progress of development and are likely to reach the market in the near future.

In recent years, with the development of pharmaceutics techniques, there have been several novel derivates produced, some of which exhibit even greater efficiency and powerful therapeutic effects than original natural pure compounds. Because SAA has a relatively small chemical structure, it could be used for the production of further derivates with structural modifications. Some of these SAA-derived compounds have already been applied to CVD, and further novel synthetic derivates are expected to be produced.

To this end, this drug and its derivates have much potential and multiple prospective uses.

Appendix

Appendix A. Antibodies Used in Western Blotting for Akt/eNOS

No.	Antibody	Cat. No.	Brand
1	**Beta-actin (D6A8) Rabbit mAb (100ul)**	8457S	Cell Signaling Technology
2	**Akt (pan) (11E7) Rabbit mAb (100ul)**	4685S	Cell Signaling Technology
3	**Phospho-Akt (Thr308) (244F9) Rabbit mAb (100ul)**	4056S	Cell Signaling Technology
4	**eNOS (D9A5L) Rabbit mAb (100ul)**	32027S	Cell Signaling Technology
5	**Phospho-eNOS (Ser1177) (C9C3) Rabbit mAb (100ul)**	9570S	Cell Signaling Technology
6	**HO-1 Antibody (Source: rabbit; 100ul)**	70081S	Cell Signaling Technology
7	**GAPDH (14C10) Rabbit mAb, 100ul**	2118S	Cell Signaling Technology
8	**Goat anti-rabbit IgG HRP (200ug/0.5mL)**	sc-2004	Santa Cruz Biotechnology

Appendix B. Main HPLC Materials and Accessories Used in the Measurement of Homocysteine Level

Product	Catalogue No.	Supplier
DL-Homocysteine,	53510-250MG	Sigma
N-(2-mercaptopropionyl)-glycine,	M6636-5G	Sigma
Potassium tetraborate tetrahydrate,	60541-250G	Sigma-Aldrich
7-Fluorobenzofurazan-4-sulfonic acid ammonium salt,	46640-5MG-F	Sigma-Aldrich
Tris-(2-carboxyethyl)-phosphine hydrochloride,	C4706-2G	Aldrich
Trichloroacetic acid, purchase min. quantity	T6399-100G	Sigma-Aldrich
Methanol, HPLC grade	DUKSAN-62-4L	Oriental Chemicals
KH_2PO_4 ,analytical grade	60218-100G	Sigma
Insert 150uL with preinstalled plastic spring	WAT094171	Waters
Guard cartridge - Waters Symmetry C_{18}, 5 µm, 3.9 × 20 mm	WAT054225	Waters

Guard column holder for 3.9 x 20 mm cartridge	WAT046910	Waters
Column - Agilent Zorbax Eclipse XDB-C_{18}, 5 µm, 4.6 × 150 mm	993967-902	Agilent

References

Abubakar, I., T. Tillmann, et al. (2015). "Global, regional, and national age-sex specific all-cause and cause-specific mortality for 240 causes of death, 1990-2013: a systematic analysis for the Global Burden of Disease Study 2013." Lancet **385**(9963): 117-171.

Alegria, J. R., T. D. Miller, et al. (2007). "Infarct size, ejection fraction, and mortality in diabetic patients with acute myocardial infarction treated with thrombolytic therapy." American heart journal **154**(4): 743-750.

Alon, T., I. Hemo, et al. (1995). "Vascular endothelial growth factor acts as a survival factor for newly formed retinal vessels and has implications for retinopathy of prematurity." Nature medicine **1**(10): 1024-1028.

Alp, N. J., S. Mussa, et al. (2003). "Tetrahydrobiopterin-dependent preservation of nitric oxide-mediated endothelial function in diabetes by targeted transgenic GTP-cyclohydrolase I overexpression." Journal of Clinical Investigation **112**(5): 725-735.

Alter, P., H. Rupp, et al. (2010). "Association of hyperhomocysteinemia with left ventricular dilatation and mass in human heart." Clinical chemistry and laboratory medicine **48**(4): 555-560.

American-Diabetes-Association (2016). "8. Cardiovascular disease and risk management." Diabetes care **39**(Supplement 1): S60-S71.

AmericanHeartAssociation (2016). What Is Cardiomyopathy in Adults?

Atlas, I. D. (2015). "International Diabetes Federation, Brussels, 2015." Available from:[Last accessed: 5 March 2014].

Avogaro, A., G. P. Fadini, et al. (2006). "Endothelial dysfunction in type 2 diabetes

mellitus." Nutrition, Metabolism and Cardiovascular Diseases **16**: S39-S45.

Barouch, L. A., D. E. Berkowitz, et al. (2003). "Disruption of leptin signaling contributes to cardiac hypertrophy independently of body weight in mice." Circulation **108**(6): 754-759.

Bauman, W. A., S. Shaw, et al. (2000). "Increased intake of calcium reverses vitamin B12 malabsorption induced by metformin." Diabetes Care **23**(9): 1227-1231.

Bermudez, V., F. Bermudez, et al. (2008). "Molecular mechanisms of endothelial dysfunction: from nitric oxide synthesis to ADMA inhibition." American journal of therapeutics **15**(4): 326-333.

Bijlstra, P., P. Smits, et al. (1995). "Effect of long-term angiotensin-converting enzyme inhibition on endothelial function in patients with the insulin-resistance syndrome." Journal of cardiovascular pharmacology **25**(4): 658-664.

Binno, S. (2016). "2016 European Guidelines on cardiovascular disease prevention in clinical practice."

Bissonnette, R., E. Treacy, et al. (2001). "Fenofibrate raises plasma homocysteine levels in the fasted and fed states." Atherosclerosis **155**(2): 455-462.

Blesa, J., S. Phani, et al. (2012). "Classic and new animal models of Parkinson's disease." BioMed Research International **2012**.

Bonaccini, L., A. Karioti, et al. (2015). "Effects of salvia miltiorrhiza on CNS neuronal injury and degeneration: a plausible complementary role of tanshinones and depsides." Planta medica **81**(12/13): 1003-1016.

Bonito, P., N. Moio, et al. (2005). "Early detection of diabetic cardiomyopathy: usefulness of tissue Doppler imaging." Diabetic medicine **22**(12): 1720-1725.

Boudina, S. and E. D. Abel (2007). "Diabetic cardiomyopathy revisited." Circulation **115**(25): 3213-3223.

Boudina, S. and E. D. Abel (2010). "Diabetic cardiomyopathy, causes and effects." Reviews in Endocrine and Metabolic Disorders **11**(1): 31-39.

Brazzelli, V., V. Grasso, et al. (2010). "Homocysteine, vitamin B12 and folic acid levels in psoriatic patients and correlation with disease severity." International journal of immunopathology and pharmacology **23**(3): 911-916.

Buse, J. B., H. N. Ginsberg, et al. (2007). "Primary prevention of cardiovascular diseases in people with diabetes mellitus: a scientific statement from the American Heart Association and the American Diabetes Association." Diabetes Care **30**(1): 162-172.

Cai, H. and D. G. Harrison (2000). "Endothelial dysfunction in cardiovascular diseases: the role of oxidant stress." Circulation Research **87**(10): 840-844.

Cai, L., Y. Wang, et al. (2006). "Attenuation by metallothionein of early cardiac cell death via suppression of mitochondrial oxidative stress results in a prevention of diabetic cardiomyopathy." Journal of the American College of Cardiology **48**(8): 1688-1697.

Calabrese, V., C. Cornelius, et al. (2010). "Cellular stress responses, the hormesis paradigm, and vitagenes: novel targets for therapeutic intervention in neurodegenerative disorders." Antioxidants & redox signaling **13**(11): 1763-1811.

Calles-Escandon, J. and M. Cipolla (2001). "Diabetes and endothelial dysfunction: a clinical perspective." Endocrine reviews **22**(1): 36-52.

Cao, Y., J. G. Chai, et al. (2009). "Beneficial effects of danshensu, an active component of Salvia miltiorrhiza, on homocysteine metabolism via the trans-sulphuration pathway in rats." Br J Pharmacol **157**(3): 482-490.

Chan, K., S. Chui, et al. (2004). "Protective effects of Danshensu from the aqueous

extract of Salvia miltiorrhiza (Danshen) against homocysteine-induced endothelial dysfunction." Life sciences **75**(26): 3157-3171.

Chang, Z., D. Jia, et al. (2015). Chinese materia medica, PMPH-USA.

Chen, Y., Y. Cao, et al. (2009). "Mechanism-based pharmacokinetic-pharmacodynamic modeling of bidirectional effect of danshensu on plasma homocysteine in rats." Pharmaceutical research **26**(8): 1863-1873.

Cheng, T. O. (2006). "Danshen: a versatile Chinese herbal drug for the treatment of coronary heart disease." International journal of cardiology **113**(3): 437-438.

Cheng, T. O. (2007). "Cardiovascular effects of Danshen." International journal of cardiology **121**(1): 9-22.

Cheng, Z.-J., X. Yang, et al. (2009). "Hyperhomocysteinemia and endothelial dysfunction." Current hypertension reviews **5**(2): 158-165.

Chico, A., A. Perez, et al. (1998). "Plasma homocysteine is related to albumin excretion rate in patients with diabetes mellitus: a new link between diabetic nephropathy and cardiovascular disease?" Diabetologia **41**(6): 684-693.

Cho, S.-G., Y. H. Lee, et al. (2001). "Glutathione S-transferase mu modulates the stress-activated signals by suppressing apoptosis signal-regulating kinase 1." Journal of Biological Chemistry **276**(16): 12749-12755.

Chong, C.-M., Z.-Y. Zhou, et al. (2013). "Danshensu protects against 6-hydroxydopamine-induced damage of PC12 cells in vitro and dopaminergic neurons in zebrafish." Neuroscience letters **543**: 121-125.

Chousos, I., D. Perrea, et al. (2010). "Acute hyperhomocysteinaemia blunts endothelial-dependent and endothelial independent vasodilatation in diabetic patients." Diabetes and Vascular Disease Research **7**(3): 186-194.

Cohen, R. A. (1995). "The role of nitric oxide and other endothelium-derived

vasoactive substances in vascular disease." Progress in cardiovascular diseases **38**(2): 105-128.

Collaboration, T. H. S. (2002). "Homocysteine and risk of ischemic heart disease and stroke." A meta-analysis. JAMA **288**.

Comin, D., L. Gazarini, et al. (2010). "Vitamin E improves learning performance and changes the expression of nitric oxide-producing neurons in the brains of diabetic rats." Behavioural brain research **210**(1): 38-45.

Commission, C. P. (2010). Pharmacopoeia of the People's Republic of China. 1 (2010), China Medical Science Press.

Commission, C. P. (2010). "Pharmacopoeia of the People's Republic of China: 2010 (Chinese Version)." Beijing: China Medicine and Technology Publishing House.

Creager, M., A. Goldin, et al. (2006). "Advanced glycation end products-Sparking the development of diabetic vascular injury." Circulation **114**: 597-605.

de Dios, S. T., C. G. Sobey, et al. (2010). Oxidative stress and endothelial dysfunction. Endothelial Dysfunction and Inflammation, Springer**:** 37-64.

de Jager, J., A. Kooy, et al. (2010). "Long-term treatment with metformin in patients with type 2 diabetes and risk of vitamin B-12 deficiency: randomised placebo-controlled trial." BMJ **340**: c2181.

De Ruijter, W., R. G. Westendorp, et al. (2009). "Use of Framingham risk score and new biomarkers to predict cardiovascular mortality in older people: population based observational cohort study." BMJ **338**: a3083.

Deanfield, J., A. Donald, et al. (2005). "Working Group on Endothelin and Endothelial Factors of the European Society of Hypertension. Endothelial function and dysfunction. Part I: Methodological issues for assessment in the different

vascular beds: a statement by the Working Group on Endothelin and Endothelial Factors of the European Society of Hypertension." J Hypertens **23**(1): 7-17.

Dej-adisai, S. and T. Pitakbut (2015). "Determination of α-glucosidase inhibitory activity from selected Fabaceae plants." Pak J Pharm Sci **28**(5): 1679-1683.

Deng, J.-Y., J.-P. Huang, et al. (2007). "Impairment of cardiac insulin signaling and myocardial contractile performance in high-cholesterol/fructose-fed rats." American Journal of Physiology-Heart and Circulatory Physiology **293**(2): H978-H987.

Deplancke, B. and H. R. Gaskins (2002). "Redox control of the transsulfuration and glutathione biosynthesis pathways." Current Opinion in Clinical Nutrition & Metabolic Care **5**(1): 85-92.

Dickinson, D. A. and H. J. Forman (2002). "Glutathione in defense and signaling." Annals of the New York Academy of Sciences **973**(1): 488-504.

Dimmeler, S., I. Fleming, et al. (1999). "Activation of nitric oxide synthase in endothelial cells by Akt-dependent phosphorylation." Nature **399**(6736): 601-605.

Ding, N. (2002). "Development and clinical application of compound danshen dripping pills." Chin Tradit Herb Drugs **33**: 1147-1148.

Doshi, S. N., I. F. McDowell, et al. (2001). "Folate Improves Endothelial Function in Coronary Artery Disease An Effect Mediated by Reduction of Intracellular Superoxide?" Arteriosclerosis, thrombosis, and vascular biology **21**(7): 1196-1202.

Doupis, J., I. Eleftheriadou, et al. (2010). "Acute hyperhomocysteinemia impairs endothelium function in subjects with type 2 diabetes mellitus." Experimental

and clinical endocrinology & diabetes **118**(07): 453-458.

Duncan, E. R., P. A. Crossey, et al. (2008). "Effect of endothelium-specific insulin resistance on endothelial function in vivo." Diabetes **57**(12): 3307-3314.

Ebesunun, M. O. and E. O. Obajobi (2012). "Elevated plasma homocysteine in type 2 diabetes mellitus: a risk factor for cardiovascular diseases." Pan African Medical Journal **12**(1).

Emoto, M., H. Kanda, et al. (2001). "Impact of insulin resistance and nephropathy on homocysteine in type 2 diabetes." Diabetes Care **24**(3): 533-538.

Epstein, F. H., G. N. Welch, et al. (1998). "Homocysteine and atherothrombosis." New England Journal of Medicine **338**(15): 1042-1050.

Eslami, A. and J. Lujan (2010). "Western blotting: sample preparation to detection." Journal of visualized experiments: JoVE(44).

Félétou, M. and P. M. Vanhoutte (1999). "The alternative: EDHF." Journal of molecular and cellular cardiology **31**(1): 15-22.

Förstermann, U. and T. Münzel (2006). "Endothelial nitric oxide synthase in vascular disease from marvel to menace." Circulation **113**(13): 1708-1714.

Fallon, U., P. Elwood, et al. (2001). "Homocysteine and ischaemic stroke in men: the Caerphilly study." Journal of Epidemiology & Community Health **55**(2): 91-96.

Fallon, U. B., J. Virtamo, et al. (2003). "Homocysteine and cerebral infarction in Finnish male smokers." Stroke **34**(6): 1359-1363.

Favaro, E., I. Miceli, et al. (2008). "Hyperglycemia induces apoptosis of human pancreatic islet endothelial cells: effects of pravastatin on the Akt survival pathway." The American journal of pathology **173**(2): 442-450.

Fennema, O. R. and S. R. Tannenbaum (1996). Food Additives. New York, Marcel

Dekker, Inc.

Ferrara, N. (2004). "Vascular endothelial growth factor: basic science and clinical progress." Endocrine reviews **25**(4): 581-611.

Ferrara, N., H.-P. Gerber, et al. (2003). "The biology of VEGF and its receptors." Nature medicine **9**(6): 669-676.

Finkelstein, J. (1998). "The metabolism of homocysteine: pathways and regulation." European journal of pediatrics **157**(2): S40-S44.

Fiordaliso, F., R. Bianchi, et al. (2004). "Antioxidant treatment attenuates hyperglycemia-induced cardiomyocyte death in rats." Journal of molecular and cellular cardiology **37**(5): 959-968.

Fischer, V. W., H. B. Barner, et al. (1984). "Pathomorphologic aspects of muscular tissue in diabetes mellitus." Human pathology **15**(12): 1127-1136.

Fonseca, V., A. Dicker-Brown, et al. (2000). "Effects of a high-fat-sucrose diet on enzymes in homocysteine metabolism in the rat." Metabolism **49**(6): 736-741.

Fonseca, V. A., L. M. Fink, et al. (2003). "Insulin sensitivity and plasma homocysteine concentrations in non-diabetic obese and normal weight subjects." Atherosclerosis **167**(1): 105-109.

Franco, R. and J. Cidlowski (2009). "Apoptosis and glutathione: beyond an antioxidant." Cell Death & Differentiation **16**(10): 1303-1314.

Fujio, Y. and K. Walsh (1999). "Akt mediates cytoprotection of endothelial cells by vascular endothelial growth factor in an anchorage-dependent manner." Journal of Biological Chemistry **274**(23): 16349-16354.

Gallego, M., A. Alday, et al. (2009). "Transient outward potassium channel regulation in healthy and diabetic hearts This article is one of a selection of papers from the NATO Advanced Research Workshop on Translational Knowledge for

Heart Health (published in part 1 of a 2-part Special Issue)." Canadian journal of physiology and pharmacology **87**(2): 77-83.

Gao, L., P. M. Siu, et al. (2017). "Cardiovascular Protective Effects of Salvianic Acid A on db/db Mice with Elevated Homocysteine Level." Oxidative Medicine and Cellular Longevity **2017**.

Gao, S., D. Ho, et al. (2011). "Echocardiography in mice." Current protocols in mouse biology: 71-83.

Gao, Y., Z. Liu, et al. (2009). "Acute and subchronic toxicity of danshensu in mice and rats." Toxicology mechanisms and methods **19**(5): 363-368.

Garg, S., J. Narula, et al. (2005). "Apoptosis and heart failure: clinical relevance and therapeutic target." Journal of molecular and cellular cardiology **38**(1): 73-79.

Gerber, H.-P., K. J. Hillan, et al. (1999). "VEGF is required for growth and survival in neonatal mice." Development **126**(6): 1149-1159.

Gersh, B. J., B. J. Maron, et al. (2011). "2011 ACCF/AHA guideline for the diagnosis and treatment of hypertrophic cardiomyopathy." Circulation: CIR. 0b013e318223e318222bd.

Ghosh, S., T. Pulinilkunnil, et al. (2005). "Cardiomyocyte apoptosis induced by short-term diabetes requires mitochondrial GSH depletion." American Journal of Physiology-Heart and Circulatory Physiology **289**(2): H768-H776.

Giltay, E., E. Hoogeveen, et al. (1998). "Insulin resistance is associated with elevated plasma total homocysteine levels in healthy, non-obese subjects." Atherosclerosis **139**(1): 197-198.

Gimbrone, M. A. and G. García-Cardeña (2016). "Endothelial cell dysfunction and the pathobiology of atherosclerosis." Circulation research **118**(4): 620-636.

Green, D. R. and G. Kroemer (2004). "The pathophysiology of mitochondrial cell

death." Science **305**(5684): 626-629.

GROOT, P. G., C. WILLEMS, et al. (1983). "Endothelial cell dysfunction in homocystinuria." European journal of clinical investigation **13**(5): 405-410.

Guan, S., J. Ma, et al. (2013). "Danshen (Salvia miltiorrhiza) injection suppresses kidney injury induced by iron overload in mice."

Guan, Y., Y. Yin, et al. (2013). "Dissection of mechanisms of a Chinese medicinal formula: danhong injection therapy for myocardial ischemia/reperfusion injury in vivo and in vitro." Evidence-Based Complementary and Alternative Medicine **2013**.

Guan, Z., M. Sun, et al. (2000). "Modern Diabetes Mellitus." Tianjin Science and Technology Press: Tianjin.

Guo, J. (1992). "Research and Clinical Application of the Root of Salvia Miltiorrhiza Bunge." Chinese Medicine and Technology Press: Beijing, China: 143-181.

Gupte, S., N. Labinskyy, et al. (2010). "Role of NAD (P) H oxidase in superoxide generation and endothelial dysfunction in Goto-Kakizaki (GK) rats as a model of nonobese NIDDM." PLoS One **5**(7): e11800.

Hakamata, W., M. Kurihara, et al. (2009). "Design and screening strategies for α-glucosidase inhibitors based on enzymological information." Current topics in medicinal chemistry **9**(1): 3-12.

Han, J.-Y., J.-Y. Fan, et al. (2008). "Ameliorating effects of compounds derived from Salvia miltiorrhiza root extract on microcirculatory disturbance and target organ injury by ischemia and reperfusion." Pharmacology & therapeutics **117**(2): 280-295.

Han, J.-Y., Y. Horie, et al. (2009). "Potential of 3, 4-dihydroxy-phenyl lactic acid for ameliorating ischemia-reperfusion-induced microvascular disturbance in rat

mesentery." American Journal of Physiology-Gastrointestinal and Liver Physiology **296**(1): G36-G44.

Han, J. Y., J. Y. Fan, et al. (2008). "Ameliorating effects of compounds derived from Salvia miltiorrhiza root extract on microcirculatory disturbance and target organ injury by ischemia and reperfusion." Pharmacol Ther **117**(2): 280-295.

Handy, D. E., Y. Zhang, et al. (2005). "Homocysteine down-regulates cellular glutathione peroxidase (GPx1) by decreasing translation." Journal of Biological Chemistry **280**(16): 15518-15525.

Hink, U., H. Li, et al. (2001). "Mechanisms Underlying Endothelial Dysfunction in Diabetes Mellitus." Circulation Research **88**(2): e14-e22.

Ho, F. M., W. W. Lin, et al. (2006). "High glucose-induced apoptosis in human vascular endothelial cells is mediated through NF-κB and c-Jun NH 2-terminal kinase pathway and prevented by PI3K/Akt/eNOS pathway." Cellular signalling **18**(3): 391-399.

Hoogeveen, E. K., P. J. Kostense, et al. (1998). "Hyperhomocysteinemia Is Associated With an Increased Risk of Cardiovascular Disease, Especially in Non–Insulin-Dependent Diabetes Mellitus A Population-Based Study." Arteriosclerosis, thrombosis, and vascular biology **18**(1): 133-138.

Hossain, G. S., J. V. van Thienen, et al. (2003). "TDAG51 is induced by homocysteine, promotes detachment-mediated programmed cell death, and contributes to the development of atherosclerosis in hyperhomocysteinemia." Journal of Biological Chemistry **278**(32): 30317-30327.

Huang, T., S. Asimi, et al. (2012). "Plasma phospholipid polyunsaturated fatty acids and homocysteine in Chinese type 2 diabetes patients." Asia Pacific journal of clinical nutrition **21**(3): 394-399.

Huang, T., Y. Chen, et al. (2012). "Meta-analysis of B vitamin supplementation on plasma homocysteine, cardiovascular and all-cause mortality." Clinical Nutrition **31**(4): 448-454.

Hummel, K. P., M. M. Dickie, et al. (1966). "Diabetes, a New Mutafton in the Mouse." Science **153**(3740): 1127-1128.

Jacobsen, D. W. (2000). "Hyperhomocysteinemia and oxidative stress time for a reality check?" Arteriosclerosis, thrombosis, and vascular biology **20**(5): 1182-1184.

Jacques, P. F., A. G. Bostom, et al. (2001). "Determinants of plasma total homocysteine concentration in the Framingham Offspring cohort." The American Journal of Clinical Nutrition **73**(3): 613-621.

Jay, D., H. Hitomi, et al. (2006). "Oxidative stress and diabetic cardiovascular complications." Free Radical Biology and Medicine **40**(2): 183-192.

Jeremy, J., N. Shukla, et al. (2002). "Homocysteine and cardiovascular disease in diabetes mellitus." Atherosclerosis **164**(2): 383-384.

Jia, L.-q., G.-l. Yang, et al. (2012). "Tanshinone IIA reduces apoptosis induced by hydrogen peroxide in the human endothelium-derived EA. hy926 cells." Journal of ethnopharmacology **143**(1): 100-108.

Jia, W., W. Gao, et al. (2003). "Antidiabetic herbal drugs officially approved in China." Phytotherapy research **17**(10): 1127-1134.

Jiang, M., M. Zhou, et al. (2013). "Identification of NF-κB Inhibitors in Xuebijing injection for sepsis treatment based on bioactivity-integrated UPLC-Q/TOF." Journal of ethnopharmacology **147**(2): 426-433.

Jiang, Z. Y., Y.-W. Lin, et al. (1999). "Characterization of selective resistance to insulin signaling in the vasculature of obese Zucker (fa/fa) rats." Journal of Clinical Investigation **104**(4): 447-457.

Jin, L., R. Caldwell, et al. (2007). "Homocysteine induces endothelial dysfunction via inhibition of arginine transport." Journal of physiology and pharmacology **58**(2): 191.

Jin, L., R. B. Caldwell, et al. (2007). "Homocysteine induces endothelial dysfunction via inhibition of arginine transport." Journal of Physiology and Pharmacology **58**(2): 191.

Jones, D. P., J. L. Carlson, et al. (2000). "Redox state of glutathione in human plasma." Free Radical Biology and Medicine **28**(4): 625-635.

Kang, S.-S., P. W. Wong, et al. (1992). "Hyperhomocyst (e) inemia as a risk factor for occlusive vascular disease." Annual review of nutrition **12**(1): 279-298.

Kang, Y. J. (2011). "Copper and homocysteine in cardiovascular diseases." Pharmacol Ther **129**(3): 321-331.

Karason, K., L. Sjöström, et al. (2003). "Impact of blood pressure and insulin on the relationship between body fat and left ventricular structure." European heart journal **24**(16): 1500-1505.

Kato, I., A. Dnistrian, et al. (1999). "Serum folate, homocysteine and colorectal cancer risk in women: a nested case–control study." British journal of cancer **79**(11-12): 1917.

Khullar, M., A. A.-R. S. Al-Shudiefat, et al. (2010). "Oxidative stress: a key contributor to diabetic cardiomyopathy This review is one of a selection of papers published in a Special Issue on Oxidative Stress in Health and Disease." Canadian journal of physiology and pharmacology **88**(3): 233-240.

Kim, C.-S., Y.-R. Kim, et al. (2011). "Homocysteine promotes human endothelial cell dysfunction via site-specific epigenetic regulation of p66shc." Cardiovascular research **92**(3): 466-475.

Kim, D.-O., K. W. Lee, et al. (2002). "Vitamin C equivalent antioxidant capacity (VCEAC) of phenolic phytochemicals." Journal of Agricultural and Food Chemistry **50**(13): 3713-3717.

Kim, S., P. A. Thiessen, et al. (2015). "PubChem substance and compound databases." Nucleic acids research **44**(D1): D1202-D1213.

Kitaoka, H. (2001). "Hypertrophic cardiomyopathy in the elderly: significance of atrial fibrillation." Journal of cardiology **37**: 133-138.

Kuhad, A. and K. Chopra (2008). "Effect of sesamol on diabetes-associated cognitive decline in rats." Experimental Brain Research **185**(3): 411-420.

Kurian, A. K. and K. M. Cardarelli (2007). "Racial and ethnic differences in cardiovascular disease risk factors: a systematic review." Ethnicity and Disease **17**(1): 143.

Kwon, G., H. J. Kim, et al. (2014). "Anxiolytic-like effect of danshensu [(3-(3, 4-dihydroxyphenyl)-lactic acid)] in mice." Life sciences **101**(1): 73-78.

Lai, W. K. C. and M. Y. Kan (2015). "Homocysteine-induced endothelial dysfunction." Annals of nutrition and metabolism **67**(1): 1-12.

Lam, F. F. Y., J. H. K. Yeung, et al. (2007). "Relaxant effects of danshen aqueous extract and its constituent danshensu on rat coronary artery are mediated by inhibition of calcium channels." Vascular pharmacology **46**(4): 271-277.

Lam, F. F. Y., J. H. K. Yeung, et al. (2007). "Relaxant effects of danshen aqueous extract and its constituent danshensu on rat coronary artery are mediated by inhibition of calcium channels." Vascular pharmacology **46**(4): 271-277.

Lam, F. F. Y., J. H. K. Yeung, et al. (2005). "Mechanisms of the dilator action of Danshen (Salvia miltiorrhiza) on rat isolated femoral artery." Journal of cardiovascular pharmacology **46**(3): 361-368.

Legoabe, L., J. Kruger, et al. (2011). "Monoamine oxidase inhibition by selected anilide derivatives." European journal of medicinal chemistry **46**(10): 5162-5174.

Lei, X.-L. and G. C. Chiou (1986). "Cardiovascular pharmacology of Panax notoginseng (Burk) FH Chen and Salvia miltiorrhiza." The American journal of Chinese medicine **14**(03n04): 145-152.

Lei, X.-L. and G. C. Chiou (1986). "Studies on cardiovascular actions of Salvia miltiorrhiza." The American journal of Chinese medicine **14**(01n02): 26-32.

Letonja, M. and D. Petrovič (2014). "Is diabetic cardiomyopathy a specific entity?" World journal of cardiology **6**(1): 8.

Lewerenz, J. and P. Maher (2011). "Control of redox state and redox signaling by neural antioxidant systems." Antioxidants & redox signaling **14**(8): 1449-1465.

Li, C., K. Yung, et al. (1990). "Hypotensive action of Salvia miltiorrhiza cell culture extract." The American journal of Chinese medicine **18**(03n04): 157-166.

Li, G., Y. Gao, et al. (2009). "Study on toxicity of danshensu in beagle dogs after 3-month continuous intravenous infusion." Toxicology mechanisms and methods **19**(6-7): 441-446.

Li, R. W.-S., C. Yang, et al. (2015). "Relaxation effect of a novel Danshensu/tetramethylpyrazine derivative on rat mesenteric arteries." Eur J Pharmacol **761**: 153-160.

Li, Z., L. Sun, et al. (2003). "Elevated plasma homocysteine was associated with hemorrhagic and ischemic stroke, but methylenetetrahydrofolate reductase gene c677t polymorphism was a risk factor for thrombotic stroke a multicenter case-control study in China." Stroke **34**(9): 2085-2090.

Mao, H.-p., X.-y. Wang, et al. (2016). "Danhong injection attenuates isoproterenol-

induced cardiac hypertrophy by regulating p38 and NF-κb pathway." Journal of ethnopharmacology **186**: 20-29.

Marí, M., A. Morales, et al. (2009). "Mitochondrial glutathione, a key survival antioxidant." Antioxidants & redox signaling **11**(11): 2685-2700.

Maron, B. J., J. A. Towbin, et al. (2006). "Contemporary definitions and classification of the cardiomyopathies." Circulation **113**(14): 1807-1816.

Martin, J. L. R., M. Sainz-Pardo, et al. (2007). "Review: benzodiazepines in generalized anxiety disorder: heterogeneity of outcomes based on a systematic review and meta-analysis of clinical trials." Journal of Psychopharmacology **21**(7): 774-782.

Martinov, M. V., V. M. Vitvitsky, et al. (2000). "A substrate switch: a new mode of regulation in the methionine metabolic pathway." Journal of theoretical biology **204**(4): 521-532.

McCully, K. S. (1969). "Vascular pathology of homocysteinemia: implications for the pathogenesis of arteriosclerosis." The American journal of pathology **56**(1): 111.

McCully, K. S. (1993). "Chemical pathology of homocysteine. I. Atherogenesis." Annals of Clinical & Laboratory Science **23**(6): 477-493.

McLean, R. R., P. F. Jacques, et al. (2004). "Homocysteine as a predictive factor for hip fracture in older persons." New England Journal of Medicine **350**(20): 2042-2049.

Mendis, S., P. Puska, et al. (2011). Global atlas on cardiovascular disease prevention and control, World Health Organization.

Milstien, S. and Z. Katusic (1999). "Oxidation of tetrahydrobiopterin by peroxynitrite: implications for vascular endothelial function." Biochemical and biophysical

research communications **263**(3): 681-684.

Miranda, C. L., J. F. Stevens, et al. (2000). "Antioxidant and prooxidant actions of prenylated and nonprenylated chalcones and flavanones in vitro." Journal of Agricultural and Food Chemistry **48**(9): 3876-3884.

Mishra, P. K., N. Tyagi, et al. (2010). "Synergism in hyperhomocysteinemia and diabetes: role of PPAR gamma and tempol." Cardiovasc Diabetol **9**(49): 1-8.

Moll, S. and E. A. Varga (2015). "Homocysteine and MTHFR mutations." Circulation **132**(1): e6-e9.

Moncada, S., R. Palmer, et al. (1991). "Nitric oxide: physiology, pathophysiology, and pharmacology." Pharmacological reviews **43**(2): 109-142.

Mosharov, E., M. R. Cranford, et al. (2000). "The quantitatively important relationship between homocysteine metabolism and glutathione synthesis by the transsulfuration pathway and its regulation by redox changes." Biochemistry **39**(42): 13005-13011.

Muniyappa, R., M. Montagnani, et al. (2007). "Cardiovascular actions of insulin." Endocrine reviews **28**(5): 463-491.

Muntean, D. M., A. Sturza, et al. (2016). "The role of mitochondrial reactive oxygen species in cardiovascular injury and protective strategies." Oxidative medicine and cellular longevity **2016**.

Muthuramu, I., F. Jacobs, et al. (2013). "Selective homocysteine lowering gene transfer improves infarct healing, attenuates remodelling, and enhances diastolic function after myocardial infarction in mice." PloS one **8**(5): e63710.

Muthuramu, I., N. Singh, et al. (2015). "Selective homocysteine-lowering gene transfer attenuates pressure overload-induced cardiomyopathy via reduced oxidative stress." Journal of molecular medicine **93**(6): 609-618.

NARIN, F., N. Narin, et al. (2002). "The effect of folic acid, vitamin B6 and vitamin B12 on the homocysteine levels in rabbits fed by methionine-enriched diets." The Tohoku journal of experimental medicine **198**(2): 99-105.

Nasir, K., M. Tsai, et al. (2007). "Elevated homocysteine is associated with reduced regional left ventricular function." Circulation **115**(2): 180-187.

Neilan, T. G., S. L. Blake, et al. (2007). "Disruption of nitric oxide synthase 3 protects against the cardiac injury, dysfunction, and mortality induced by doxorubicin." Circulation **116**(5): 506-514.

Nikolaidis, L. A., A. Sturzu, et al. (2004). "The development of myocardial insulin resistance in conscious dogs with advanced dilated cardiomyopathy." Cardiovascular research **61**(2): 297-306.

Noctor, G., L. Gomez, et al. (2002). "Interactions between biosynthesis, compartmentation and transport in the control of glutathione homeostasis and signalling." Journal of experimental botany **53**(372): 1283-1304.

Nolin, T. D., M. E. McMenamin, et al. (2007). "Simultaneous determination of total homocysteine, cysteine, cysteinylglycine, and glutathione in human plasma by high-performance liquid chromatography: application to studies of oxidative stress." Journal of Chromatography B **852**(1): 554-561.

Nordberg, J. and E. S. Arner (2001). "Reactive oxygen species, antioxidants, and the mammalian thioredoxin system." Free Radical Biology and Medicine **31**(11): 1287-1312.

Nunes, S., A. P. Rolo, et al. (2017). Diabetic Cardiomyopathy: Focus on Oxidative Stress, Mitochondrial Dysfunction and Inflammation. Cardiomyopathies-Types and Treatments, InTech.

Nunes, S., E. Soares, et al. (2013). "Early cardiac changes in a rat model of prediabetes:

brain natriuretic peptide overexpression seems to be the best marker." Cardiovascular diabetology **12**(1): 44.

Nygård, O., H. Refsum, et al. (1997). "Coffee consumption and plasma total homocysteine: The Hordaland Homocysteine Study." The American Journal of Clinical Nutrition **65**(1): 136-143.

Olivotto, I., F. Cecchi, et al. (2001). "Impact of atrial fibrillation on the clinical course of hypertrophic cardiomyopathy." Circulation **104**(21): 2517-2524.

Papapetropoulos, A., G. García-Cardeña, et al. (1997). "Nitric oxide production contributes to the angiogenic properties of vascular endothelial growth factor in human endothelial cells." Journal of Clinical Investigation **100**(12): 3131.

Park, K.-H. and W. J. Park (2015). "Endothelial dysfunction: clinical implications in cardiovascular disease and therapeutic approaches." Journal of Korean medical science **30**(9): 1213-1225.

Parng, C., N. M. Roy, et al. (2007). "Neurotoxicity assessment using zebrafish." Journal of pharmacological and toxicological methods **55**(1): 103-112.

Penumathsa, S. V., M. Thirunavukkarasu, et al. (2008). "Resveratrol enhances GLUT-4 translocation to the caveolar lipid raft fractions through AMPK/Akt/eNOS signalling pathway in diabetic myocardium." Journal of cellular and molecular medicine **12**(6a): 2350-2361.

Pieper, G. M. (1997). "Acute amelioration of diabetic endothelial dysfunction with a derivative of the nitric oxide synthase cofactor, tetrahydrobiopterin." Journal of cardiovascular pharmacology **29**(1): 8-15.

Qu, W., H. Huang, et al. (2014). "Danshensu-mediated protective effect against hepatic fibrosis induced by carbon tetrachloride in rats." Pathologie Biologie **62**(6): 348-353.

Raaf, L., C. Noll, et al. (2011). "Myocardial fibrosis and TGFB expression in hyperhomocysteinemic rats." Molecular and cellular biochemistry **347**(1-2): 63-70.

Rahangdale, S., S. Y. Yeh, et al. (2008). "Therapeutic interventions and oxidative stress in diabetes." Frontiers in bioscience: a journal and virtual library **14**: 192-209.

Rajpathak, S. N., D. J. Kumbhani, et al. (2009). "Statin therapy and risk of developing type 2 diabetes: a meta-analysis." Diabetes Care **32**(10): 1924-1929.

Rivett, A. J. and J. A. Roth (1982). "Kinetic studies on the O-methylation of dopamine by human brain membrane-bound catechol O-methyltransferase." Biochemistry **21**(8): 1740-1742.

Rosenkranz, A. C., S. G. Hood, et al. (2003). "B-Type Natriuretic Peptide Prevents Acute Hypertrophic Responses in the Diabetic Rat Heart." Diabetes **52**(9): 2389-2395.

Rubler, S., J. Dlugash, et al. (1972). "New type of cardiomyopathy associated with diabetic glomerulosclerosis." The American journal of cardiology **30**(6): 595-602.

Ruhui, L., J. Jinfa, et al. (2015). "Influence of hyperhomocysteinemia on left ventricular diastolic function in Chinese patients with hypertension." Herz **40**(4): 679-684.

Sahin, M., N. B. Tutuncu, et al. (2007). "Effects of metformin or rosiglitazone on serum concentrations of homocysteine, folate, and vitamin B12 in patients with type 2 diabetes mellitus." Journal of diabetes and its complications **21**(2): 118-123.

Satoh, T., S.-I. Okamoto, et al. (2006). "Activation of the Keap1/Nrf2 pathway for neuroprotection by electrophillic phase II inducers." Proceedings of the

National Academy of Sciences of the United States of America **103**(3): 768-773.

Sattar, N., D. Preiss, et al. (2010). "Statins and risk of incident diabetes: a collaborative meta-analysis of randomised statin trials." The Lancet **375**(9716): 735-742.

Schalkwijk, C. G. and C. D. Stehouwer (2005). "Vascular complications in diabetes mellitus: the role of endothelial dysfunction." Clinical science **109**(2): 143-159.

Schröder, M. and R. J. Kaufman (2005). "ER stress and the unfolded protein response." Mutation Research/Fundamental and Molecular Mechanisms of Mutagenesis **569**(1): 29-63.

Serpillon, S., B. C. Floyd, et al. (2009). "Superoxide production by NAD (P) H oxidase and mitochondria is increased in genetically obese and hyperglycemic rat heart and aorta before the development of cardiac dysfunction. The role of glucose-6-phosphate dehydrogenase-derived NADPH." American Journal of Physiology-Heart and Circulatory Physiology **297**(1): H153-H162.

Seshadri, S., A. Beiser, et al. (2002). "Plasma homocysteine as a risk factor for dementia and Alzheimer's disease." New England Journal of Medicine **346**(7): 476-483.

Shaikh, M. K., B. R. Devrajani, et al. (2012). "Plasma homocysteine level in patients with diabetes mellitus." World Applied Sciences Journal **16**(9): 1269-1273.

Shukla, N., C. Thompson, et al. (2002). "Homocysteine enhances impairment of endothelium-dependent relaxation and guanosine cyclic monophosphate formation in aortae from diabetic rabbits." Diabetologia **45**(9): 1325-1331.

Singh, S., Y. K. Loke, et al. (2007). "Long-term risk of cardiovascular events with rosiglitazone: a meta-analysis." Jama **298**(10): 1189-1195.

Sipkens, J. A., N. Hahn, et al. (2013). "Homocysteine-induced apoptosis in endothelial

cells coincides with nuclear NOX2 and peri-nuclear NOX4 activity." Cell biochemistry and biophysics **67**(2): 341-352.

Siu, P. M., S. Bae, et al. (2007). "Response of caspase-independent apoptotic factors to high salt diet-induced heart failure." Journal of molecular and cellular cardiology **42**(3): 678-686.

Soinio, M., J. Marniemi, et al. (2004). "Elevated plasma homocysteine level is an independent predictor of coronary heart disease events in patients with type 2 diabetes mellitus." Annals of internal medicine **140**(2): 94-100.

Sood, H. S., M. J. Hunt, et al. (2003). "Peroxisome proliferator ameliorates endothelial dysfunction in a murine model of hyperhomocysteinemia." American Journal of Physiology-Lung Cellular and Molecular Physiology **284**(2): L333-L341.

Sorescu, D. and K. K. Griendling (2002). "Reactive oxygen species, mitochondria, and NAD (P) H oxidases in the development and progression of heart failure." Congestive Heart Failure **8**(3): 132-140.

Srianta, I., N. Kusumawati, et al. (2013). "In vitro α-glucosidase inhibitory activity of Monascus-fermented durian seed extracts." International Food Research Journal **20**(2): 533-536.

Stühlinger, M. C., P. S. Tsao, et al. (2001). "Homocysteine impairs the nitric oxide synthase pathway role of asymmetric dimethylarginine." Circulation **104**(21): 2569-2575.

Stipanuk, M. H. and I. Ueki (2011). "Dealing with methionine/homocysteine sulfur: cysteine metabolism to taurine and inorganic sulfur." Journal of inherited metabolic disease **34**(1): 17-32.

Story, C. (2017). "What is cardiomyopathy?". URL: http://www.healthline.com/health/heart-disease/cardiomyopathy#overview1

Suematsu, N., C. Ojaimi, et al. (2007). "Hyperhomocysteinemia alters cardiac substrate metabolism by impairing nitric oxide bioavailability through oxidative stress." Circulation **115**(2): 255-262.

Sundström, J., L. Sullivan, et al. (2004). "Relations of plasma homocysteine to left ventricular structure and function: the Framingham Heart Study." European heart journal **25**(6): 523-530.

Tan, K. C., W. S. Chow, et al. (2002). "Effects of angiotensin II receptor antagonist on endothelial vasomotor function and urinary albumin excretion in type 2 diabetic patients with microalbuminuria." Diabetes/metabolism research and reviews **18**(1): 71-76.

Taniyama, Y. and K. Walsh (2002). "Elevated myocardial Akt signaling ameliorates doxorubicin-induced congestive heart failure and promotes heart growth." Journal of molecular and cellular cardiology **34**(10): 1241-1247.

Tawakol, A., T. Omland, et al. (1997). "Hyperhomocyst (e) inemia is associated with impaired endothelium-dependent vasodilation in humans." Circulation **95**(5): 1119-1121.

Tchaikovski, V., S. Olieslagers, et al. (2009). "Diabetes mellitus activates signal transduction pathways resulting in vascular endothelial growth factor resistance of human monocytes." Circulation **120**(2): 150-159.

Thiene, G., D. Corrado, et al. (2004). "Cardiomyopathies: is it time for a molecular classification?" European heart journal **25**(20): 1772-1775.

Topal, G., A. Brunet, et al. (2004). "Homocysteine induces oxidative stress by uncoupling of NO synthase activity through reduction of tetrahydrobiopterin." Free Radical Biology and Medicine **36**(12): 1532-1541.

Tousoulis, D., A.-M. Kampoli, et al. (2012). "Diabetes mellitus and vascular

endothelial dysfunction: current perspectives." Current vascular pharmacology **10**(1): 19-32.

Townsend, N., L. Wilson, et al. (2016). "Cardiovascular disease in Europe: epidemiological update 2016." European heart journal **37**(42): 3232-3245.

Tuomilehto, J. and J. Lindström (2003). "The major diabetes prevention trials." Current diabetes reports **3**(2): 115-122.

Tyagi, S. C., W. Rodriguez, et al. (2005). "Hyperhomocysteinemic diabetic cardiomyopathy: oxidative stress, remodeling, and endothelial-myocyte uncoupling." Journal of cardiovascular pharmacology and therapeutics **10**(1): 1-10.

Tyagi, S. C., L. M. Smiley, et al. (1999). "Homocyst (e) ine impairs endocardial endothelial function." Canadian journal of physiology and pharmacology **77**(12): 950-957.

Ueland, P. M., H. Refsum, et al. (1992). "Plasma homocysteine and cardiovascular disease." Atherosclerotic cardiovascular disease, hemostasis, and endothelial function. New York: Marcel Dekker **183**.

Ueland, P. M., H. Refsum, et al. (1993). "Total homocysteine in plasma or serum: methods and clinical applications." Clinical Chemistry **39**(9): 1764-1779.

Ungvari, Z., A. Csiszar, et al. (2003). "Increased superoxide production in coronary arteries in hyperhomocysteinemia." Arteriosclerosis, thrombosis, and vascular biology **23**(3): 418-424.

Upchurch, G. R., G. N. Welch, et al. (1997). "Homocyst (e) ine decreases bioavailable nitric oxide by a mechanism involving glutathione peroxidase." Journal of Biological Chemistry **272**(27): 17012-17017.

Vásquez-Vivar, J., B. Kalyanaraman, et al. (1998). "Superoxide generation by

endothelial nitric oxide synthase: the influence of cofactors." Proceedings of the National Academy of Sciences **95**(16): 9220-9225.

Van den Oever, I. A., H. G. Raterman, et al. (2010). "Endothelial dysfunction, inflammation, and apoptosis in diabetes mellitus." Mediators of inflammation **2010**.

Van Hoeven, K. and S. M. Factor (1990). "A comparison of the pathological spectrum of hypertensive, diabetic, and hypertensive-diabetic heart disease." Circulation **82**(3): 848-855.

Velagaleti, R. S., P. Gona, et al. (2010). "Relations of insulin resistance and glycemic abnormalities to cardiovascular magnetic resonance measures of cardiac structure and function: the Framingham Heart Study." Circulation: Cardiovascular Imaging: CIRCIMAGING. 109.911438.

Velez-Carrasco, W., M. Merkel, et al. (2008). "Dietary methionine effects on plasma homocysteine and HDL metabolism in mice." The Journal of nutritional biochemistry **19**(6): 362-370.

Vitvitsky, V., E. Mosharov, et al. (2003). "Redox regulation of homocysteine-dependent glutathione synthesis." Redox report **8**(1): 57-63.

Wald, D. S., M. Law, et al. (2002). "Homocysteine and cardiovascular disease: evidence on causality from a meta-analysis." BMJ **325**(7374): 1202.

Waltenberger, J. (2009). "VEGF resistance as a molecular basis to explain the angiogenesis paradox in diabetes mellitus." Biochemical Society Transactions **37**(6): 1167.

Wang, D., G. Fan, et al. (2013). "Vascular reactivity screen of Chinese medicine danhong injection identifies Danshensu as a NO-independent but PGI2-mediated relaxation factor." Journal of cardiovascular pharmacology **62**(5):

457-465.

Wang, F., Y.-Y. Liu, et al. (2009). "The attenuation effect of 3, 4-dihydroxy-phenyl lactic acid and salvianolic acid B on venular thrombosis induced in rat mesentery by photochemical reaction." Clinical hemorheology and microcirculation **42**(1): 7-18.

Wang, J., Z. Ma, et al. (2011). "Tissue distribution in mice of danshensu from sodium danshensu and Salvia miltiorrhiza injection." China journal of Chinese materia medica **36**(11): 1516-1518.

Wang, J., X. Xiong, et al. (2013). "Cardiovascular effects of salvianolic acid B." Evidence-Based Complementary and Alternative Medicine **2013**.

Wang, T., F. Fu, et al. (2012). "Danshensu ameliorates the cognitive decline in streptozotocin-induced diabetic mice by attenuating advanced glycation end product-mediated neuroinflammation." Journal of Neuroimmunology **245**(1): 79-86.

Wang, W.-M. and H.-Z. Jin (2017). "Homocysteine: A Potential Common Route for Cardiovascular Risk and DNA Methylation in Psoriasis." Chinese Medical Journal **130**(16): 1980.

Wang, X.-J., Z.-B. Wang, et al. (2005). "Effect of salvianic acid A on lipid peroxidation and membrane permeability in mitochondria." Journal of ethnopharmacology **97**(3): 441-445.

Wang, X., L. Cui, et al. (2012). "Homocysteine induces cardiomyocyte dysfunction and apoptosis through p38 MAPK-mediated increase in oxidant stress." Journal of molecular and cellular cardiology **52**(3): 753-760.

Washio, T., K. Nomoto, et al. (2011). "Relationship between plasma homocysteine levels and congestive heart failure in patients with acute myocardial

infarction." International heart journal **52**(4): 224-228.

Weissmann, N., S. Winterhalder, et al. (2001). "NO and reactive oxygen species are involved in biphasic hypoxic vasoconstriction of isolated rabbit lungs." American Journal of Physiology-Lung Cellular and Molecular Physiology **280**(4): L638-L645.

Wile, D. J. and C. Toth (2010). "Association of metformin, elevated homocysteine, and methylmalonic acid levels and clinically worsened diabetic peripheral neuropathy." Diabetes Care **33**(1): 156-161.

Willcox, J. K., S. L. Ash, et al. (2004). "Antioxidants and prevention of chronic disease." Critical reviews in food science and nutrition **44**(4): 275-295.

Wright, E., J. Scism-Bacon, et al. (2006). "Oxidative stress in type 2 diabetes: the role of fasting and postprandial glycaemia." International journal of clinical practice **60**(3): 308-314.

Xiao-Yong, L., C. Chun-Lin, et al. (2008). "Effects of danshensu on the incidence of ischemia-reperfusion induced arrhythmia in hypertrophy rat heart." Chinese Journal of Natural Medicines **6**(6): 461-465.

Yan, T. T., Q. Li, et al. (2010). "Homocysteine impaired endothelial function through compromised vascular endothelial growth factor/Akt/endothelial nitric oxide synthase signalling." Clinical and Experimental Pharmacology and Physiology **37**(11): 1071-1077.

Yang, F., H.-M. Tan, et al. (2005). "Hyperhomocysteinemia and atherosclerosis." Sheng li xue bao:[Acta physiologica Sinica] **57**(2): 103-114.

Yang, R.-x., S.-y. Huang, et al. (2010). "Danshensu protects vascular endothelia in a rat model of hyperhomocysteinemia." Acta Pharmacologica Sinica **31**(10): 1395.

Ye, G., N. S. Metreveli, et al. (2003). "Metallothionein prevents diabetes-induced deficits in cardiomyocytes by inhibiting reactive oxygen species production." Diabetes **52**(3): 777-783.

Yin, Y., Y. Guan, et al. (2013). "Cardioprotective effect of Danshensu against myocardial ischemia/reperfusion injury and inhibits apoptosis of H9c2 cardiomyocytes via Akt and ERK1/2 phosphorylation." European journal of pharmacology **699**(1): 219-226.

Yin, Y., Y. Guan, et al. (2013). "Cardioprotective effect of Danshensu against myocardial ischemia/reperfusion injury and inhibits apoptosis of H9c2 cardiomyocytes via Akt and ERK1/2 phosphorylation." Eur J Pharmacol **699**(1): 219-226.

Yin, Y., Y. Guan, et al. (2013). "Cardioprotective effect of Danshensu against myocardial ischemia/reperfusion injury and inhibits apoptosis of H9c2 cardiomyocytes via Akt and ERK1/2 phosphorylation." Eur J Pharmacol **699**(1-3): 219-226.

Yu, P.-F., W.-Y. Wang, et al. (2011). "The role of P-glycoprotein in transport of Danshensu across the blood-brain barrier." Evidence-Based Complementary and Alternative Medicine **2011**.

Yue, P., T. Arai, et al. (2007). "Magnetic resonance imaging of progressive cardiomyopathic changes in the db/db mouse." American Journal of Physiology-Heart and Circulatory Physiology **292**(5): H2106-H2118.

Zeng, G., F. H. Nystrom, et al. (2000). "Roles for insulin receptor, PI3-kinase, and Akt in insulin-signaling pathways related to production of nitric oxide in human vascular endothelial cells." Circulation **101**(13): 1539-1545.

Zhang, C., Y. Cai, et al. (2001). "Homocysteine induces programmed cell death in

human vascular endothelial cells through activation of the unfolded protein response." Journal of Biological Chemistry **276**(38): 35867-35874.

Zhang, N., H. Zou, et al. (2010). "Biphasic effects of sodium danshensu on vessel function in isolated rat aorta." Acta Pharmacologica Sinica **31**(4): 421.

Zhao, G.-R., Z.-J. Xiang, et al. (2006). "Antioxidant activities of Salvia miltiorrhiza and Panax notoginseng." Food Chemistry **99**(4): 767-774.

Zhao, G.-R., H.-M. Zhang, et al. (2008). "Characterization of the radical scavenging and antioxidant activities of danshensu and salvianolic acid B." Food and Chemical Toxicology **46**(1): 73-81.

Zhou, X., S. W. Chan, et al. (2012). "Danshensu is the major marker for the antioxidant and vasorelaxation effects of Danshen (Salvia miltiorrhiza) water-extracts produced by different heat water-extractions." Phytomedicine **19**(14): 1263-1269.

Zieman, S. J., V. Melenovsky, et al. (2007). "Advanced glycation endproduct crosslink breaker (alagebrium) improves endothelial function in patients with isolated systolic hypertension." Journal of Hypertension **25**(3): 577-583.